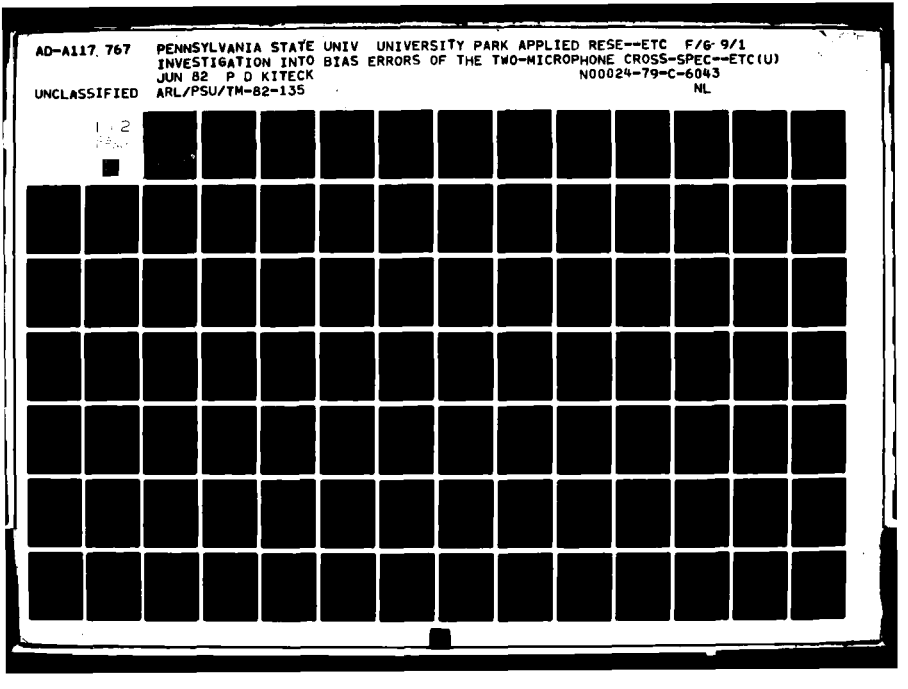
AD-A117 767
PENNSYLVANIA STATE UNIV UNIVERSITY PARK APPLIED RESE--ETC F/G 9/1
INVESTIGATION INTO BIAS ERRORS OF THE TWO-MICROPHONE CROSS-SPEC--ETC(U)
JUN 82 P D KITECK
N00024-79-C-6043
UNCLASSIFIED
ARL/PSU/TM-82-135
NL
1 2

AD A117767

(6)

INVESTIGATION INTO BIAS ERRORS OF THE TWO-MICROPHONE CROSS-SPECTRAL METHOD TO MEASURE ACOUSTIC INTENSITY

Paul D. Kiteck

Technical Memorandum
File No. TM 82-135
June 2, 1982
Contract No. N00024-79-C-6043

Copy No. 5

The Pennsylvania State University
Intercollege Research Programs and Facilities
APPLIED RESEARCH LABORATORY
Post Office Box 30
State College, PA 16801

DTIC
ELECTE
AUG 3 1982
H

DTIC FILE COPY

**APPROVED FOR PUBLIC RELEASE
DISTRIBUTION UNLIMITED**

NAVY DEPARTMENT

NAVAL SEA SYSTEMS COMMAND

82 08 03 084

Unclassified

SECURITY CLASSIFICATION OF THIS PAGE (When Data Entered)

REPORT DOCUMENTATION PAGE		READ INSTRUCTIONS BEFORE COMPLETING FORM
1. REPORT NUMBER TM82-135	2. GOVT ACCESSION NO. AD-A117767	3. RECIPIENT'S CATALOG NUMBER
4. TITLE (and Subtitle) Investigation Into Bias Errors of the Two-Microphone Cross-Spectral Method to Measure Acoustic Intensity		5. TYPE OF REPORT & PERIOD COVERED M.S. Thesis, August 1982 6. PERFORMING ORG. REPORT NUMBER TM82-135
7. AUTHOR(s) Paul D. Kiteck		8. CONTRACT OR GRANT NUMBER(s) N00024-79-C-6043
9. PERFORMING ORGANIZATION NAME AND ADDRESS The Pennsylvania State University Applied Research Laboratory, P.O.Box 30 State College, PA 16801		10. PROGRAM ELEMENT, PROJECT, TASK AREA & WORK UNIT NUMBERS
11. CONTROLLING OFFICE NAME AND ADDRESS Naval Sea Systems Command Department of the Navy Washington, DC 20362		12. REPORT DATE June 2, 1982 13. NUMBER OF PAGES 163 pages
14. MONITORING AGENCY NAME & ADDRESS(if different from Controlling Office)		15. SECURITY CLASS. (of this report) Unclassified, Unlimited 15a. DECLASSIFICATION/DOWNGRADING SCHEDULE

16. DISTRIBUTION STATEMENT (of this Report)

Approved for public release, distribution unlimited, per NSSC (Naval Sea Systems Command), July 7, 1982.

17. DISTRIBUTION STATEMENT (of the abstract entered in Block 20, if different from Report)

18. SUPPLEMENTARY NOTES

19. KEY WORDS (Continue on reverse side if necessary and identify by block number)

thesis, acoustic, intensity, measurement

20. ABSTRACT (Continue on reverse side if necessary and identify by block number)

The practical application of the two-microphone cross-spectral method of measuring acoustic intensity has recently gained great popularity in the field of noise control and soon will become the standard method of measuring the sound power of a noise source in-situ.

The cross-spectral intensity technique contains inherent limitations which must be thoroughly understood before applying the measuring method in the field. These errors of the cross-spectral intensity method can be classified in terms of both bias and random errors, and if the coherence

DD FORM 1 JAN 73 1473 EDITION OF 1 NOV 65 IS OBSOLETE

Unclassified

between the two receivers approaches unity and the random errors are sufficiently reduced by an appropriate amount of averaging by the FFT analyzer, the bias errors are then considered to be the major contributor to the deficiencies of the two-microphone intensity technique.

These bias errors of the cross-spectral intensity technique have been theoretically analyzed in the literature but not completely verified experimentally. Therefore, the purpose of this work is to experimentally investigate the bias errors of the cross-spectral method of measuring acoustic intensity and also provide a current review of the technique.

Accession For
NTIS GRA&I
DTIC TAB
Unannounced
Justification
By
Distribution/
Availability Codes
Dist | Avail and/or Special
A

DTIC COPY INSPECTED 2

ABSTRACT

The two-microphone cross-spectral intensity method of measuring acoustic intensity represents a new approach of determining the sound power of a sound source but contains inherent limitations which must be thoroughly understood before applying the measuring method in the field. These errors of the cross-spectral intensity method can be classified in terms of both bias and random errors, and if the coherence between the two receivers approaches unity and the random errors are sufficiently reduced by an appropriate amount of averaging by the FFT analyzer, the bias errors are then considered to be the major contributor to the deficiencies of the two-microphone intensity technique.

The purpose of this work is to experimentally investigate the bias errors of the cross-spectral method of measuring acoustic intensity which are analyzed in the literature but not completely verified experimentally and also provide a current review of the technique.

It was found, for the most part, that the empirical results correlated well with the predicted bias errors. In the situation where theoretical results were not available, the experimental evidence shows that the acoustical scattering by the intensity probe produces only a minimal amount of error when certain precautions are taken. Also, the calibration procedures were analyzed, and recommendations for correct application are presented. It was shown that the intensity can be successfully measured in semi-reverberant and reverberant sound fields. In general, the intensity technique performs well when qualifying a noise source located in its normal operating acoustic environment and offers new adventures for many acoustical measurements.

TABLE OF CONTENTS

Accession For
NTIS GRA&I
DTIC TAB
Unannounced
Justification
By
Distribution/
Availability Codes
Dist | Avail and/or Special
A

DTIC COPY INSPECTED 2

LIST OF FIGURES

LIST OF SYMBOLS

a	indicates the measured system a
A/D	analog to digital
b	indicates the measured system b
B	resolution bandwidth of the analysis
B&K	Bruel & Kjaer
c	velocity of sound in air (m/sec)
$C_{12}(f)$	coincident spectral density function between acoustic pressures $P_1(f)$ and $P_2(f)$
dB	decibel: where rms sound pressure level is referenced to 0.00002 Newton/$_m$2; sound intensity level is referenced to 10^{-12} watt/$_m$2; and sound power level is referenced to 10^{-12} watt.
$d\hat{S}$	product of a normal unit vector and an incremental area about the measurement surface
E	expected value of the quantity (ensemble average) or estimation of the quantity
f	frequency in Hertz (Hz)
FFT	Fast Fourier Transform
$\hat{G}_{ab}(f)$	estimated one-sided cross-spectral density function between the measured pressures $P_a(f)$ and $P_b(f)$
$\hat{G}^s_{ab}(f)$	switched cross-spectral density function
$G_1(f)$	one-sided power spectral density function (autospectrum) of microphone 1
$G_2(f)$	one-sided power spectral density function of microphone 2
$G_{12}(f)$	one-sided cross-spectral density function between the acoustic pressures $P_1(f)$ and $P_2(f)$
$G'_{12}(f)$	one-sided cross-spectral density function due only to the secondary source
$G_{12}(f)_{cal}$	calibrated one-sided cross-spectral density function
$H_a(f)$	complex frequency response of the measuring system a

$H_{ab}(f)$	relative transfer function between the two microphone measuring systems
$\|H_{ab}(f)\|$	relative gain difference between the two microphone measuring systems
$H_b(f)$	complex frequency response of the measuring system b
$\|H_1\|$	gain factor of microphone system 1
$\|H_2\|$	gain factor of microphone system 2
H_{10}	transfer function between the primary source and the measurement point 1
$H_{10'}$	transfer function between the secondary source and the measurement point 2
H_{20}	transfer function between the primary source and the measurement point 2
$H_{20'}$	transfer function between the secondary source and the measurement point 2
$\vec{I}$	vector component of acoustic intensity
$I(f)$	intensity level due only to the primary source
$I'(f)$	intensity level due only to the secondary source
I_c	complex acoustic intensity
I_{IM}	imaginary (reactive) sound intensity
I_n	normal component of acoustic intensity
I_r	acoustic intensity in the r-direction
Im	imaginary part of the quantity
j	indicates an imaginary quantity and equals the square root of -1
k	wavenumber of sound in air (ω/c)
L_{ps}	intensity level of the primary source (ps)
L_{ss}	intensity level of the secondary source (ss)
m	modal density in an acoustic enclosure
n_d	number of data samples of a mathematical process of the FFT analyzer

$p(t)$	acoustic pressure
$P(f)$	Fourier transform of the acoustic pressure
P_c	complex acoustic pressure
$P'(f)$	acoustic pressure due only to the secondary source
Q	directivity constant of a sound source
$Q_{12}(f)$	quadrature spectral density function between the acoustic pressures $P_1(f)$ and $P_2(f)$
r	distance between the sound source and the measurement point
r_1, r_2	center distances of microphones 1 and 2, respectively, from the source
Δr	separation distance between the two closely-spaced microphones
R_{xx}	general expression for the auto-correlation function
R_{xy}	general expression for the cross-correlation function
Re	real part of the quantity
rms	root mean square value
S	area of the enclosed surface
S_{xy}	general expression for a two-sided cross-spectral density function
$S_1(f)$	two-sided power spectral density function at microphone 1
$S_2(f)$	two-sided power spectral density function at microphone 2
$S_{12}(f)$	two-sided cross-spectral density function between the acoustic pressures $P_1(f)$ and $P_2(f)$
S.F.	smoothing factor
t	time (sec)
T	length of the time average or the integration time
T_{60}	reverberation time (sec)
$u(t)$	acoustic particle velocity
$U(f)$	Fourier transform of the acoustic particle velocity

u_c	complex acoustic particle velocity
u_r	r-component of particle velocity
W	acoustic power (watts)

LIST OF GREEK SYMBOLS

β	non-dimensional parameter representing the ratio of Δr to r
$\gamma_{12}^2(f)$	coherence between the measuring points 1 and 2
∂	partial differentiation of the quantity
$\varepsilon_b(f)$	normalized bias error
$\varepsilon_{b_{IM}}(f)$	normalized bias error for reactive intensity
θ	angle of incidence for an incoming sound wave
θ_{ss}	angle that the secondary source is located with respect to the primary source (in the same plane)
λ	wavelength of sound (c/f)
λ_{min}	minimum wavelength of interest
π	equal to 3.14159
ρ	density of air (Kg/m^3)
ρc	characteristic acoustic impedance of the medium (air in this case)
τ	general symbol expressing time value
$\phi_{12}(f)$	phase angle between the two pressures $P_1(f)$ and $P_2(f)$, in the direction of wave propagation, for a specific microphone distance Δr
$\Delta\phi_{ab}(f)$	relative phase difference between the two microphone measuring systems
$\Delta\hat{\phi}_{ab}(f)$	estimated phase angle $\{\phi_{12}(f)\}$ between the two measured pressures $P_a(f)$ and $P_b(f)$ and including any phase difference of the two measuring systems
ω	angular frequency (rad/sec)

LIST OF OTHER SYMBOLS

0	represents the primary source
0′	represents the secondary source
1	indicates the true measuring system 1
2	indicates the true measuring system 2
*	complex conjugate of the variable
< >	time averaging of the quantity
^	estimated value of the quantity
| |	absolute value or magnitude of the quantity
≈	represents an approximate value
~	proportionality symbol
<<	much less than
>>	much greater than
$\iint_S$	integration over the measuring surface

ACKNOWLEDGEMENTS

The author would like to express his sincere appreciation to the many people associated with The Applied Research Laboratory at The Pennsylvania State University who have contributed to the success of this work. A special thanks is extended to Dr. Jiri Tichy for his assistance and guidance throughout the course of this research, and to the members of the thesis committee, Gerald Lauchle and Oliver McDaniel, for their suggestions which were helpful in the preparation of this study. Also, a very sincere thank you is given to Gary Elko for his helpful discussions and due interest.

This research was supported under the general funding of the Exploratory and Foundational Research Program directed by Dr. M. T. Pigott and other projects at The Applied Research Laboratory.

CHAPTER 1

INTRODUCTION

1.1 General Background and Research Objectives

The practical application of the two-microphone cross-spectral method of measuring acoustic intensity has recently gained great popularity in the acoustics field, particularly in relation with noise control. With the recent advances in electronics and digital signal processing techniques (FFT dual-channel analyzers), the cross-spectral intensity method has developed into a viable technique of measuring sound intensity for the purpose of quantifying and ranking noise sources in semi-reverberant spaces and in-situ (noise source in its natural or original position for operation) while providing a useful and practical supplement to traditional methods.

It has recently been reported that experimental results using the cross-spectral intensity method compare favorably to existing methods for determination of sound power levels requiring special acoustical facilities (15,25). For the cross-spectral intensity method to prove successful, the calculation of sound power levels from a source in-situ should be in reasonable agreement with existing precision methods for broad-band, narrow-band sound power determination.

The potential sources of error inherent in the two-microphone cross-spectral intensity estimation which limit the intensity formulation when employed in empirical conditions are: (1) errors associated with the digital signal processing (owing to the

effectiveness of the FFT algorithm and process) of the cross-spectrum; (2) a methodological error related to the developmental mathematical approximation of intensity using two finite-pressure microphones; (3) errors due to the deficiencies of the measuring instrumentation; (4) errors from the acoustical scattering by the finite-size intensity probe; and (5) errors influenced by the acoustic measuring environment. In general, all used methods to measure the sound power of a noise source (using either the intensity meter or special acoustical facilities) have accuracy restrictions, and the precision of these sound power measurement methods will be equilvalent only after understanding the limitations of each.

The theoretical errors associated with the cross-spectral acoustic intensity estimation have been well documented in recent literature (58,61). Some experimental examination of these predicted errors, particularly bias errors, has been accomplished. Because of the necessity to fully understand the deficiencies related to the cross-spectral intensity technique, an experimental investigation of these errors was performed, and the results are presented in this study. Also, the problem of measuring the intensity far from the source in a semi-reverberant or reverberant acoustic environment was investigated, and it was found that intensity measurements in such cases are feasible. Because the classical sound power determination from sound pressure measurements is not possible in the reverberant sound field, the cross-spectral intensity method provides a favorable alternative of measuring the sound power of a noise source in-situ while opening new realms for rapid acoustical data aquisition.

1.2 Brief Historical Background

Attempts to produce a viable sound intensity meter were tried as early as 1932 when H.F. Olson (44) patented a method to measure the system response to energy flow of sound waves using the difference between the acoustic pressures measured at two closely-spaced pressure microphones. In 1941, Clapp and Firestone (19) employed a combination of two crystal pressure microphones and a ribbon velocity microphone to measure sound energy flow. Then, in 1943, Bolt and Petrauskas (8) applied the pressure-sum pressure-difference principle between two pressure microphones to measure the pressure and pressure gradient to evaluate acoustic impedance of a surface. This was the first use of the pressure-sum pressure-difference principle to produce acoustical measurements from two closely-spaced pressure microphones.

1.2.1 Continuation with Pressure Sum-Difference Methods

In the next decade, interest in sound intensity measurements diminished until Baker (2) and Schultz (54) revived the intensity measurement research with their own individual acoustic wattmeter devices. Schultz made a thorough investigation into the performance of a back-to-back, double electrostatic microphone transducer for measuring sound intensity. Then Schultz, Smith, and Malme (55) were contracted to investigate some aspects of intensity measurements in nearfields and reverberant spaces, and later they described applications of Schultz's acoustic wattmeter to the calibration of an acoustic source in both an anechoic and a reverberant enclosure (56). Other intensity meters were tried during the early 70's by Burger et al (9) and colleagues van Zyl

and Anderson (66). Their conclusions suggested that the pressure-sum pressure-difference principle may provide a better practical solution. And indeed, this principle was used to develop an instrument for measuring sound intensity and mapping intensity flow lines, as applied to automobile acoustics, by Stahel and Lambrich (59) at Unikeller in 1975. Other significant investigations and applications pertaining to this pressure-sum pressure-difference method of measuring sound intensity were also accomplished by Fahy (25,26) and Pavic (47), and the method has been described thoroughly in a recent report by Jacobsen (33).

1.2.2 Cross-Correlation and Cross-Spectral Acoustic Measurements

Applications of the cross-correlation coefficient (the Fourier transform of a cross-spectrum function) between the sound pressures at two points a distance Δr apart for acoustical measurements have been studied since the early 1950's by Cook and Waterhouse et al (20) and Goff (29). At that time, it was predicted that the cross-correlation measurement could be used to define the acoustical quality of a closed room. Blake and Waterhouse (6), Bodlund (7), Schroeder, and others continued this initial spatial cross-correlation work by employing the cross-spectral density between two closely-spaced microphones to understand the diffusion and energy density of reverberant and partially reverberant sound fields.

The two-receiver cross-correlation technique was then applied to noise source identification which provided the initiative for cross-correlation measurements between surface velocity and surface acoustic

pressure to measure radiated acoustic power (30,31). After the success of a surface acoustical intensity method using two transducers (a microphone and an accelerometer) Fahy (24) presented the first significant publication describing a method of evaluating the acoustic vector intensity by measuring the imaginary part of the cross-spectral density between two closely-spaced pressure microphones. Then Chung (11,13,14), from General Motors Research Laboratory, provided important practical application of the cross-spectral formulation using a modern FFT analyzer.

There were initial problems with gain and phase errors between the two-microphone systems used in sensing and recording the signals, but adequate solutions to these phase and gain-mismatch errors were presented by Chung (12), Seybert and Ross (57), and Krishnappa (35). Recent applications of the cross-spectral intensity technique by Chung et al (10), Alfredson (1), Reinhart (52), and others have confirmed the overall accuracy and effectiveness of the acoustic intensity method. Though the experimental results appear encouraging, there are a number of errors inherent in the intensity estimation procedure which very recently have been theoretically analyzed by Thompson and Tree (61) and Seybert (58).

1.2.3 Other Applications

Other applications of the two-microphone cross-spectral technique are now in use or are being developed. In addition to noise source ranking and identification, the procedure can be applied in evaluating acoustic properties of materials in an impedance tube (16,17,57), to

estimate ground-reflection characteristics (28,65), to measure structure borne power flow (41,48,62), and eventually to problems in underwater acoustics (60).

1.3 Scope of the Study

Chapter II describes the general theory of acoustic intensity as related to the sound power determination of a noise source and compares the standard qualifications in specialized acoustic environments with in-situ measurement methods.

In Chapter III, the cross-spectral technique to measure acoustic intensity by two closely-spaced microphones is discussed in detail. First, the expressions for the active acoustic intensity developed in Chapter II are combined with the linear wave equation to produce approximations of sound pressure and particle velocity at a single point in space with two closely-spaced sound pressures, and this is then used to develop the cross-spectral intensity theory. Next, a description of the physical set-up, data processing, and calibration for implementing the technique is detailed. Then, the directional characteristics of the two-microphone device and other possible higher-order receivers are described. Also, limitations of the measuring environment as related to the test facility used for all measurements are mentioned. Finally and most important to this study, a general discussion of the random and bias errors associated with the cross-spectral intensity method is presented.

The next four chapters, Chapters IV to VII, develop the theoretical expressions and examine the related empirical results of the bias errors

mentioned in Chapter III. Chapter IV describes a methodology bias error inherent in the cross-spectral intensity approximation. Chapter V investigates the very important phase and gain-mismatch errors of the measuring instrumentation. Then, Chapter VI analyzes the acoustic scattering by the finite-size intensity probe. Chapter VII concludes the study by examining bias errors from the measuring environment (secondary sound sources and the reverberant sound field) and the reactive sound field.

Chapter VIII provides a summary of the intensity technique employed and states the conclusions of the experimental results. Also, some final comments on the subject and recommendations for future study are presented.

CHAPTER 2

MEASUREMENT OF SOUND POWER AS RELATED TO ACOUSTIC INTENSITY

2.1 Sound Power and Acoustic Intensity Expressions

Acoustic intensity is a vector quantity (power flow vector) which describes sound energy flow through a unit surface S normal to the direction of propagation in unit time. Thus, the acoustic power flow passing through a surface S of a sound source can be determined by integrating the normal component of acoustic intensity (I_n) over a surface enclosing the source and expressed as

$$W(S,t) = \iint_S \vec{I}\cdot d\vec{S} = \iint_S I_n dS \ . \qquad (2.1)$$

This fundamental relationship defines the total radiated sound power and is the principle supporting the usefulness of the concept of sound intensity.

In a medium without mean background flow[1] (the steady state sound field), the vector intensity is equilvalent to the time-averaged product of the pressure and the corresponding particle velocity (in the direction of propagation) at the same location and is defined by:

$$\vec{I} = \lim_{T\to\infty} \frac{1}{T} \int_{-\frac{T}{2}}^{\frac{T}{2}} p(t)\vec{u}(t)dt = \langle p(t)\vec{u}(t)\rangle \ , \qquad (2.2)$$

---

[1] the acoustic medium is assume to be at rest, and the continuity of sound power appears as a consequence of energy conservation.

where the pointed brackets denote time averaging. This product of two real functions, sound pressure and particle velocity, averaged over time represents the fundamental definition of acoustic intensity and can be used to determine the radiated sound power over the measurement surface enclosing a sound source at any distance from the source, even at the surface of the source itself.

The acoustic intensity expression (2.2) accounts for the energy transmitted (called the active or real intensity) in which one of the two components of the farfield velocity is in-phase with the pressure. However, when close to a radiating surface where the pressure and one component of the particle velocity are 90^{o} out-of-phase, there will exist a reactive field (energy fluctuations with zero-mean value in time-space) in which some of the acoustic energy is stored. Therefore, the acoustic intensity may be described as a complex quantity, the real part of which represents the intensity radiated into the farfield and the imaginary part of which represents hydrodynamic flow near the source.

Using the acoustic anology for the complex power (60,64), the complex vector intensity is given by

$$I_c(r) = \tfrac{1}{2} p_c(r,t) u_c^*(r,t) \tag{2.3}$$

where $p_c(r,t)$ and $u_c(r,t)$ are the space-dependent complex pressure and particle velocity, respectively, and the asterisk denotes the complex conjugate. The complex intensity can also be written in real and imaginary parts as

$$\text{Re } I_c(r) = \tfrac{1}{4}[p_c(r,t) u_c^*(r,t) + p_c^*(r,t) u_c(r,t)] \tag{2.4}$$

$$\text{Im } I_c(r) = (\tfrac{1}{4}j)[p_c(r,t)u_c^*(r,t) - p_c^*(r,t)u_c(r,t)] \qquad (2.5)$$

with

$$I_c(r) = \text{Re } I_c(r) + j\text{Im } I_c(r) \ , \qquad (2.6)$$

whereby the imaginary part becomes negligible when $kr \gg 1$, but when $kr \lesssim 1$, the reactive field becomes appreciable.

In general, only the active acoustic vector intensity of a sinusoidal sound field will be measured and written as

$$I(r) = \tfrac{1}{2}\text{Re}[p(r,t)u^*(r,t)] \ , \qquad (2.7)$$

which is the time-average of the product of two complex sound field quantities each oscillating with the same frequency but not necessarily in phase. This real quantity of sound intensity (Equation 2.7) can also be expressed in the alternative form (39), using rms (root-mean-square) values for pressure and velocity, as

$$I(r) = \tfrac{1}{2}[p_{rms}^*(r,t)u_{rms}(r,t) + p_{rms}(r,t)u_{rms}^*(r,t)] \ . \qquad (2.8)$$

2.2 Sound Power Measurements from Specialized Acoustic Environments

Another useful form of sound intensity can be derived from the previous vector intensity expression (2.7). Considering a traveling wave in a uniform nonviscous medium of infinite extent (the free-field), the far-field particle velocity is in the direction of propagation of the sound wave, and the sound intensity is related to the mean-square pressure by

$$I_r = p_{rms}^2/\rho c \qquad (2.9)$$

where ρ and c are, respectively, the density of air and the velocity of sound in air. The subscript r indicates the direction of wave propagation, and because the plane wave pressure is in phase with the velocity, ρc is called the characteristic acoustic impedance of the medium.

This far-field approximation of acoustic intensity (2.9) is a convenient approach to evaluate the sound power of a noise source because it is only necessary to integrate the measured mean-square acoustic pressures on a sphere (or a hemisphere) which is large enough to ensure that far-field conditions are satisfied over this surface. The method is very accurate and can provide information about the directional characteristics of the source. However, this method of determining sound power can only be accomplished in an anechoic environment with far-field pressure measurements and cannot be used in the acoustic nearfield of the sound source or in reverberant sound fields.

The other acoustic environment used to determine the sound power of a sound source is the reverberation room. Without going into detail, the reverberation room sound power measurements can be performed using a normal mode analysis or a statistical analysis of spatially averaged mean-square pressures or a combination of both procedures. The normal mode analysis is particulary appropriate for the low-frequency situation but is not restricted to low frequencies. The statistical analysis method is more useful for the measurement of sound power within the medium and at high frequencies where it can be assumed that the sound

field is diffused (the sound field has high modal overlapping). Both methods should probably be used in determining the radiated sound power of a broad-band noise source. Both measuring procedures entail a significant amount of mathematics, and considerable knowledge of experimental accuracy is essential. There are very excellent and extensive investigations into this subject of sound power measurement in reverberation rooms (two recent comprehensive and cumulative references on the subject are by Jacobsen (32,34)).

2.3 Sound Power Measurements In-Situ

The two environments of a free-field (anechoic) enclosure and a reverberation room are used for sound power determination because only under these so-called well-defined conditions can a general relation between the sound power and the sound pressure exist. Therefore, when sound pressure measurements are used to predict the sound power of a source in its normal physical location for operation (in-situ), many environmental acoustic problems may result. The radiated sound power can, under certain in-situ conditions, be estimated from sound pressure measurements on two (or three) surfaces surrounding the source at different distances, but not all in-situ pressure measurements may be used for calculating the sound-power level of a noise source. Only by satisfying prescribed qualification procedures which provide that the measurements are not contaminated by the reverberant field, extraneous noise, or nearfield pressures may the data be considered as accurate. Because the investigator has little control over the acoustic environment enclosing the sound source, the sound-power levels received

from the in-situ sound pressure measurement methods are usually unacceptable.

In the noise control field, there is the necessity for in-situ sound power measurements because it may be impractical to determine the sound power of a noise source from special facilities, such as an anechoic room or a reverberation chamber. The accuracy of sound power via in-situ sound pressure measurements has been previously established as undesirable. Therefore, the logical approach to in-situ sound power measurement would be to use the exact method of integrating the time-averaged product of the instantaneous pressure and particle velocity (the vector intensity) over a surface. This method of determining sound power, in principle, is rigorous with accuracy limited by the number of intensity measurement positions and imperfections associated with the sound intensity measurement technique. Because sound intensity is a vector quantity (indicates the direction of energy flow), this method will work for all outgoing waves from a noise source under test, irrespective of the environment. If the enclosed measuring surface contains negligable absorption, noise sources outside this surface will, theoretically, not affect the measurements (provided that the noise is steady, which may be questionably). Also, in contrast to pressure measurements, the intensity measurements take into account the phase difference between pressure and velocity, thus making measurements in the nearfield of the sound source feasible which, furthermore, results in the possibility for noise source identification. For these reasons, the intensity method is very suitable for approximating the sound power of a noise source in-situ.

Next it will be established that the imaginary part of the cross-spectrum between two closely-spaced microphones is proportional to the vector intensity of sound. With the advent of dual-channel FFT analyzers, the cross-spectral measurements required in evaluating acoustic intensity can be easily realizable and therefore, provides a viable technique of estimating the sound power of a in-situ noise source.

CHAPTER 3

THE CROSS-SPECTRAL INTENSITY TECHNIQUE

3.1 Approximation with Sound Pressure Values in Closely-Spaced Locations

The relationship between the vector acoustic intensity and the sound pressure and particle velocity is derived from the statement of Newton's second law (the first-order equation of motion). This linear wave equation with zero-mean (medium) flow relates the particle velocity and acoustic pressure gradient in the following manner:

$$\rho \partial u(x,y,z,t)/\partial t = -\text{grad } p(x,y,z,t) \quad \text{[three-dimensional equation]} \quad (3.1)$$

and

$$\rho \partial u(x,t)/\partial t = -\partial p(x,t)/\partial x \quad \text{[one-dimensional equation]} \quad (3.2)$$

where grad p(x,y,z,t) denotes the pressure gradient of p(x,y,z,t). This equation of motion in the r-direction of velocity can then be written as

$$\rho \partial u_r(r,t)/\partial t = -\partial p(r,t)/\partial r \,. \quad (3.3)$$

The particle velocity can be estimated by integrating the one-dimensional acoustic pressure gradient as

$$u_r(r,t) = -\frac{1}{\rho}\int_{-\infty}^{t} \partial p(r,t_1)/\partial r \, dt_1 \,, \quad (3.4)$$

where the lower limit $-\infty$ indicates the moment pertaining to the beginning of the measurement. This equation (3.4) is the basis for

describing the intensity of sound as related to the time-averaged product of pressure and particle velocity (Equation 2.2).

Next, consider the acoustic pressure at two points, r_1 and r_2, separated by the distance Δr ($\Delta r = r_2 - r_1$) in the r-direction. The pressure gradient $\partial p(r,t)/\partial r$ can be approximated by the pressure difference divided by Δr (the physical spacing between two acoustic pressure points), noting that this assumption will be valid if Δr is small compared to the shortest wavelength of interest, λ_{min}. With this in mind, the pressure gradient can be written as

$$\partial p(r,t)/\partial r \approx [p(r_2,t) - p(r_1,t)]/\Delta r$$

$$\approx [p_2(t) - p_1(t)]/\Delta r \qquad (3.5)$$

where the notations $p_1(t)$ and $p_2(t)$ are the complex pressures measured at microphones 1 and 2, respectively.

The component of particle velocity midway between two closely-spaced microphones in the direction of the first microphone to the second microphone can be approximated by substituting the pressure gradient estimation (Equation 3.5) into the linear equation of motion (3.4), resulting in the particle velocity

$$\hat{u}_r(r,t) = -\frac{1}{\rho\Delta r}\int_{-\infty}^{t}[p_2(t_1) - p_1(t_1)]dt_1 \qquad (3.6)$$

with $\hat{u}_r(r,t) \approx u_r(r,t)$ for $\Delta r << \lambda_{min}$. The circumflex symbol (^) denotes an estimated value of the quantity.

Similarly, the corresponding approximation for the acoustic pressure midway between two closely-spaced microphones is given by

$$\hat{p}(r,t) = \tfrac{1}{2}[p(r_1,t) + p(r_2,t)]$$

$$= \frac{1}{2}[p_1(t) + p_2(t)] \quad . \tag{3.7}$$

These expressions for the acoustic pressure (3.7) and particle velocity via the pressure gradient (3.6) can be substituted into the equation for radial acoustic intensity (2.2), resulting in an intensity estimation of the form

$$\hat{I}_r = -\frac{1}{\rho \Delta r} \langle \hat{p}(r,t) \int_{-\infty}^{t} [p_2(t_1) - p_1(t_1)] dt_1 \rangle \tag{3.8}$$

and

$$\hat{I}_r = -\frac{1}{2\,\rho \Delta r} \langle [p_1(t) + p_2(t)] \int_{-\infty}^{t} [p_2(t_1) - p_1(t_1)] dt_1 \rangle \quad . \tag{3.9}$$

The intensity meter using the pressure-sum pressure-difference principle was developed based on the Equations 3.8 and 3.9, but no additional details of this particular device will be discused. Further information in the literature pertaining to this specific subject can be obtained in other references (26,33).

3.2 Development of the Cross-Spectral Intensity

The formulation of the cross-spectral acoustic intensity method has been developed extensively in the literature by Fahy (24,26), Chung (11,13), Jacobsen (33), Okubo (42), and Reinhart (52). All of their respective mathematical formulations associated with the cross-spectral intensity technique are derived by slightly different, but all valid, procedures. Therefore, an indifferent approach to the development of the cross-spectral intensity method will be accomplished which will be theoretically equal to the others.

Beginning by substituting the general expression

$$z(t) = \int_{-\infty}^{t} p(t_1)dt_1 \tag{3.10}$$

into the acoustic intensity estimation (Equation 3.9) developed in Section 3.1, the estimated intensity can be rewritten as

$$\hat{I}_r = -\{\langle p_1(t)z_2(t)\rangle + \langle p_2(t)z_2(t)\rangle - \langle p_1(t)z_1(t)\rangle - \langle p_2(t)z_1(t)\rangle\}/_{2\rho\Delta r}. \tag{3.11}$$

The cross-correlation function between the two general random processes x(t) and y(t) is defined as

$$R_{xy}(\tau) = \langle x(t)y(t+\tau)\rangle$$

$$= \frac{1}{2\pi}\int_{-\infty}^{\infty} S_{xy}(\omega)e^{j\omega\tau}d\omega \ , \tag{3.12}$$

where $S_{xy}(\omega)$ is the cross-spectral density function between the two processes x(t) and y(t).

If it is assumed that $\tau = 0$, which would be true if there is no time delay between the two closely-spaced microphone receivers, then the general cross-correlation kernel (Equation 3.12) can be expressed as

$$R_{xy}(0) = \langle x(t)y(t)\rangle$$

$$= \frac{1}{2\pi}\int_{-\infty}^{\infty} S_{xy}(\omega)d\omega \ . \tag{3.13}$$

The resulting expression for acoustic intensity (3.11), using the general cross-correlation function between x(t) and y(t), becomes

$$\hat{I}_r = -\{R_{p_1z_2}(0) + R_{p_2z_2}(0) - R_{p_1z_1}(0) - R_{p_2z_1}(0)\}/_{2\rho\Delta r} \ , \tag{3.14}$$

where $R_{p_1z_2}$, $R_{p_2z_1}$ are the respective cross-correlation functions and $R_{p_1z_1}$, $R_{p_2z_2}$ the respective auto-correlation functions between $p_1(t)$, $z_1(t)$, $p_2(t)$, and $z_2(t)$.

Taking the Fourier transform of the general expression (Equation 3.10) for $z(t)$,[1] it follows that

$$S_{xz}(\omega) = \frac{1}{j\omega} S_{xy}(\omega) \ . \tag{3.15}$$

Using the corresponding cross-spectral density functions for $R_{p_1z_2}$, $R_{p_2z_1}$ and the corresponding auto-spectral density functions for $R_{p_1z_1}$, $R_{p_2z_2}$; the estimated acoustic intensity (Equation 3.14) can be represented as

$$\begin{aligned} \hat{I}_r &= \int_{-\infty}^{-\infty} \hat{I}_r(\omega) \cdot d\omega \\ &= \frac{-1}{2\rho\Delta r} \int_{-\infty}^{-\infty} \{S_{p_1p_2}(\omega) + S_{p_2}(\omega) - S_{p_1}(\omega) - S_{p_2p_1}(\omega)\}/_{j\omega} \cdot d\omega \end{aligned} \tag{3.16}$$

and rewritten as

$$\hat{I}_r(\omega) = -\{S_{p_1p_2}(\omega) + S_{p_2}(\omega) - S_{p_1}(\omega) - S_{p_2p_1}(\omega)\}/_{2j\omega\rho\Delta r} \ . \tag{3.17}$$

Since $p_1(t)$ and $p_2(t)$ are real functions, then

$$S_{p_1p_2}(\omega) = S^*_{p_2p_1}(\omega) \ . \tag{3.18}$$

Using the mathematical manipulation of

$$(A - A^*) = 2j\mathrm{Im}\ A \ ,$$

the intensity estimation is then expressed as

$$\hat{I}_r(\omega) = -[S_{p_2}(\omega) - S_{p_1}(\omega) + j2\mathrm{Im}\{S_{p_2p_1}(\omega)\}]/_{2j\omega\rho\Delta r} \ . \tag{3.19}$$

---

[1] this will be true if the transforms do indeed exists and $S(\omega)/_{\omega}$ is bounded at $\omega = 0$.

The intensity estimate will consist of the real part related to the in-phase component of pressure and particle velocity,

$$\mathrm{Re}\{\hat{I}_r(\omega)\} = -\mathrm{Im}\{S_{p_2p_1}(\omega)\}/_{\omega\rho\Delta r} , \tag{3.20}$$

and an imaginary part, expressing the product of the out-of-phase components called the reactive intensity,

$$\mathrm{Im}\{\hat{I}_r(\omega)\} = \hat{I}_{IM}(\omega) = \{S_{p_2}(\omega) - S_{p_1}(\omega)\}/_{2\omega\rho\Delta r} . \tag{3.21}$$

For practical applications, the measurement of the acoustic intensity using Equations 3.20 and 3.21 will be performed by a real-time FFT spectral analyzer. Therefore, the one-sided cross-spectral and auto-spectral density functions will be more appertainable and are related to the two-sided cross-spectral and auto-spectral densities (4) as

$$2S_{p_1p_2}(\omega) = G_{p_1p_2}(\omega) = G_{12}(\omega) \tag{3.22}$$

$$2S_{p_1p_1}(\omega) = G_{p_1p_1}(\omega) = G_{11}(\omega) \tag{3.23}$$

The one-sided cross-spectral density can now be placed into the real intensity estimation (Equation 3.20) to form the expresssion

$$\hat{I}_r(f) = -\mathrm{Im}[G_{12}(f)]/_{4\pi f\rho\Delta r} , \tag{3.24}$$

which shows the estimated real acoustic intensity as a function of the imaginary part of the cross-spectrum between two closely-spaced microphone receivers, and if $G_{12}(f)$ is converted for rms quantities, the intensity expression will be

$$\hat{I}_r(f) = -\mathrm{Im}[G_{12}(f)]/_{2\pi f\rho\Delta r} . \tag{3.25}$$

3.3 Implementating the Technique

Basically, the cross-spectral intensity technique requires two measuring microphones of any type, their associated electronics (cathode followers, power supplies, pre-ammplifiers, and optional filters), a Fourier dual-channel spectral analyzer to perform the cross-spectral operation, and a computer system to collect and manipulate the cross-spectral data into intensity form (unless a programmable spectral analyzer is used). The measuring instrumentation must have good stability characteristics to retain circumscribed amplitude and phase factors, a wide dynamic range to give an acceptable signal-to-noise ratio, and a broad frequency response to provide a sufficient spectral bandwidth for the measurements. In addition, the two measuring microphones must have small physical dimensions (the microphones can then be closely spaced) and should have omnidirectional responses. All of these requirements are necessary to assure precision of the intensity measurements.

The actual implementation of the intensity technique with the equipment mentioned can be an arduous and non-trivial task. Many practical problems must be resolved before the cross-spectral intensity theory can be experimentally applied. Therefore, the following sections describe in detail the physical setup of the system, the developmental software for data processing, and the calibration of the intensity measurement technique utilized in this work.

3.3.1 The Physical Setup

The instrumentation system used to implement the cross-spectral intensity technique is diagramed in Figure 3.1. The pressure measuring system consists of either a randomly-selected pair of Bruel & Kjaer (B&K) 1/2" microphones (model 4133) or a pair of specially-chosen "phase-matched" B&K 1/4" microphones (model 4135) and their necessary electronics; B&K cathode followers (model 2619) and a B&K two-channel power supply (model 2807). The electrical signals representing the measured sound pressure were amplified by Ithaco pre-amplifiers (model 453) and optionally filtered by coupled Ithaco filters (model 4113). The two amplified signals were then processed by a Spectral Dynamics SD360 dual-channel spectral analyzer consisting of an analog-to-digital (A/D) converter, an X-Y display unit, and the FFT processor. All of the processed cross-spectral data from the spectral analyzer were stored in a DEC (Digital Electronics Company) PDP-11/34 computer system with help from a software package provided by Spectral Dynamics, the Annotated Graphics Package (AGP). This cross-spectral information could then be manipulated into acoustic intensity data by other Fortran software developed by the author and later displayed on a CRT graphrics terminal (Tektronix 40006-1) or plotted on a digital plotter (Tektronix 4662).

The intensity probe used for all measurements, consisting of either the 1/2" or 1/4" microphone pair and the device to hold the two microphones, is shown in Figure 3.2. Typically, the two cylindrically-shaped microphones were placed in parallel with their respective membranes in one plane. The microphone holder was a small rectangular aluminum "block" (25x28x76 mm) with two adjustable microphone mounting

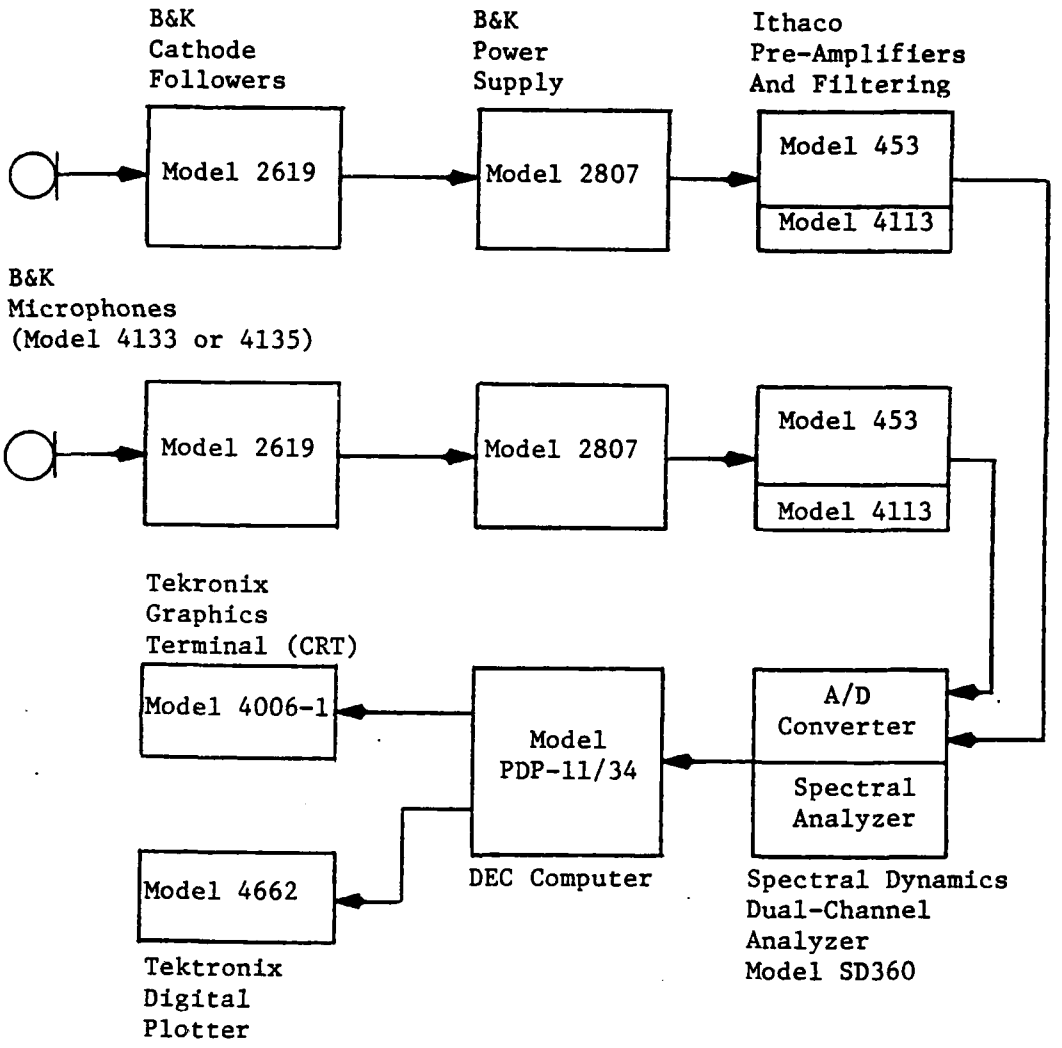

Figure 3.1: Instrumentation Used to Implement the Cross-Spectral Intensity Technique

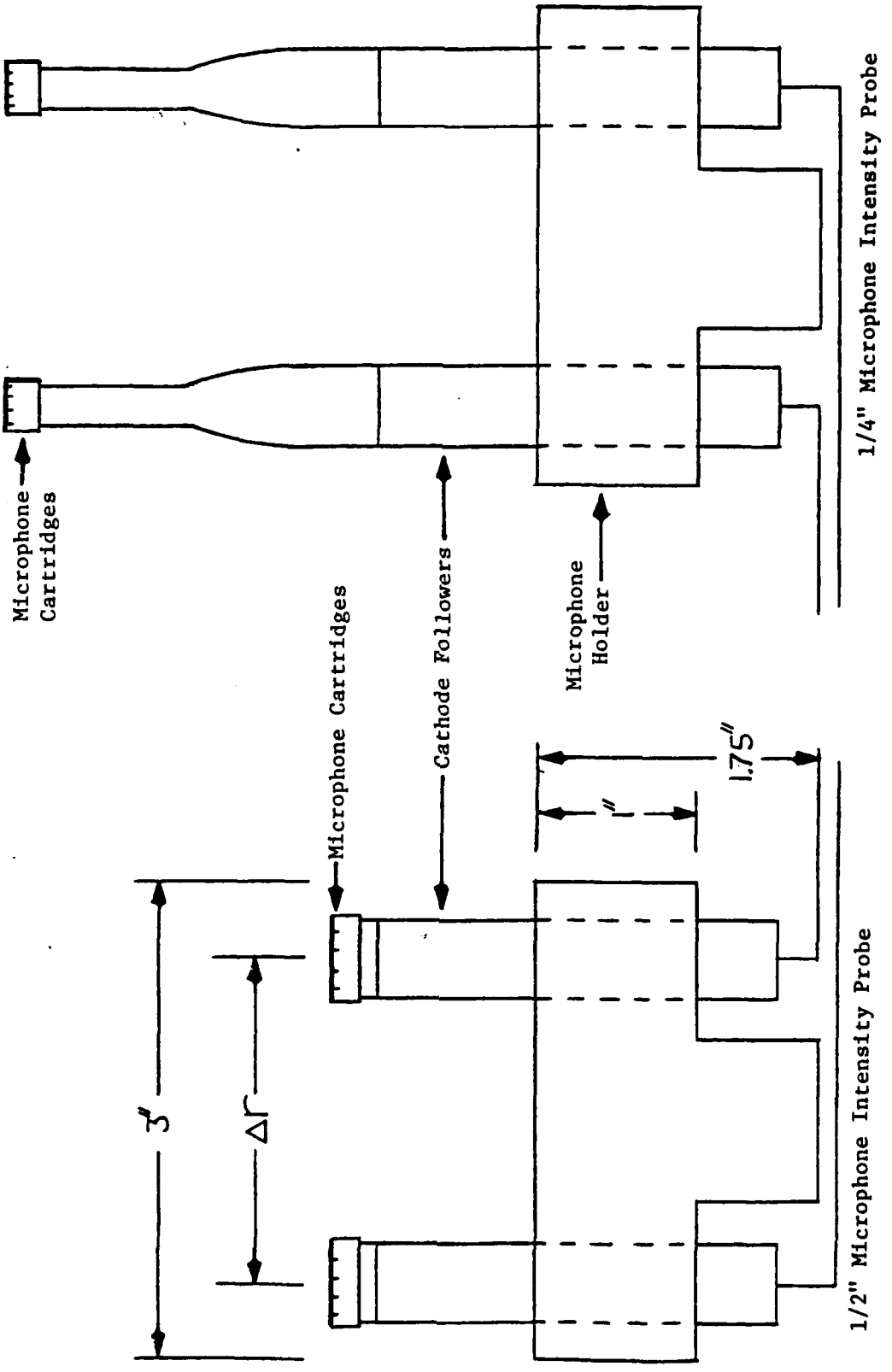

Figure 3.2: Two-Microphone Acoustic Intensity Probe

brackets for variability of the microphone separation distance. This two-microphone configuration is probably the most practical and most commonly used arrangement to date because these high quality microphones are physically easy to mount and are usually available in a noise control laboratory.

Other more complicated microphone configurations are used for acoustic intensity and power flow measurements by various people (1,33,49). The Bruel & Kjaer Company even provide their own version of the intensity probe (51) with the B&K Sound Intensity Analysing System (Type 3360).

3.3.2 Processing the Cross-Spectral Data

Developing the method of measuring acoustic intensity from the cross-spectrum between two microphone receivers requires transferring the cross-spectral data from the SD360 spectral analyzer to the computer, storing the data in the computer, and manipulating this collected data with the computer. Spectral Dynamics does provide a basic graphics program, the Annotated Graphics Package (AGP), which supplies the system operator of the DEC PDP-11/34 computer the capability to remotely program and execute all the SD360 spectral analyzer hardwired functions. The AGP software gives the operator the ability to transfer the cross-spectral data (prospective intensity data) or any data from the specified functions (mathematical operations) of the analyzer to the DEC computer for storage and plotting.

The limitations of the AGP software is two-fold: only twenty-five individual data files can be stored at one time and most important, the

raw cross-spectral data which have been stored cannot easily be retrived for further processing into the intensity data of interest. Therefore, it was necessary to locate or develop additional software which would give the operator the ability to access the raw cross-spectral data that have been transferred from the SD360 spectral analyzer (via the annotated graphics program).

At first, it was thought that this additional software could be easily acquirred from the software-developing personnel at Spectral Dynamics or another facility requiring similar operation of the same equipment. After a lengthy time period of searching without success for the needed software, the software was finally developed by a hired programing specialists (Lynn Rothrock) and a fellow graduate student (Gary Elko).

To develop this additional data acquisition software, the complete source listing of the AGP software was required. From this AGP source listing, the specific file name (DSPDAT.DAT) containing the processed data words from the spectral analyzer was located. Then these data files of the AGP could be opened for direct access of the twenty-five stored data files. This gives the operator the capability of recording a large number of individual data blocks onto the computer as easily excessable file names for further processing, independent of the AGP. It should be also noted that the individual data words which represent measured data values from a specified function (mathematical operation) of the spectral analyzer are represented as ascending linear numbers. This fact will be useful in the development of the calibration technique used in the acoustic intensity process (Section 3.3.3).

3.3.3 Calibration

Acoustic intensity must be calibrated to a known reference source before absolute intensity levels can be measured in an acoustic environment. All acoustic intensity calculations were performed with the aid of the SD360 spectral analyzer, the AGP software on a DEC computer, and the additional processing software mentioned earlier (Section 3.3.2). The calibration of acoustic intensity then could be accomplished by understanding the format representing the data received from the spectral analyzer. The output data from the mathematical operation 'Forward Transform' of the analyzer were received as 1024 data words with the first 512 data words representing the sound pressure spectrum (the autospectrum). The output data from the mathematical operation 'Cross-Spectrum' were received also as 1024 data words in which the last 512 data words represent the imaginary part of the cross-spectrum. All the output data words (either forward transform or the cross-spectrum) were represented by ascending linear scaled numbers which relate to but were not equilvalent to the numerical values (dB or linear) exhibited on the spectral analyzer's LED display control. Therefore, the logical approach for calibration of a sound source would be to place a known absolute signal into the spectral analyzer and receive an absolute output linear value in which all other output linear amplitude values will be relative to.

A pistonphone sound source and a calibrated sound level meter were the two choices when calibrating absolute sound pressure levels The pistonphone's sound pressure level was found to be somewhat unstable, and the frequency of the pistonphone's sound pressure amplitude varied

slightly with individual microphones.[2] One also must be concerned with the inaccuracies introduced by the resolution bandwidth of the spectral analyzer whereby minimum errors occur when the resonance frequency coincides with the band centre frequency (63). Therefore, it was decided to use a precision sound level meter to calibrate the equipment. Locating the microphone of the sound level meter in the direct field of a smooth stationary sound source, a flat diaphragm mid-range loudspeaker from Technics (53), a known arbitrary sound pressure from a stable pure tone input (stable in both amplitude and frequency) at 1200 Hz was used as the absolute input signal to the spectral analyzer. The linear output value processed from the analyzer and representing this absolute sound pressure input signal could then be used to scale all other linear output values from any arbitary sound pressure level.

For calibrating the two-microphone cross-spectral acoustic intensity, both microphones were adjusted for equal output response to the same sound pressure input. The free-field acoustic intensity at the midpoint between the two microphone receivers could therefore be estimated from knowing the absolute sound pressure level at each respective microphone location. Placing the two-microphone intensity probe at the exact location that was used to calibrate the sound pressure level, the cross-spectral measurement was performed using the same 1200 Hz pure tone. The linear output value representing this absolute sound intensity (from the cross-spectrum) could then be used to

---

[2] the B&K pistonphone is rated at 124 dB ($\pm$0.2 dB) at a calibrated frequency of 250 Hz. The pistonphone's frequency used for these measurements varied between 246 Hz and 247 Hz.

scale all other linear output values representing any arbitary sound intensity level.

It was necessary to choose the reference frequency value of the pure tone input signal at a high enough value whereby any phase mismatch between two microphones would not bias the absolute intensity approximation (discussed in Chapter 5). Also, a low enough reference frequency value was choosen to prevent any significant bias error due to the finite-difference approximation between two microphones (discussed in Chapter 4). Because of these two factors, the pure tone of 1200 Hz was used as the reference input signal for calibration of acoustic intensity.

3.4 Directional Characteristics

The two-microphone acoustic intensity device is considered to be a sound receiver of the first-order[3], which results when two receivers of the zero-order, having the same sensitivity, are placed a distance Δr apart in space, so that the voltage produced is proportional to the pressure difference (p_2-p_1) where p_1 and p_2 are the pressures acting on each of the zero-order receivers. The microphone separation distance of Δr will only be realized if the propagating wavefront of sound flows perpendicular to an imaginary line connecting the two closely-spaced microphones. For the other directions of an incident wave, this

---

[3] a zero-order (omni-directional) receiver is an electroacoustic transducer which transforms an incident sound wave into a voltage approximately proportional to one of the parameters of the incident acoustic wave, such as sound pressure (37).

imaginary line connecting the points 1 and 2 of the corresponding microphone pressures p_1 and p_2 actually makes an angle θ with the direction of sound-wave propagation (see Figure 3.3, the normalized linear and logarithmic directional responses). Therefore, the centerpoints of the microphone diaphragms are separated by a distance $\Delta r\cos\theta$ in the direction of the propagation of an incident sound wave, and this gives precisely the cosine dependence upon the angle of incidence which is characteristic of the pressure gradient and consequently the two-microphone intensity device.

Because the acoustic intensity device is a directional microphone, this first-order sound measuring meter will have a definite advantage over the zero-order receiver when measuring a noise source in-situ. Where the omni-directional microphone would be influenced significantly by the reactive sound field, by other secondary (contaminating) sound sources, and the reverberant field; the two-microphone intensity device should be better capable of measuring only the energy flux transmitted (the active sound field) while rejecting, for the most part, any contamination from secondary sources and the reactive sound field. Note also that the sensitivity of the velocity function at $\theta=180^{o}$ of the first-order receiver is the same as the velocity function at $\theta=0^{o}$ but opposite in sign. Therefore, this intensity measurement technique can thus be able to delineate and quantify the real energy flow and the direction of the energy flow.

It may be useful to have a more pronounced directional

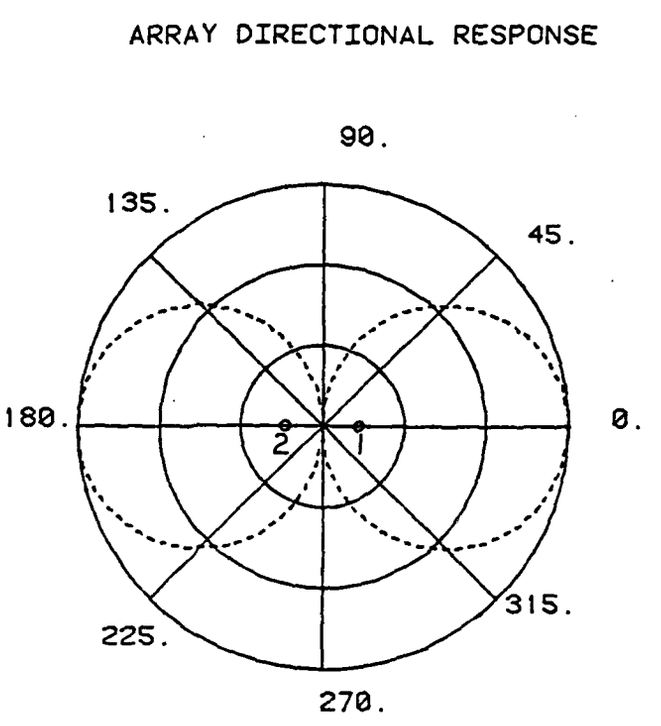

Figure 3.3(a): The Normalized Linear Directional Response of the Two-Microphone Acoustic Intensity Device

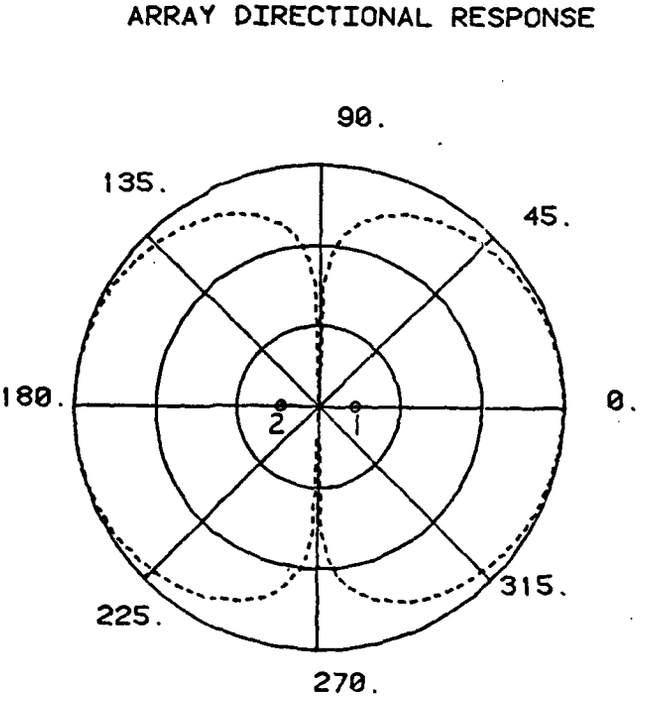

Figure 3.3(b): The Normalized Log Directional Response of the Two-Microphone Acoustic Intensity Device

characteristic for the acoustic intensity device. A second-order receiver[4] consisting of four equally and closely-spaced zero-order receivers will have a directional characteristic (as related to the pressure gradient) which is proportional to $\cos^2\theta$ where θ is an angle the propagating sound-wave makes with an imaginary line connecting the points 1,2,3,4 of the corresponding microphone pressures (see Figure 3.4, the normalized linear and logarithmic directional characteristics in a plane containing the acoustic axis of the receiver). It is then apparent that compared with first-order receivers, the second-order receivers show a more pronounced directional effect. It is of interest to note that for $\theta=180^\circ$, the sensitivity of the velocity function is the same as for $\theta=0^\circ$ ($\cos^2(\pm\theta)$ always has a positive value). Therefore, the second-order receiver, in contrast to the first-order receiver and as far as the phase of the output voltage is concerned, does not distinguish between the sound waves coming from the front or from the rear.

It should be noted that the theory for the directional characteristics of the first and second-order receivers was derived under the assumption that the receiver is a point body, and will only be approximately true in practice if the dimensions of the receiver are considerably smaller than the wavelength of sound in the medium in which the receivers are placed. Also, for the first-order and second-order receivers to have the directional properties shown in Figures 3.3 and 3.4, the zero-order receivers that comprise these higher-order receivers

---

[4] a second-order receiver will result if two first-order receivers are connected so that the difference of their output is obtained (37).

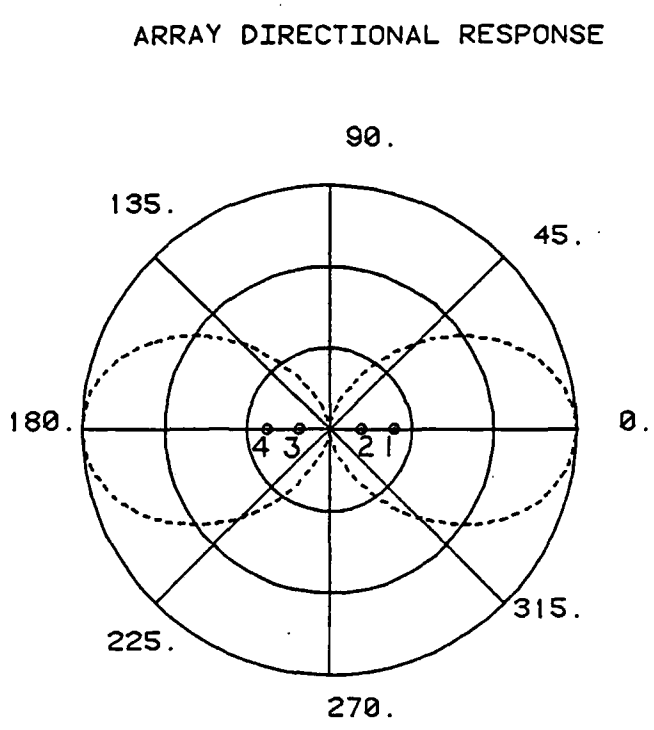

Figure 3.4(a): The Normalized Linear Directional Response of a Second-Order Microphone Receiver

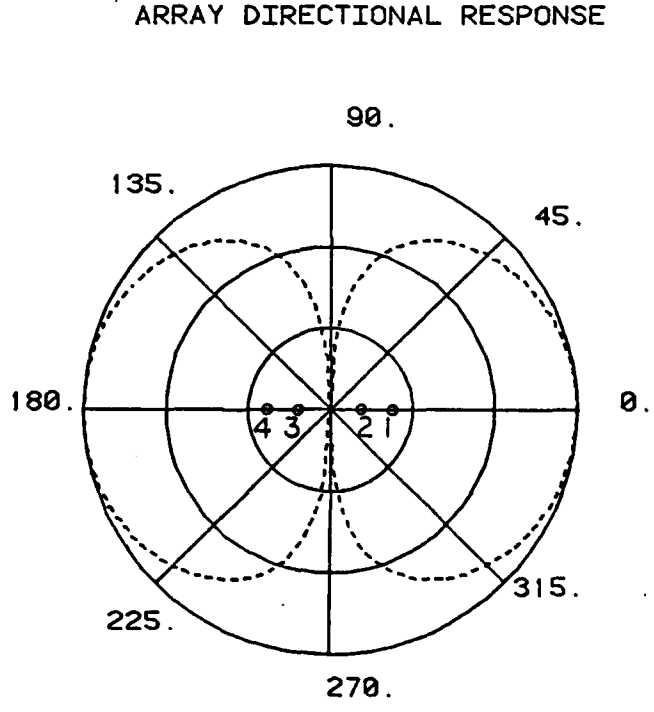

Figure 3.4(b): The Normalized Log Directional Response of a Second-Order Microphone Receiver

must have omni-directional characteristics over the measurement frequencies of interest.

3.5 The Testing Environment

The estimation of the acoustic intensity of a specific source developed in Sections 3.1 and 3.2 fails to accurately describe the acoustic intensity through the measurement point if there is the presence of a strong reverberant field or a significant amount of background noise.

The cross-spectral intensity data of a specific sound source in-situ may be influenced by secondary acoustic sources (background noise), especially if there are a number of contaiminating sources and their sound levels are similar to or greater than that of the primary sound source. Also, the reverberant acoustic field of the measuring environment is yet another detriment of the intensity measurements because the estimation of the pressure and pressure gradient by two separate pressure measurements can not accurately specify the sound field.[5] In the case where there is the presence of a reactive intensity component (in the very nearfield of the source), the resulting intensity expression involves not only the imaginary part of the cross-spectral density but also the difference between the autospectrums of the two microphones (41).

---

[5] note that in a perfectly diffused reverberant field, there would be equal probability of energy flow in all directions, and the acoustic intensity would be theoretically zero (32).

It is clearly advantageous to locate the enclosing measurement surface in the direct field of the sound source away from sound reflectors and secondary acoustic sources. Therefore, a free-field acoustic environment (an anechoic room) would be the most suitable location to investigate other errors of the cross-spectral intensity method which are unrelated to errors from the complex measuring environment (errors of the intensity technique from the reverberant field and secondary sources are separately discussed in greater detail in Chapter 7).

3.6 The Test Facility Used

All the equipment necessary for these acoustic intensity measurements was located in a quiet work area of The Applied Research Laboratory. Therefore, it was predicted that this laboratory room could be suitable for the intensity measurements, and an anechoic room (a free-field acoustic environment where one can assume little interference from sound reflections and background noise) would not have to be used.

The room constants (representing the room's absorbing power) and corresponding critical distances (the distance from a sound source one must be to assure that the direct field predominates) were calculated from reverberation time measurements (T_{60}) in order to understand the acoustical characteristics of the test area used for the intensity measurements (Figure 3.5(a)). The laboratory room (dimensions shown in Figure 3.5(b)) was found to be a rather low-reverberant room in which intensity measurements in the direct field of a sound source could be accomplished without interference from the reverberant field or

No.	T_{60} (Ave.)	1/3 Octave Frequency	Room Constant	Critical Distance	Q
1)	1.02 sec.	80 Hz	550.3	3.31 ft.	1
2)	.75 sec.	125 Hz	748.5	3.86 ft.	1
3)	.56 sec.	250 Hz	1002.4	4.47 ft.	1
4)	.51 sec.	500 Hz	1100.7	4.68 ft.	1
5)	.46 sec.	1000 Hz	1220.3	4.93 ft.	1
6)	.46 sec.	2000 Hz	1220.3	4.93 ft.	1
7)	.42 sec.	4000 Hz	1336.5	5.16 ft.	1

Figure 3.5(a): Acoustical Characteristics of the Laboratory Room Used for the Acoustic Intensity Measurements

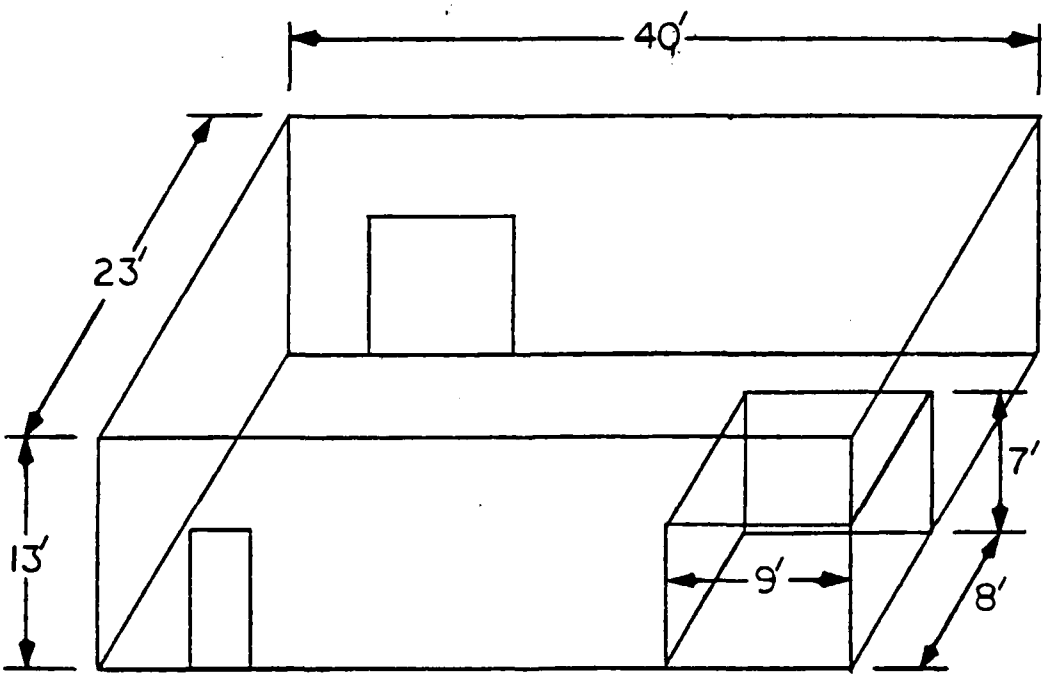

Figure 3.5(b): Physical Dimensions of the Laboratory Room Used for the Acoustic Intensity Measurements

nearfield. The background noise in the room was somewhat significant but still acceptable for these measurements. Therefore, all of the acoustic intensity testing was conducted in the forementioned laboratory room with the two-microphone probe arranged normal and on-axis to the primary sound source at a distance which was in the direct field but not near any significant sound reflectors (except in the case when results in the reverberant field or with reflectors were done purposely).

3.7 Statistical Errors of the Technique Employed

The errors of the cross-spectral intensity method can be classified statistically as both bias and random errors (where acoustic intensity is a random process). The random (variance) errors are a direct result of the averaging operations performed by the FFT processer with a finite number of sample records N or over a single sample record of finite length T (finite averaging time). The bias error is a systematic error that will appear with the same magnitude and in the same direction from one intensity analysis to the next.

Random errors of the cross-spectral intensity measurements have only very recently been documented by Seybert (58) and Pascal (46). Without going into the development detail, Seybert derived a first order approximation equation of the normalized standard error $\varepsilon(\hat{I})$ as

$$\varepsilon(\hat{I}) = \left(\frac{1}{n_d}\right)^{\frac{1}{2}} \left[1/\gamma_{12}^2(f) + \cot^2\phi_{12}\{1-\gamma_{12}^2(f)\}/2\gamma_{12}^2(f)\right]^{\frac{1}{2}}, \quad (3.26)$$

where n_d represents the number of data samples performed, $\gamma_{12}^2(f)$ is the coherence function between the two receivers, and $\phi_{12}(f)$ is the phase

angle between the two pressure receivers, in the direction of wave propagation, for a microphone separation distance Δr. For high-frequency measurements (large phase angles), the normalized standard error approaches the value

$$\varepsilon(\hat{I}) = [1/(n_d)\gamma_{12}^2(f)]^{\frac{1}{2}} . \qquad (3.27)$$

For low-frequency measurements (small phase angles,, the normalized standard error is dominated by the second term of equation (3.21) containing the phase angle $\phi_{12}(f)$. At high frequencies, the normalized standard error can be made sufficiently small by appropriate selection of the number of data samples (n_d). However, if the coherence is low (which can be true for measurements in the testing environment with substantial background noise and/or a strong reverberant field), the normalized standard error will be quite large. Typically, if the suggestions in Section 3.5 pertaining to the measurement of a sound source in-situ are practiced and a large amount of averaging by the FFT analyzer is used, the random error of the cross-spectral intensity method can be significantly reduced. Therefore, the bias errors are considered to be the major contributor to the deficiencies of the cross-spectral intensity technique, and these bias errors are analyzed in the remainder of this work.

CHAPTER 4

FINITE DIFFERENCE APPROXIMATION

4.1 Description of the Methodology Error

The finite-difference approximation in acoustic intensity measurements results in a systematic error associated with the approximation of the local pressure gradient and pressure by finite-sum and difference quantities as expressed by the Equations 3.5 and 3.7. The bias error due to the developmental finite-difference approximation can be expressed in terms of a Taylor series expansion of the pressure gradient and pressure about a finite distance ($\pm\frac{\Delta r}{2}$) from a reference position r midway between the two measuring microphones. Therefore, considering a pure-tone sound field, the signals from the two microphones represent the one-dimensional pressure at the positions ($r+\frac{\Delta r}{2}$) and ($r-\frac{\Delta r}{2}$) and can be expanded into a Taylor series to obtain the expressions (omitting the time function $e^{j\omega t}$)

$$p(r+\tfrac{\Delta r}{2}) = p(r) + (\tfrac{\Delta r}{2})p'(r) + \tfrac{1}{2}(\tfrac{\Delta r}{2})^2 p''(r) + \tfrac{1}{6}(\tfrac{\Delta r}{2})^3 p'''(r) + \ldots \quad (4.1)$$

and

$$p(r-\tfrac{\Delta r}{2}) = p(r) - (\tfrac{\Delta r}{2})p'(r) + \tfrac{1}{2}(\tfrac{\Delta r}{2})^2 p''(r) - \tfrac{1}{6}(\tfrac{\Delta r}{2})^3 p'''(r) + \ldots \quad (4.2)$$

whereby $p'(r)$ denotes the partial derivative $\partial p(r)/\partial r$, etc. . It follows that the pressure-sum and pressure-difference equations are redefined as

$$\tfrac{1}{2}[p(r+\tfrac{\Delta r}{2}) + (p(r-\tfrac{\Delta r}{2})] = p(r) + \tfrac{1}{8}(\Delta r)^2 p''(r) + \ldots \quad (4.3)$$

and

$$p(r+\tfrac{\Delta r}{2}) - p(r-\tfrac{\Delta r}{2}) = (\Delta r)p'(r) + \tfrac{1}{24}(\Delta r)^3 p'''(r) + \ldots \quad . \qquad (4.4)$$

Placing these pressure-sum and difference expressions (4.3 and 4.4) into the estimated intensity equation developed in Chapter 3 (3.9) and using the exact expression for the acoustic intensity (2.7), the fractional error of an intensity approximation can be expressed as[1]

$$\hat{I}_r(r) = I_r(r) - \mathrm{Im}[p^*(r)p'''(r) + 3p'(r)(p''(r))^* + \\ + \text{higher-order terms}](\Delta r)^2/48\rho 2\pi f \; . \qquad (4.5)$$

It is evident that the error of the intensity estimate depends strongly on the sound field being investigated, and it is not possible to correct for the error without a rather detailed knowledge of the sound field.

Thus, the physical reason for a finite-separation error is that the second or higher-order spatial derivatives of the mathematical expansion of pressure and pressure gradient are significant and can not be ignored. Therefore, the sound field can not be accurately specified by only two separate pressure measurements. This situation can arise either because the microphone separation distance is not small compared with the acoustic wavelength of the incident sound wave, or because the microphone pair is too close to a non-idealized complex-radiating sound source.

---

[1] this Taylor series expansions for the intensity method with two-microphones is developed more thoroughly in other references (24,33,42,47), and only the final result is presented here.

Using the acoustic model of a progressive plane sound wave (pure-tone) propagating in the direction of a line joining the two microphone positions, the intensity estimate is related to the actual intensity by the expression (33)

$$\hat{I}_r = I_r[\sin(k\Delta r)/(k\Delta r)] \tag{4.6}$$

where k is the wavenumber for sound and equal to $2\pi f/c$. It is then intuitive that the greatest accuracy of the finite difference occurs with the smallest microphone separation, and the acoustic intensity is underestimated. Therefore, it should be possible to compensate for this bias error of the intensity measurement with a correction factor equilvalent to the finite-difference approximation for a finite two-microphone separation. Some of the empirical sound intensity data in this work compensates for the bias error induced by the finite-difference approximation but only as related to a simple plane-wave propagation of sound. Unfortunutely, noise sources encountered in actual in-situ measurements usually consist of more complex sound-radiation patterns which may complicate using a correction factor for realistic acoustic intensity measurements.

A very recent paper pertaining precisely to this subject of finite-difference approximation errors in acoustic intensity measurements (reference 61 with corrections in reference 23) contains theoretical development describing the errors from not only a simple point monopole source but also for the dipole and a lateral quadrupole point sources. Both the dipole and quadrupole sources have a more complicated nearfield than the single monopole whereby the radiating sound field is not purely

radial, and the reactive energy is relatively large and more concentrated near the axis. An expression similar to the plane-wave error equation (4.6) for the estimated acoustic intensity as related to the actual intensity for a point monopole source (61) is

$$\hat{I}_r = I_r[\sin(k\Delta r)/(k\Delta r)\{r^2/r_1 r_2\}] \tag{4.7}$$

$$= I_r[\sin(k\Delta r)/(k\Delta r)\{1/1-\beta^2/4\}] \tag{4.8}$$

where $\beta = \Delta r/r$ is a non-dimensional parameter, and r is the distance between the source and the measurement point with r_1, r_2 being the center distances of microphones 1 and 2, respectively, from the source.

It can now be recognized from Equation 4.8 that the measurement accuracy of a monopole source is a function of not only the microphone separation $k\Delta r$ but also the greatest possible measurement distance, $\Delta r/r$. This fact will be more substantial for the more complex sources, the dipole and lateral quadrupole. Therefore, in general, finite-difference errors are minimized by employing the smallest possible values of $k\Delta r$ and $\Delta r/r$. It is suggested (61) that the maximum value of $k\Delta r$ be approximately 0.85. It was also found that for quadrupole source measurements, there are both low-frequency and high-frequency limits to the measurement accuracy, while for the monopole and dipole sources only high-frequency limits exist. It can be stated that the high-frequency limits give an underestimation of the true acoustic intensity, and the low-frequency limits tend to produce an overestimation of the intensity. This low-frequency limitation of the intensity measurements is probably due to numerical rounding off (finite representation) of the mathematical expression used to represent the quadrupole source. For

practical cases, the low-frequency limitation is due to the presence of a reative sound field in the nearfield or caused by instrumentation errors.

There are definite optimum ranges of the measurement parameters $k\Delta r$ and $\Delta r/r$ for which the best accuracy can be achieved for intensity measurements, and this range for the optimum parameter values decreases with increasing source radiation complexity. It is suggested that the best procedure would be to select the measurement parameters base on the "worst-case" design. Therefore, for a maximum inaccuracy of ± 1.5 dB, the parameter limits of $0.1 \leq k\Delta r \leq 1.3$ and $0.0 \leq \Delta r/r \leq 0.5$ would be useful guidelines. However, if intensity measurements in the immediate vicinity of point sources are excluded, the expression for the error under plane-wave conditions and point monopole conditions gives at least a rough indication of the measurement accuracy.

In general, the finite-difference error cannot be overcome, and the only method of extending the upper frequency range of the two-microphone intensity instrument is to decrease the finite separation between the two sensors. The one drawback with this procedure is that relative phase errors between the two microphone measuring systems become much more of a factor in the lower frequencies of operation (discussed in Chapter 5). Therefore, a compromise will have to be made for sound power measurements using extended frequency ranges, whereby, it may be more useful to conduct tests using two different sets of finite-separation distances between the sensors. However, if measurements in the low-frequency spectrum are made and a large microphone separation is used, excessive proximity error could occur when measuring a complex-

radiating source. Therefore, intensity measurements would have to be made at relatively large distances from the sound source, which may not be sufficiently close to satisfy the criteria of measuring in the direct field.

4.2 Experimental Verification

Theoretical development and experimental verification of the finite-difference approximation errors have been presented rather extensively in a number of references (41,50,59). Excluding measurements in the nearfield of a sound source, most of the empirical results confirm the analytical predictions of the finite-difference errors. Therefore, only one set of data verifying the presence of the finite-difference error will be presented.

Figure 4.1(a) displays the acoustic intensity of a flat-diaphram loudspeaker measured using two different methods. Curve A of Figure 4.1(a) represents the free-field acoustic intensity of the sound source derived from the expression relating the mean-square pressure to the sound intensity (Equation 2.9). Curve B of Figure 4.1(a) shows the acoustic intensity as measured by the two-microphone cross-spectral intensity method (Equation 3.21) at the same physical location (18 cm) as the free-field intensity measurement. Then, the cross-spectral intensity was subtracted from the free-field intensity, and this difference, which represents the experimental finite-difference error, is plotted in Figure 4.1(b)(Curve A). In order to compare the empirical bias error with the analytical prediction, the theoretical finite-difference (bias) error, assuming plane-wave conditions and using the

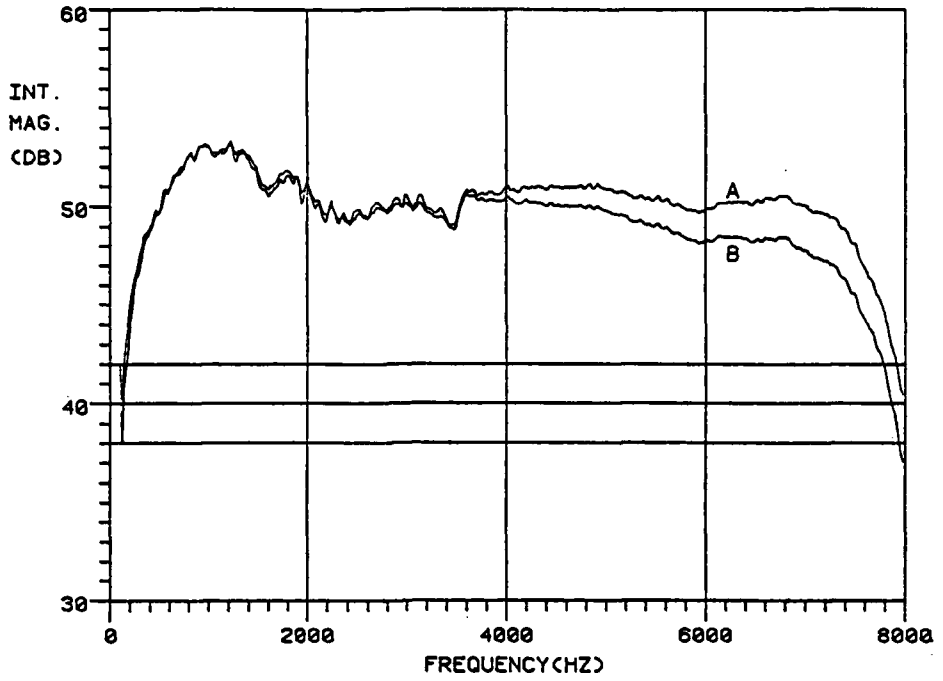

Figure 4.1(a): The Acoustic Intensity of a Flat-Diaphragm Loudspeaker
Curve A: Intensity Calculated Using Free-Field Pressure
Curve B: Intensity Measured by the Cross-Spectral Method

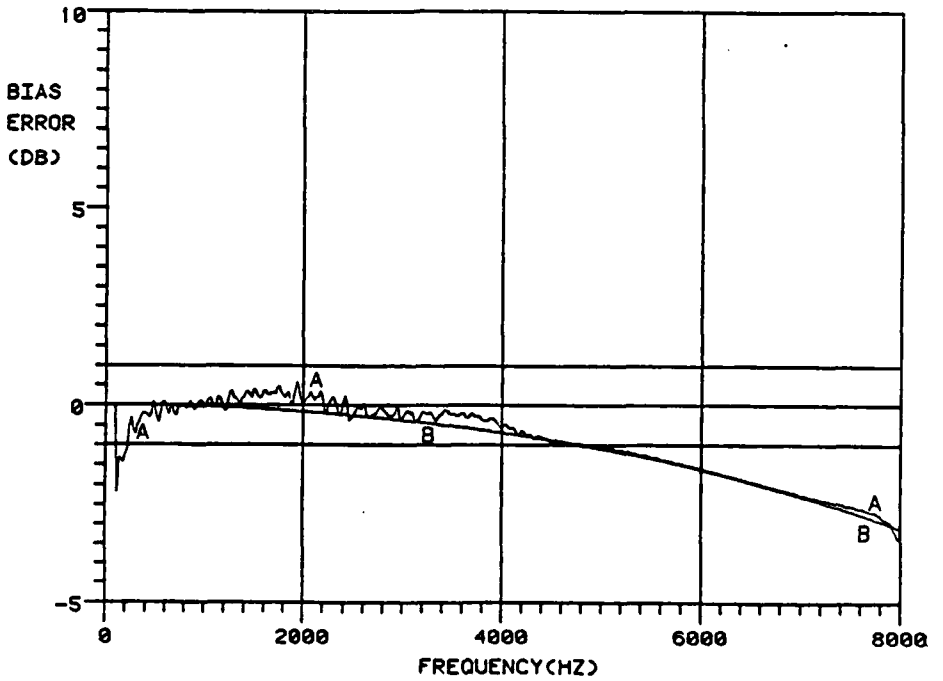

Figure 4.1(b): The Finite-Difference Bias Error Assuming Plane-Wave Conditions and Using a Flat-Diaphragm Loudspeaker
Curve A: Experimental Bias Error
Curve B: Theoretical Bias Error

same two-microphone separation distance, was calculated and is shown in Figure 4.1(b)(Curve B).

It can be noticed that there was markedly good agreement between the measured and the predicted bias error due to the finite-difference principle throughout most of the measured frequency range which indicates that the sound radiation of the source similates a plane wave and the two measuring systems were phase and gain matched (B&K 1/4" microphones where used) in the higher frequencies (above 500 Hz). The magnitude differences between the two intensity methods below 500 Hz are due to the phase mismatch between the two measuring system and background noise, and no correction for the mismatch was attempted for this particular experiment (discussed in Chapter 5).

CHAPTER 5

ERRORS DUE TO THE MEASURING INSTRUMENTATION

5.1 Phase and Gain-Mismatch Errors

It has been shown that the acoustic intensity is related to the cross-spectrum between two closely-spaced microphones (using Equation 3.24 and assuming that $\hat{I}(f) \simeq I(f)$ for $\Delta r << \lambda_{min}$) as

$$I(f) = -Im[G_{12}(f)]/_{4\pi f \rho \Delta r} , \tag{5.1}$$

where $G_{12}(f)$ is the cross-spectral density between the true complex acoustic pressures $P_1(f)$ and $P_2(f)$ (see Figure 5.1). This true cross-spectrum can be separated into real and imaginary components as[1]

$$G_{12}(f) = C_{12}(f) - jQ_{12}(f)$$

$$= |G_{12}(f)|\cos\phi_{12}(f) - j|G_{12}(f)|\sin\phi_{12}(f) , \tag{5.2}$$

where $\phi_{12}(f)$ is the actual phase delay (phase shift) between the true acoustic pressures, in the direction of wave propagation, for a microphone separation distance Δr, and $|G_{12}(f)|$ is the magnitude of the cross-spectrum. The magnitude $|G_{12}(f)|$ and the angle $\phi_{12}(f)$ are related to $C_{12}(f)$ and $Q_{12}(f)$ by

$$|G_{12}(f)| = [C_{12}^2(f) + Q_{12}^2(f)]^{\frac{1}{2}}$$

---

[1] the real part, $C_{12}(f)$, is called the coincident spectral density function, and the imaginary part, $Q_{12}(f)$, is called the quadrature spectral density function.

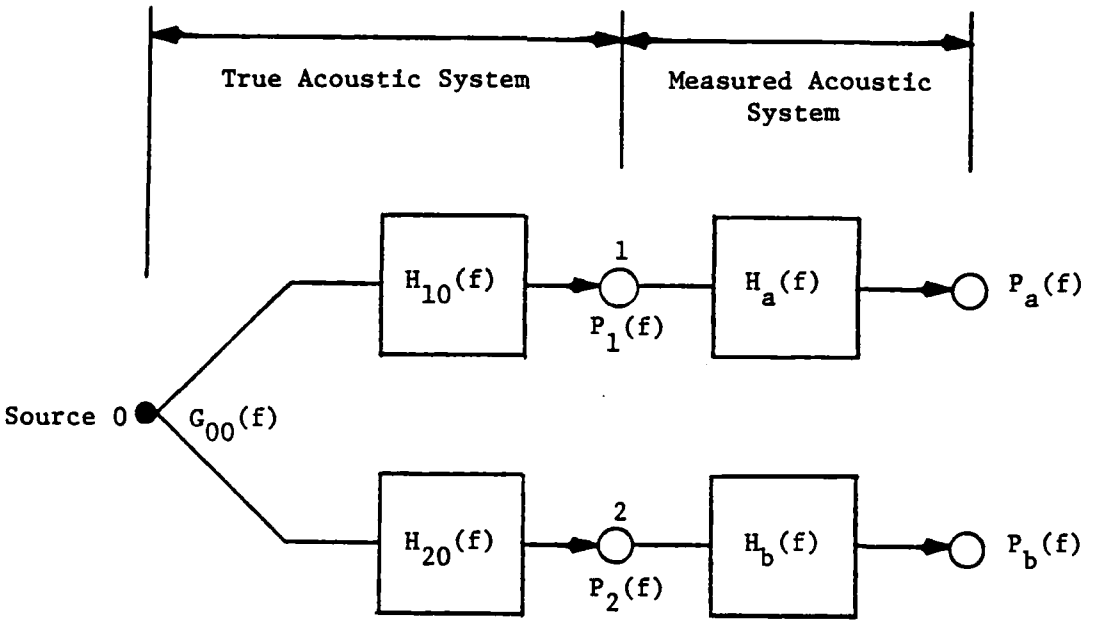

Figure 5.1: Schematic Representation of the Idealized Acoustic Intensity Measurement Using Only One Sound Source

$$\phi_{12}(f) = \tan^{-1}[Q_{12}(f)/C_{12}(f)] .$$

It can be realized that the true acoustic pressures $P_1(f)$ and $P_2(f)$ cannot be measured directly but must be represented by the measured acoustic pressures $P_a(f)$ and $P_b(f)$ via instrumentation. The measuring instrumentation (microphones, cathode followers, power supplys, pre-amplifiers, and the FFT analyzer) can often cause a significant phase and gain mismatch between the two microphone measuring systems which will in turn induce errors in the measurement of the true acoustic pressures $P_1(f)$ and $P_2(f)$. Because the microphone separation distance Δr is very small, the imaginary part of the true cross-spectrum $G_{12}(f)$ will have a very small imaginary component, and even small errors in the measuring system may bias the acoustic intensity measurement. Therefore, the measurement of the true cross-spectrum $G_{12}(f)$ will only be an estimated cross-spectrum $\hat{G}_{ab}(f)$ between the measured pressures $P_a(f)$ and $P_b(f)$ which includes any phase and gain mismatch between the two microphone channels. The estimated acoustic intensity can now be written (from Equation 5.1) as

$$\hat{I}(f) = -\text{Im}[\hat{G}_{ab}(f)]/4\pi f\rho\Delta r , \tag{5.3}$$

where the estimated cross-spectral density $\hat{G}_{ab}(f)$ is related to the true cross-spectral density $G_{12}(f)$ by the two input/two output relationship (4)

$$\hat{G}_{ab}(f) = H_a^*(f)H_b(f)G_{12}(f) . \tag{5.4}$$

This estimated cross-spectrum $\hat{G}_{ab}(f)$ can be further defined by imaginary and real components as

$$\hat{G}_{ab}(f) = |\hat{G}_{ab}(f)|\cos\hat{\phi}_{ab}(f) - j|\hat{G}_{ab}(f)|\sin\hat{\phi}_{ab}(f) \ , \qquad (5.5)$$

where $\hat{\phi}_{ab}(f)$ is the estimated phase delay between the measured acoustic pressures and includes any phase errors due to instrumentation.

5.2 Techniques to Correct Mismatch Errors

There are several techniques, described in the literature, to correct for errors due to the phase and gain mismatch between the two microphone measuring systems used in estimating acoustic intensity. All the existing techniques of correcting for the phase and gain-mismatch errors are developed from two basic methods; the microphone-switching approach and the calibration-transfer-function approach or a combination and compromise of both approaches.

5.2.1 The Microphone-Switching Approach

The microphone-switching approach was first developed and used in cross-spectral intensity measurements by Chung (11,12,14). Briefly described, the phase and gain-corrected cross-spectrum is obtained from the geometric mean of the measured cross-spectrum $\hat{G}_{ab}(f)$ determined with the original microphone configuration,

$$\hat{G}_{ab}(f) = H_a^*(f)H_b(f)G_{12}(f) \ , \qquad (5.6)$$

and the switched cross-spectrum $\hat{G}^s_{ab}(f)$,

$$\hat{G}^s_{ab}(f) = H_a^*(f)H_b(f)G_{21}(f) \ , \qquad (5.7)$$

determined by interchanging the two microphone sensing locations. The result, after some mathematical manipulation, will be a calibrated cross-spectrum

$$G_{12}(f)_{cal} = [\hat{G}_{ab}(f)\hat{G}^{s}_{ab}(f)]^{\frac{1}{2}}/|H_1||H_2| \tag{5.8}$$

where $|H_1|$ and $|H_2|$ are the microphone system's gain factors and are equal to one with proper calibration. The switching of the microphones can be accomplished either electrically or mechanically. If the microphone cartridges and other succeeding electronics (i.e., the cathode followers) are phase and gain matched, then the switching can be performed directly behind these phase-matched elements and therefore avoiding relocation errors associated with mechanical switching.

This method of correcting phase and gain-mismatch errors has proved to be very accurate because most nonstationary phase and gain differences between the two microphone systems can be eliminated. The microphone-switching method can be applied in most practical acoustic environments to quantify sound sources but would have difficulties if the measured sound source is nonstationary. The method does require double the number of cross-spectral measurements normally necessary for evaluating acoustic intensity, and this fact is a major disadvantage.

5.2.2 The Calibration-Transfer-Function Approach

The calibration-transfer-function approach to eliminate phase and gain-mismatch errors between the two microphone measuring systems has been mentioned in much of the literature pertaining to acoustic intensity measurements and acoustic properties of materials in duct

systems (18,33,57) and is summerized in a publication by Krishnappa (35). This technique involves careful measurement of the transfer function between the two microphone systems while the microphones are exposed to the same complex sound pressure, and using this stored information (the phase and gain differences between the microphone measuring systems) as a correction factor to calibrate all subsequent computed cross-spectral measurements.

Noting the schematic of the acoustic intensity measuring system in Figure 5.1, the transfer function obtained by a FFT analyzer between the two measuring systems is

$$H_{ab}(f) = G_{ba}(f)/G_{aa}(f) = H_b(f)G_{21}(f)/H_a(f)G_{11}(f) . \quad (5.9)$$

Assuming that the sound pressures $P_1(f)$ and $P_2(f)$ imposed on the two microphones are identical, it follows that the relative measured transfer function is

$$H_{ab}(f) = H_b(f)/H_a(f) , \quad (5.10)$$

where $H_a(f)$ and $H_b(f)$ are the complex frequency responses of each individual microphone channel representing the amplitude differences and phase shifts between the true acoustic pressures and the measured acoustic presures and defined as

$$H_a(f) = |H_a(f)|e^{-j\phi_a(f)} \quad (5.11)$$

$$H_b(f) = |H_b(f)|e^{-j\phi_b(f)} . \quad (5.12)$$

The transfer function $H_{ab}(f)$ (Equation 5.10) describes the relative phase and gain mismatch between the two microphone measuring systems and is further defined

$$H_{ab}(f) = |H_{ab}(f)|[\cos\Delta\phi_{ab}(f) - j\sin\Delta\phi_{ab}(f)] \qquad (5.13)$$

where $|H_{ab}(f)|$ and $\Delta\phi_{ab}(f)$ ($\Delta\phi_{ab} = \phi_b - \phi_a$) are the amplitude and phase differences respectively.

Substituting the relative transfer function (Equation 5.10) into the expression relating the true cross-spectrum $G_{12}(f)$ with the measured cross-spectrum $\hat{G}_{ab}(f)$ (Equation 5.4), the following calibrated cross-spectrum can be obtained after some simple mathematical manipulation:

$$G_{12}(f)_{cal} = \hat{G}_{ab}(f)/H_a^*(f)H_a(f)H_{ab}(f)$$

$$= \hat{G}_{ab}(f)/H_{ab}(f)|H_a(f)|^2 \cdot \qquad (5.14)$$

Therefore, knowing the phase and gain-mismatch errors created by the different sensitivity, response, and phase characteristics between the two microphone measuring systems and the frequency response of one of the channels provides the computer with complete information about the calibration transfer function used to eliminate these errors from the acoustic intensity estimation.

With proper calibration, the frequency response factor $|H_a(f)|^2$ will be equal to one, and consequently the expression for the true calibrated cross-spectrum (5.14) can be written

$$G_{12}(f)_{cal} = \hat{G}_{ab}(f)/H_{ab}(f) \cdot \qquad (5.15)$$

The acoustic intensity (Equation 5.1) can then be redefined using the calibrated cross-spectrum as

$$I(f) = -\mathrm{Im}\{\hat{G}_{ab}(f)/H_{ab}(f)\}/4\pi f\rho\Delta r \cdot \qquad (5.16)$$

This calibrated acoustic intensity requires one complex division and must be mathematically manipulated before using the expression in the computer program of this work as follows (from Equations 5.5 and 5.13):

$$\mathrm{Im}\{\hat{G}_{ab}(f)/H_{ab}(f)\} = [\sin\hat{\phi}_{ab}\cos\Delta\phi_{ab}-\cos\hat{\phi}_{ab}\sin\Delta\phi_{ab}]|\hat{G}_{ab}|/|H_{ab}| \qquad (5.17)$$

where $[\sin\hat{\phi}_{ab}\cos\Delta\phi_{ab}-\cos\hat{\phi}_{ab}\sin\Delta\phi_{ab}] = \sin(\hat{\phi}_{ab}-\Delta\phi_{ab})$.

As a result, the expression for the calibrated acoustic intensity (5.17) usable in a computer program containing the necessary stored information is

$$I(f) = -\{|\hat{G}_{ab}|/|H_{ab}|\}\sin(\hat{\phi}_{ab}-\Delta\phi_{ab})/4\pi f\rho\Delta r \; . \qquad (5.18)$$

This expression (5.18) shows that the phase and gain-mismatch errors, $\Delta\phi_{ab}$ and $|H_{ab}|$, are eliminated.

5.2.3 Methods to Produce the Transfer Function

The transfer-function approach to eliminate phase and gain errors between the two measuring microphone systems is a relatively simple method which does not require the double ensemble averaging time necessary for the microphone-switching approach. A duct system can be employed consisting of the measuring microphones rigidly flush-mounted at one end of the duct or tube with a sound source at the other end radiating an incident plane wave (identical complex sound pressure) upon the mounted microphones (the set-up of the plane-wave duct method is shown in Figure 5.2(a)).

It can be difficult to generate a broad-frequency-band signal with the necessary dynamic range (signal-to-noise ratio) in a duct or tube

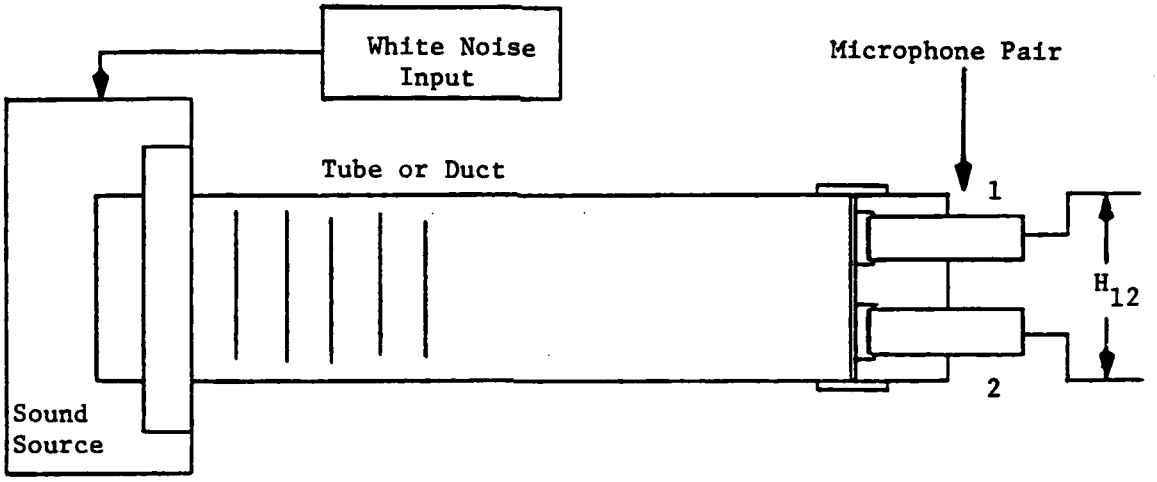

Figure 5.2(a): Plane-Wave Duct Method to Measure the Calibration-Transfer Function

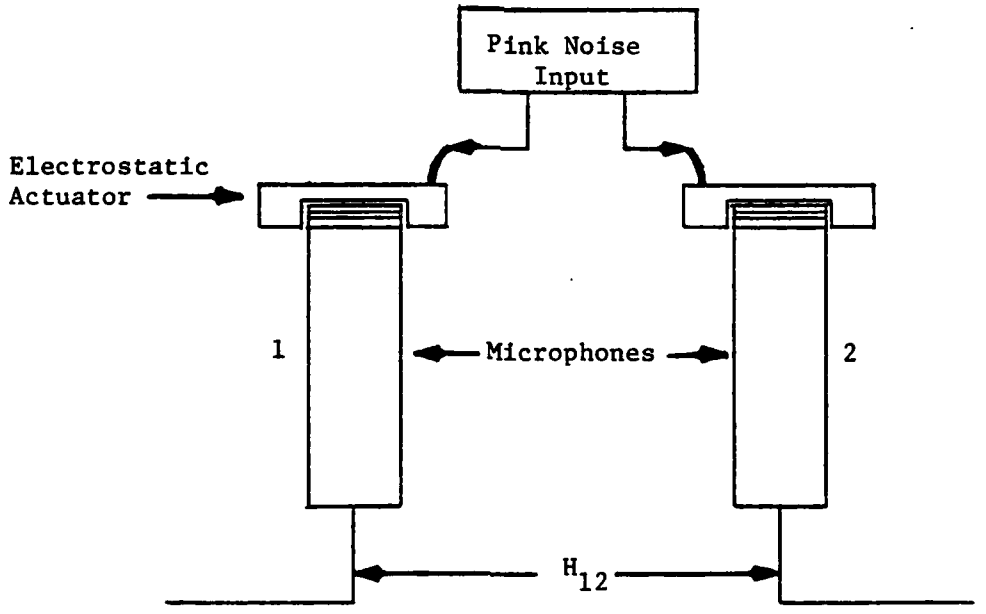

Figure 5.2(b): Dual-Electrostatic Actuator Method to Measure the Calibration-Transfer Function

because of radial modes that exist above the plane-wave cutoff frequency and difficulties in the very low-frequency radiation from a conventional loudspeaker. These problems associated with the duct system can be eliminated by using dual-electrostatic actuators to measure the calibration transfer function. This dual-actuator method uses two electrostatic actuators mounted upon the diaphragms of both microphones, and then, with the same voltage input to the actuators, the transfer function between the microphones is measured (the set-up of the dual-electrostatic actuator method is shown in Figure 5.2(b)). The electrostatic-actuator system produces a wide broad-band signal, and the dynamic range is acceptable if the measurements are accomplished in a normal, semi-quiet acoustic environment. The actuator measurements would work better in a noiseless environment (i.e., an anechoic room) because the greater the background noise level, the greater the actuator polarizing voltage must be to yield an acceptable signal-to-noise ratio. In general, the electrostatic actuator gives very good calibration results over a wide frequency range.

The plane-wave duct system used for the calibration measurements of this study consisted of a circular tube with a 1/8"-thick wall and an outside diameter of 4 inches and a total length of 11.2 feet (3.41 m). A flat-diaphragm loudspeaker was used as the radiating sound source, and aluminum end-plugs were made to hold two 1/2" microphones (shown in Figures 5.3 and 5.4). The actuator calibration of microphones was accomplished with B&K electrostatic actuators (models UA 0023 and UA 0033) and a corresponding B&K microphone calibration apparatus (model 4142). Typically, a pink-noise input gave the best dynamic range than a

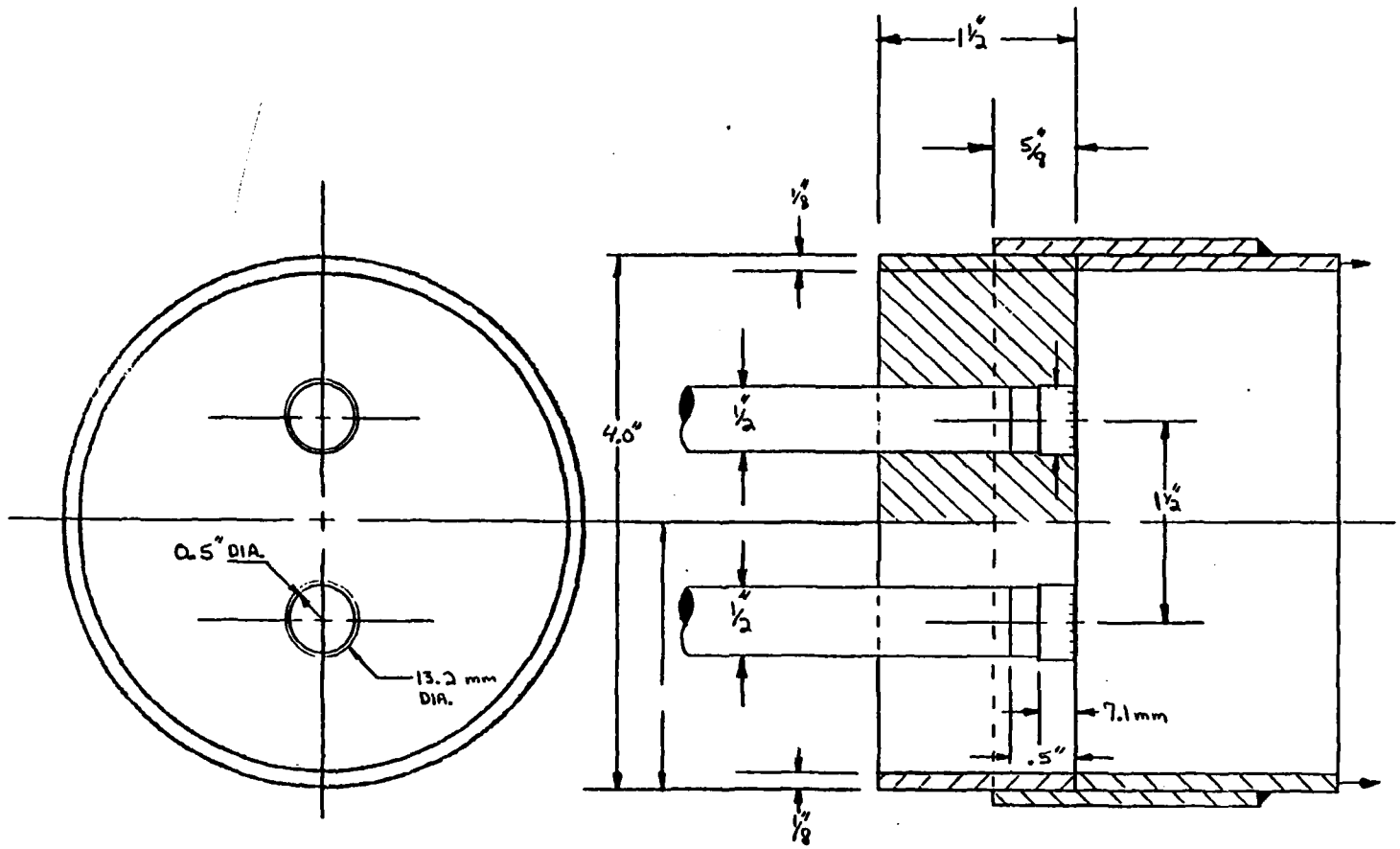

Figure 5.3: Physical Dimension of the 1/2" Microphone End-Plug Used to Hold the Microphones in the Plane-Wave Tube

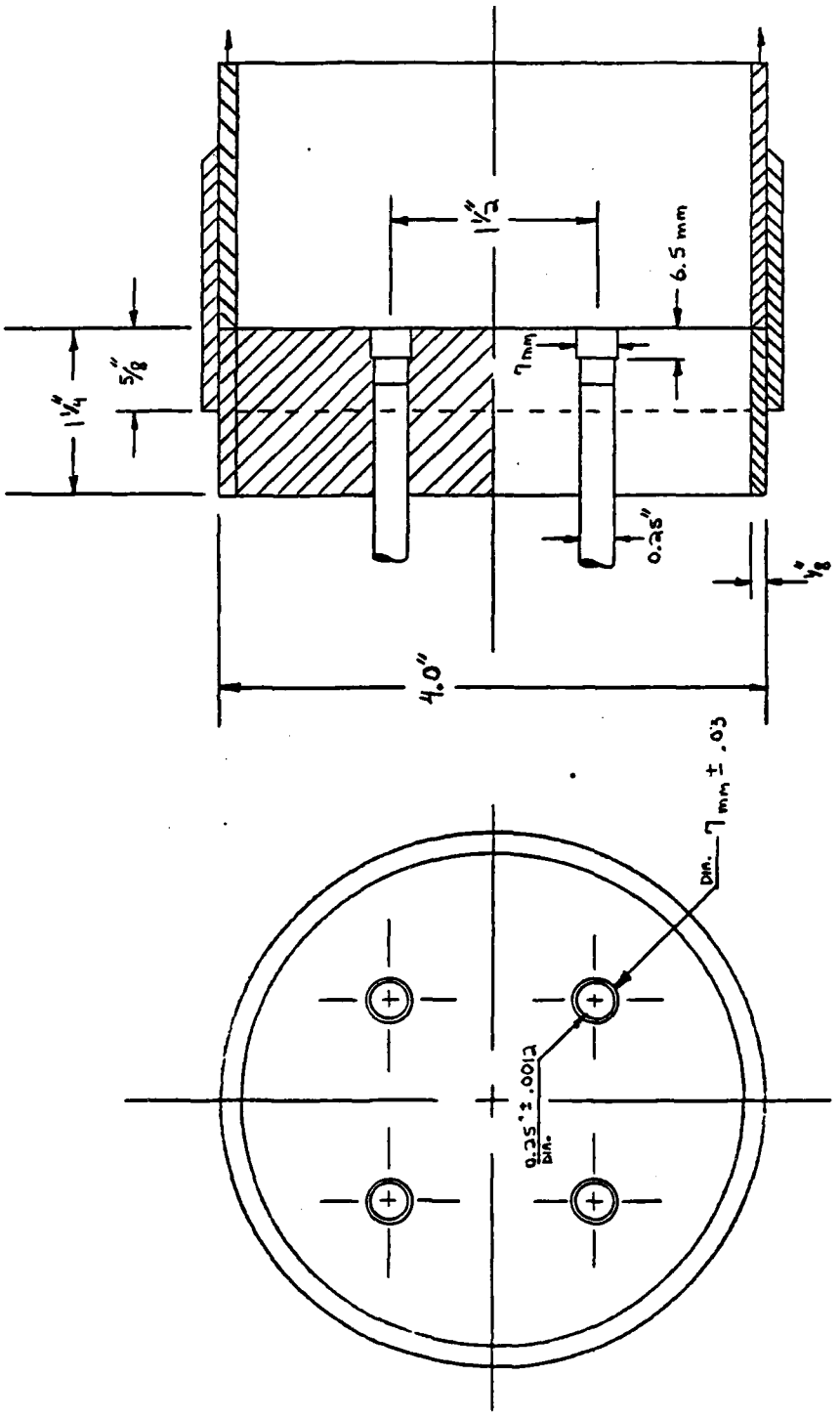

Figure 5.4: Physical Dimensions of the 1/4" Microphone End-Plug Used to Hold the Microphones in the Plane-Wave Tube

white-noise input because low-frequency noise was a problem. In general, the polarization voltages of the actuators were approximately 25 volts (rms) for the 1/2" microphones and 50 volts (rms) for the 1/4" microphones.[2]

5.3 The Normalized Bias Error

Using the idealized measurement process of Figure 5.1, the transfer functions $H_a(f)$ and $H_b(f)$ between the true complex acoustic pressures $P_1(f)$ and $P_2(f)$ and the estimated complex acoustic pressures $P_a(f)$ and $P_b(f)$ include the lumped effects of microphone gain and phase errors and the electronic magnitude and phase differences between the channels. The error in the intensity measurements due to these effects can be evaluated by using the normalized theoretical bias error of a stochastic process. Note that the effect of acoustical scattering by the intensity probe can be included in the calculation, but the bias error due to this effect will be developed in more detail in Chapter 6.

The normalized bias error for acoustic intensity is defined as (4)

$$\varepsilon_b(f) = \{E\{\hat{I}(f)\} - I(f)\}/_{I(f)} \qquad (5.19)$$

where $\hat{I}(f)$ is the measured acoustic intensity, and $I(f)$ is the true acoustic intensity.

The measured cross-spectrum between two closely-spaced microphones is related to the true cross-spectrum (Equation 5.4) as

$$\hat{G}_{ab}(f) = H_a^*(f)H_b(f)G_{12}(f)$$

---

[2] these polarization voltages were rather high values but must be to receive the needed signal-to-noise ratio for exceptable measurements.

and using Equations 5.2, 5.11, and 5.12, this relationship is written

$$\hat{G}_{ab}(f) = |H_a(f)||H_b(f)|e^{-j\Delta\phi_{ab}}|G_{12}(f)|e^{-j\phi_{12}} . \qquad (5.20)$$

Therefore, the measured acoustic intensity (taking the imaginary part of Equation 5.20) can be written as

$$\hat{I}(f) = |H_a(f)||H_b(f)||G_{12}(f)|\sin(\phi_{12} + \Delta\phi_{ab})/4\pi f\rho\Delta r \qquad (5.21)$$

where $\Delta\phi_{ab}$ is the phase shift of the lumped systems $H_a(f)$ and $H_b(f)$, and ϕ_{12} is the actual phase delay (phase shift) between the true acoustic pressures, in the direction of wave propagation, for a microphone separation distance Δr.

Placing the expressions for the true acoustic intensity (5.2) and the estimated acoustic intensity (5.21) into the equation for the normalized bias error (5.19) results in

$$\varepsilon_b(f) = |H_a||H_b|[\cos\Delta\phi_{ab} + \cot\phi_{12}\sin\Delta\phi_{ab}] - 1 . \qquad (5.22)$$

If it is assumed that $\Delta\phi_{ab}$ is small enough that $\cos\Delta\phi_{ab} \cong 1$ and $\sin\Delta\phi_{ab} \cong \Delta\phi_{ab}$, then the estimated bias error (via Equation 5.22) is

$$\varepsilon_b(f) \cong |H_a(f)||H_b(f)|(1 + \Delta\phi_{ab}\cot\phi_{12}) - 1 , \qquad (5.23)$$

where the first term $|H_a(f)||H_b(f)|$, which would be ideally equal to one, is the magnitude error, and the $\Delta\phi_{ab}(f)$ term is the phase error due to the microphones and the associated electronics.

5.4 Empirical Investigation of the Phase and Gain Differences

Typically, the phase and gain-mismatch errors between the microphone cathode followers, their respective power supplies, and the high-quality pre-amplifiers are very minimal. Figures 5.5 and 5.6 show the phase and gain differences between the channels of the power supply and pre-amplifier employed in the intensity measurements.

The major contributors to these errors was found to be, firstly, the microphone cartridges and secondly, the FFT analyzer (more precisely, the alaising filters of the A/D converter of the SD360). The measured phase and gain differences between the two channels of the A/D converter are shown in more detail in Figure 5.7. Even though the magnitude differences between the channels were stable, the phase differences varied concurrently with the measuring frequency range set on the FFT analyzer and also with the warm-up time of the A/D unit (eventually kept operating continuously). Fortunately, these phase errors are only prevalent at the higher frequencies of each selected frequency range where phase errors are much less of a problem.

The most severe phase and gain errors are contributed by the microphone cartridges. Even with so-called "phase-matched" microphones from Brual & Kjaer, low-frequency phase differences were noticable, and in some cases, phase errors developed after a short period of time, while the magnitude differences remained constant and very minimal. Because these phase problems are in the low-frequency region (below 300 Hz), the bias error from these phase differences could be rather significant.

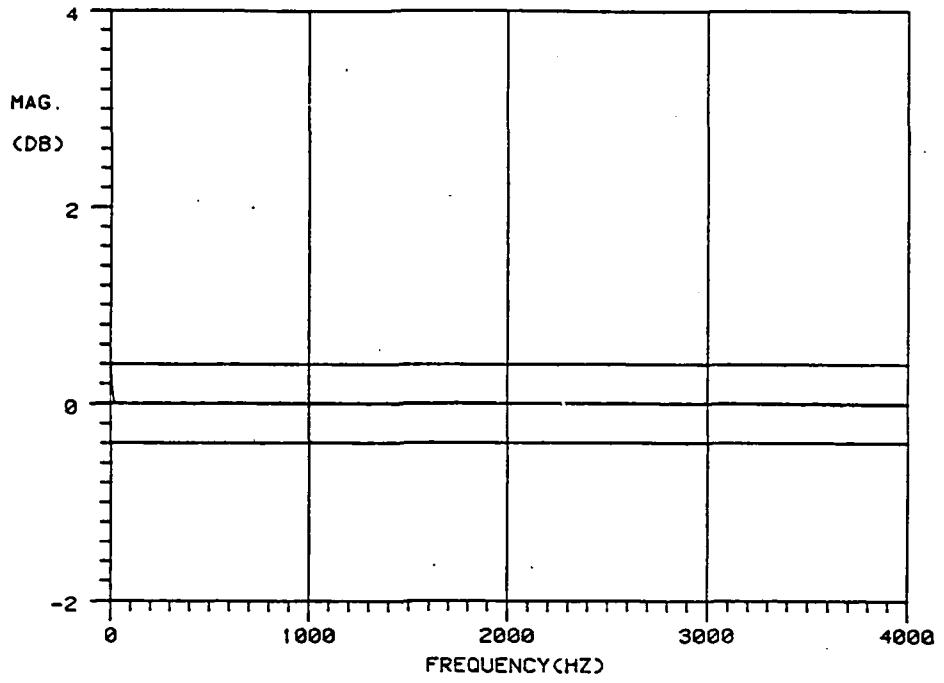

Figure 5.5(a): The Magnitude Difference Between the Two Channels of the B&K Power Supply

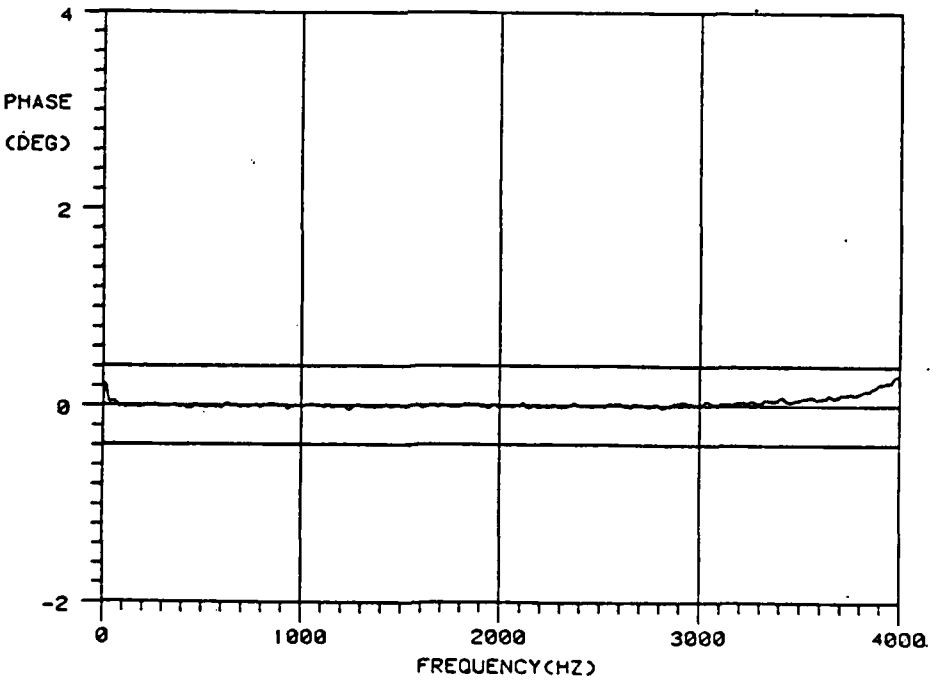

Figure 5.5(b): The Phase Difference Between the Two Channels of the B&K Power Supply

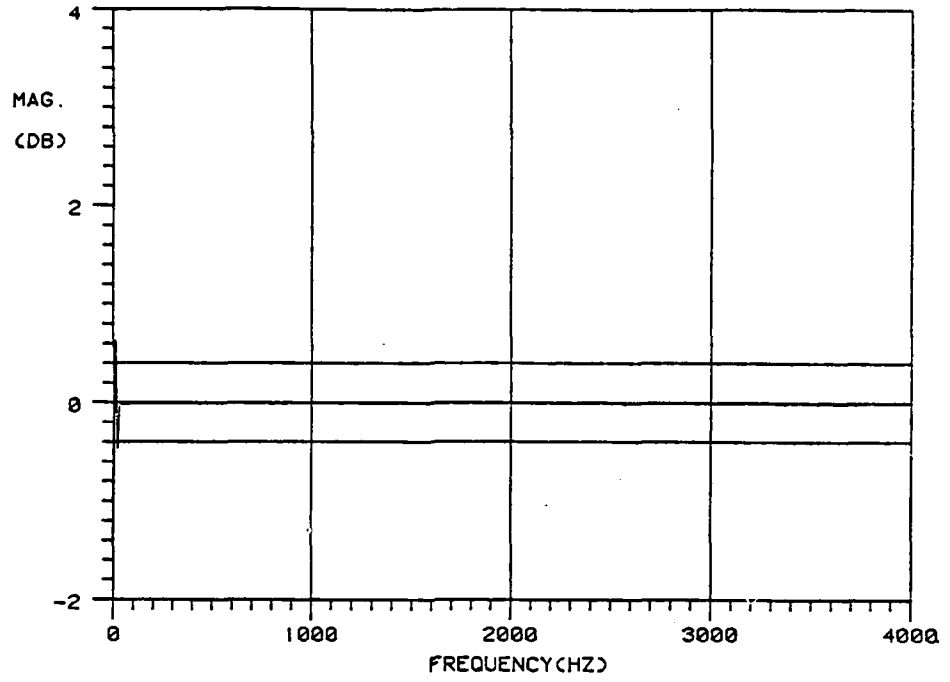

Figure 5.6(a): The Magnitude Difference Between the Two Channels of the Ithaco Pre-Amplifiers

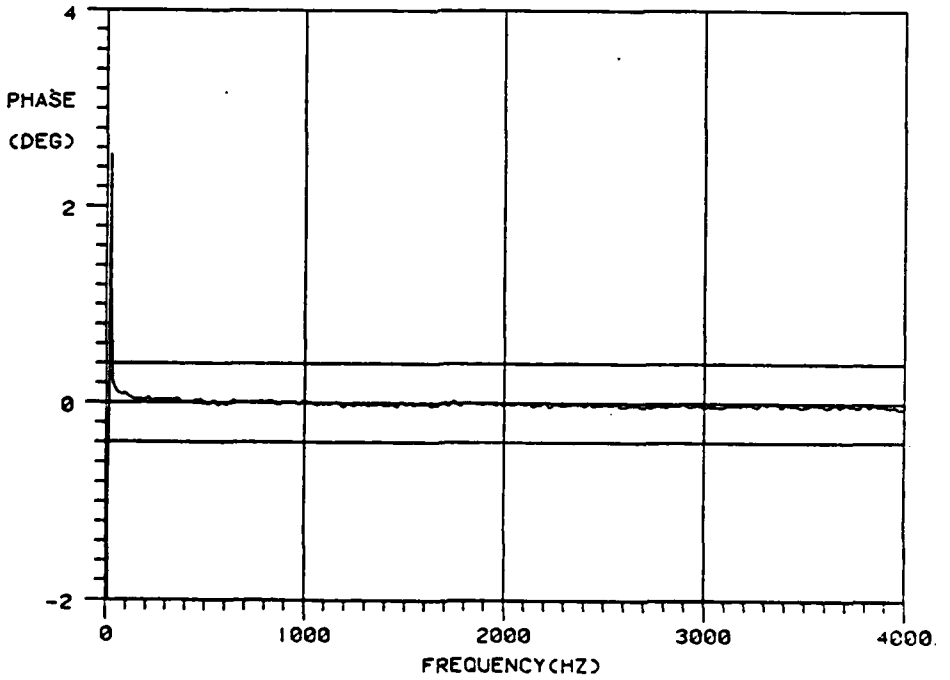

Figure 5.6(b): The Phase Difference Between the Two Channels of the Ithaco Pre-Amplifiers

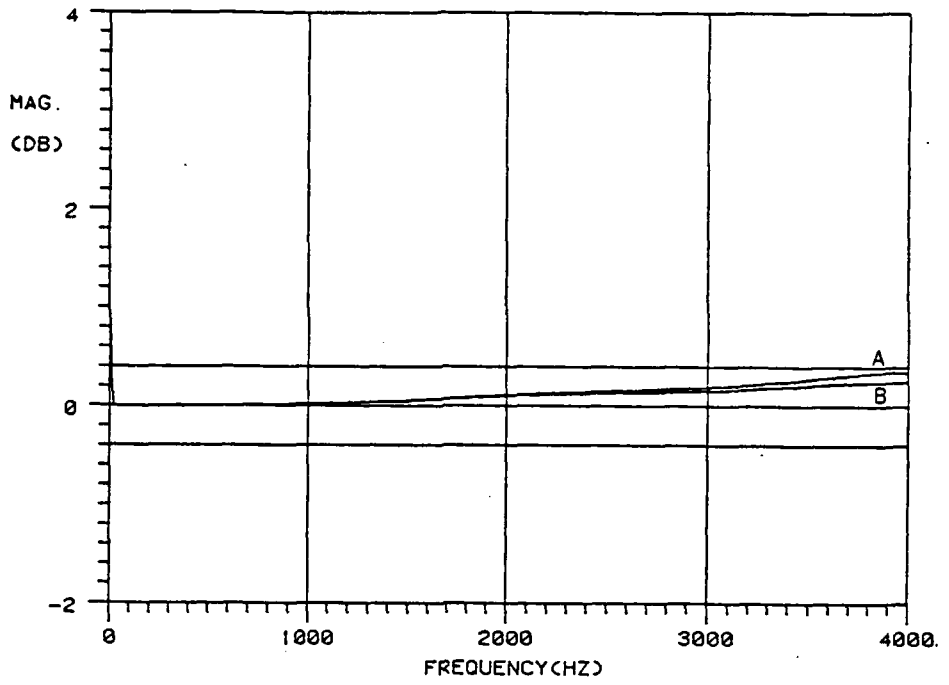

Figure 5.7(a): The Magnitude Difference Between the Two Channels of the A/D Converter
Curve A: Initial Turn-On
Curve B: One-Hour Warm-Up Time

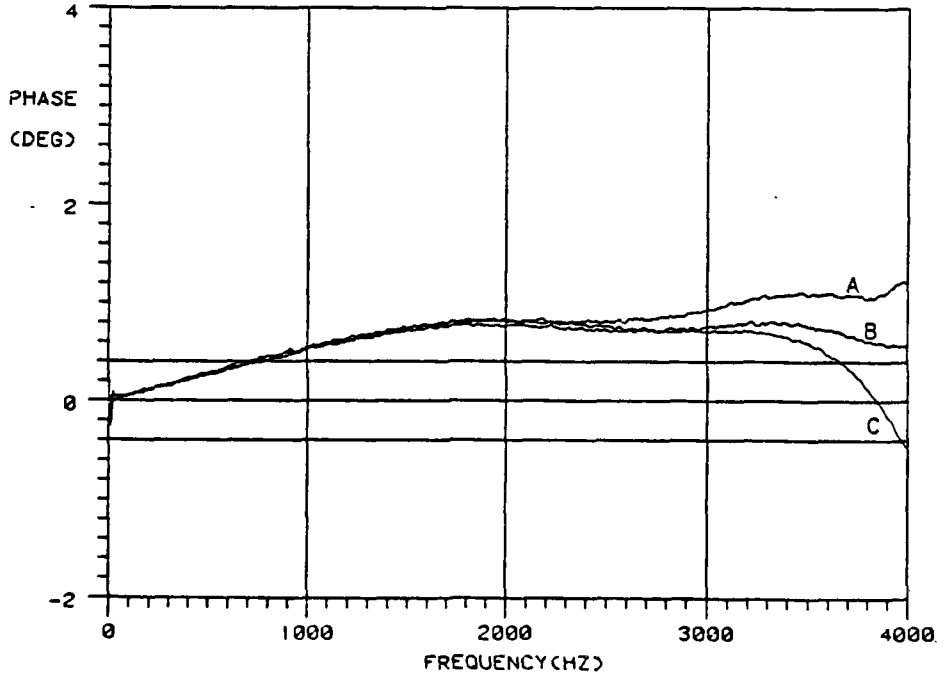

Figure 5.7(b): The Phase Difference Between the Two Channels of the A/D Converter
Curve A: Initial Turn-On
Curve B: One-Hour Warm-Up Time
Curve C: Extended Warm-Up Time

Figure 5.8 displays the phase and magnitude responses between the 1/2" microphone pair for one particular frequency range, and Figures 5.9 and 5.10 show two different frequency ranges fo the 1/4" microphone pair used for the intensity measurements. The two individual curves on each plot represent results from the two different methods of measuring the transfer function, the electrostatic actuator test (curve B) and the plane-wave duct system (curve A). The radical fluctuations in magnitude and phase of curve A for all plots above 1800 Hz designates the cutoff frequency of the tube (the frequency range where radial modes of the tube are prevalent).

Theoretically, both calibration methods should produce equilvalent results in the low-frequency region where the correction for phase differences is essential, but empirically, for both a randomly-selected pair of 1/2" B&K microphones and a "phase-matched" pair of 1/4" B&K microphones, the actuator test gave lower phase-difference values than the plane-wave duct calibration method (see Figures 5.8 and 5.9). Explaining this dilemma between the two measuring methods, it is stated (27) that at low frequencies the controlled vent of the B&K microphones, which allows pressure equalization between the two sides of the diaphragm, causes a change in the microphone's sensitivity at low frequencies, and the low-frequency limit may be altered by changing the resistance of the vent. Also, the impedance of the cavity behind the diaphragm influences the lower limiting frequency. Noting that the electrostatic actuator applies no signal to the equalization vent while the plane-wave tube method exposes the vent to a sound field, then this fact has to be important when comparing the low-frequency results from

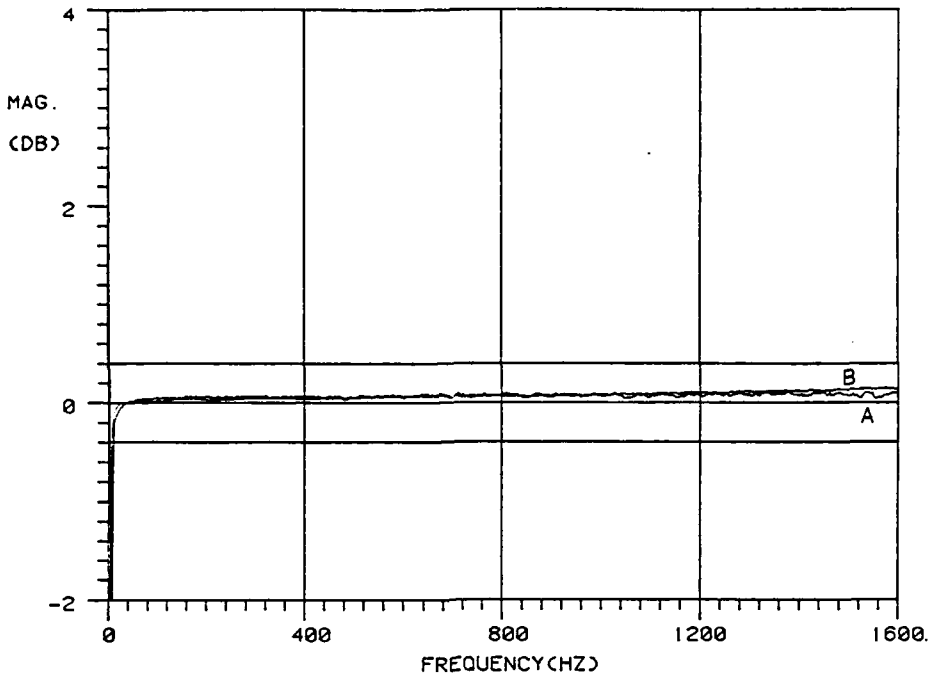

Figure 5.8(a): The Magnitude Difference Between Two B&K 1/2" Microphone Cartridges
Curve A: Results Using the Plane-Wave Duct System
Curve B: Results Using the Dual-Actuator Test

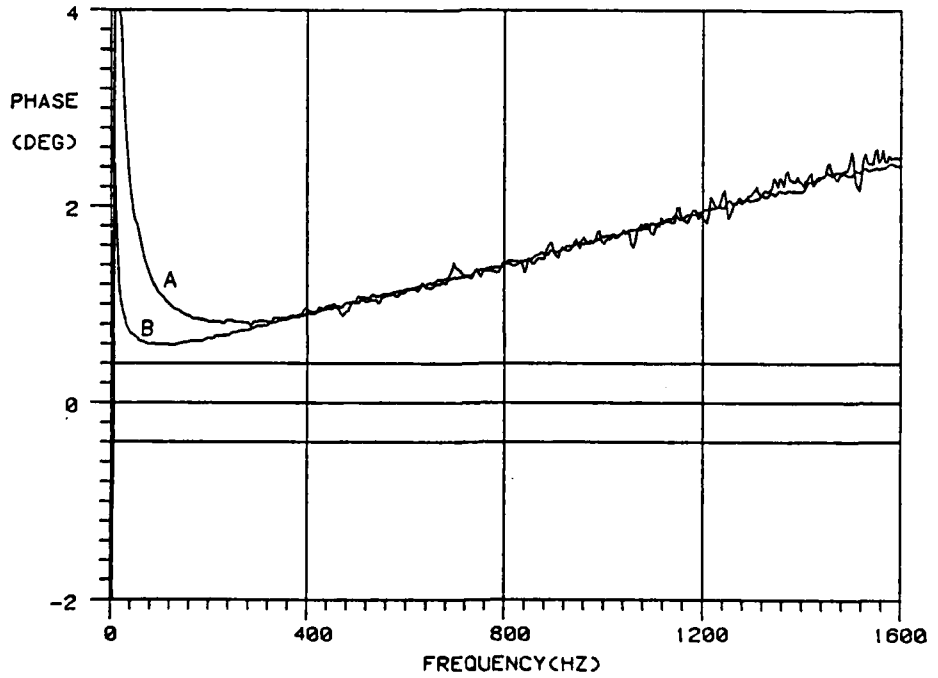

Figure 5.8(b): The Phase Difference Between Two B&K 1/2" Microphone Cartridges
Curve A: Results Using the Plane-Wave Duct System
Curve B: Results Using the Dual-Actuator Test

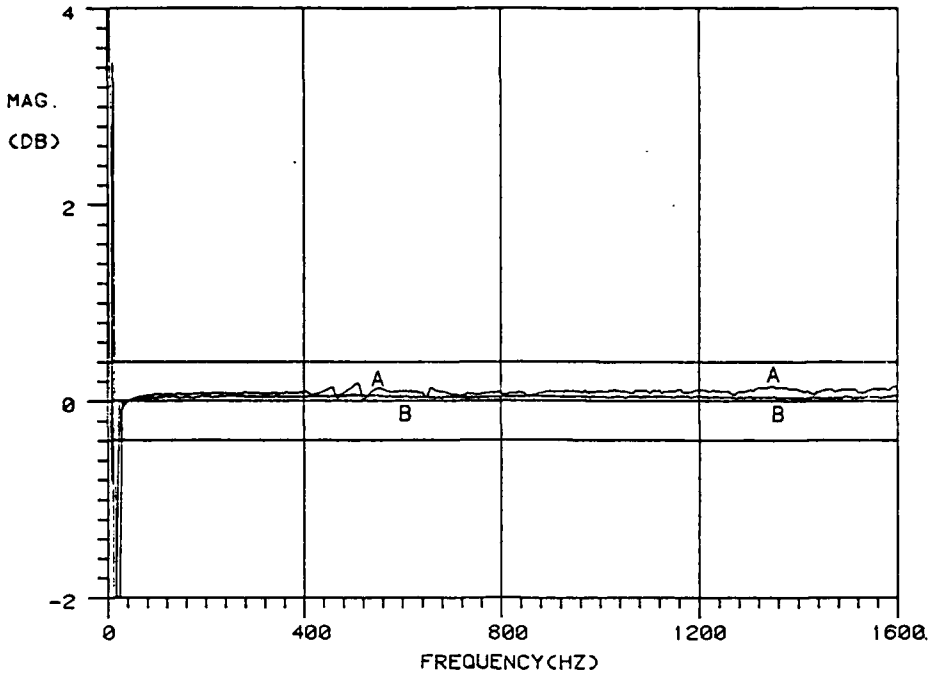

Figure 5.9(a): The Magnitude Difference Between Two B&K 1/4" Microphone Cartridges
Curve A: Results Using the Plane-Wave Duct System
Curve B: Results Using the Dual-Actuator Test

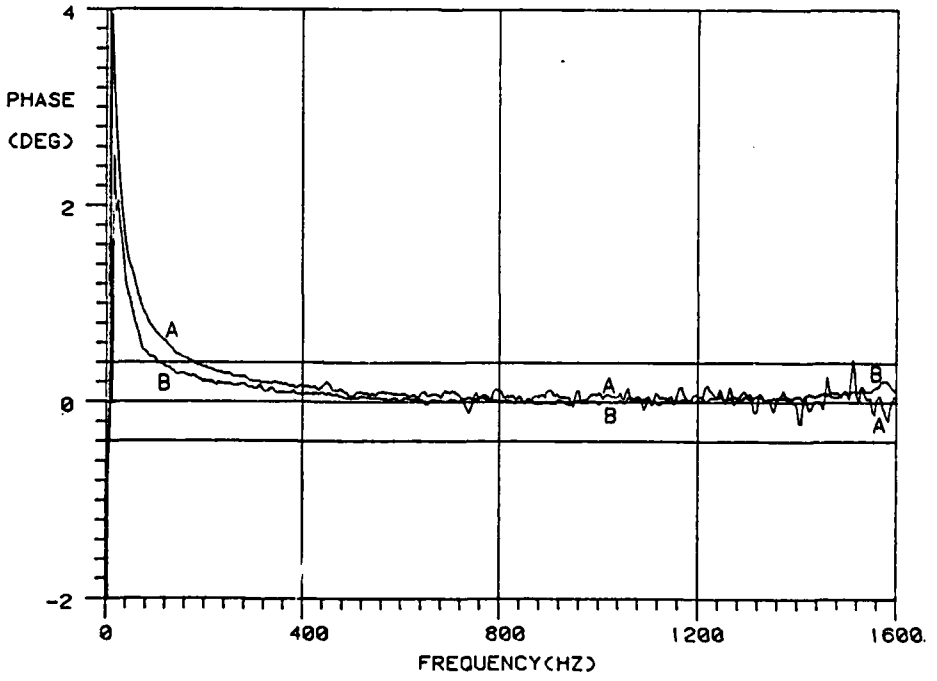

Figure 5.9(b): The Phase Difference Between Two B&K 1/4" Microphone Cartridges
Curve A: Results Using the Plane-Wave Duct System
Curve B: Results Using the Dual-Actuator Test

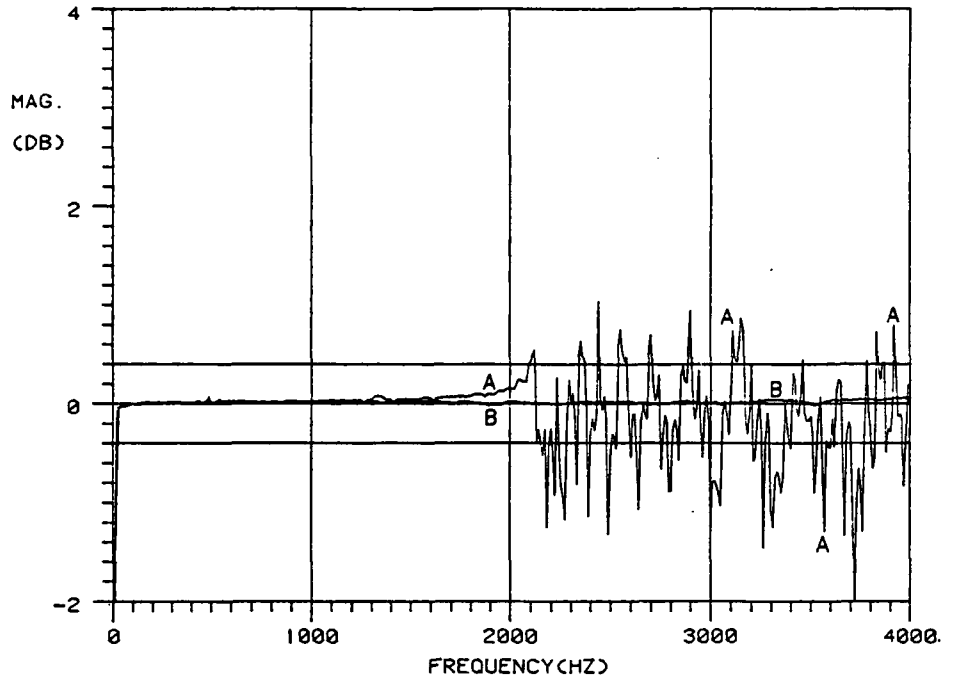

Figure 5.10(a): The Magnitude Difference Between Two B&K 1/4" Microphone Cartridges (4000 Hz Range).
Curve A: Results Using the Plane-Wave Duct System
Curve B: Results Using the Dual-Actuator Test

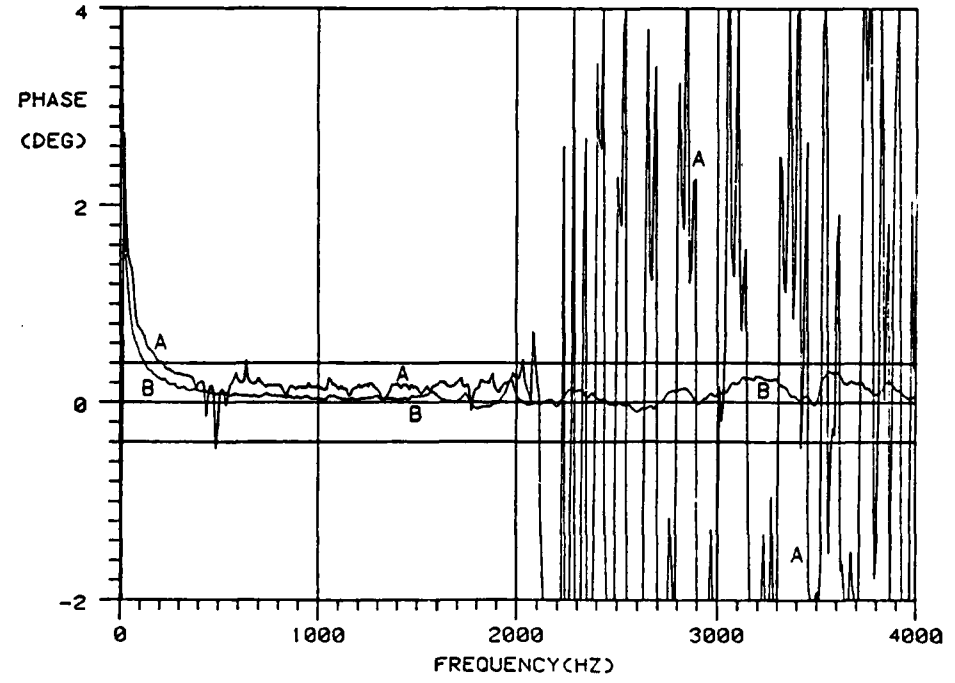

Figure 5.10(b): The Phase Difference Between Two B&K 1/4" Microphone Cartridges (4000 Hz Range)
Curve A: Results Using the Plane-Wave Duct System
Curve B: Results Using the Dual-Actuator Test

each individual calibration method. If this is true, the equalization vents of each microphone must have slightly different dimensions which evidently changes the resistance of the vent. Many attempts to experimentally justify the above deduction pertaining to the phase differences between the two calibration-transfer-function methods failed. It should be noted that the plane-wave duct method provided the more accurate cross-spectral acoustic intensity results when compared to the free-field acoustic intensity (Equation 2.9) which coincides with the above conclusions. Therefore, a practical compromise and solution to this problem would be to use the plane-wave duct method to calibrate the microphones for the low-frequency region and the actuator test to calibrate the higher frequencies of the two phase-mismatched microphones.

Aside from the two calibration methods mentioned, a low-frequency constant-pressure acoustic calibrator has been recently developed by Bruel & Kjaer Instruments, Inc. (27) which may be a more adequate device for calibrating two microphones (transducers), but this calibration unit (model UA-4221) was not available for testing.

To appreciate the amount of error in the intensity measurement if calibration of these phase differences between the microphones cartridges is not applied, the resulting bias error of intensity calculated using Equation 5.23 (as measured by the duct system) for the 1/2" and 1/4" microphone phase differences (Figures 5.8 and 5.9) is shown is Figure 5.11. Therefore, if an error below 1.0 dB is the designed criteria for the intensity measurements, the measurements below 240 Hz (for the 1/2" microphones) and 140 Hz (for the 1/4" microphones) would be unacceptable.

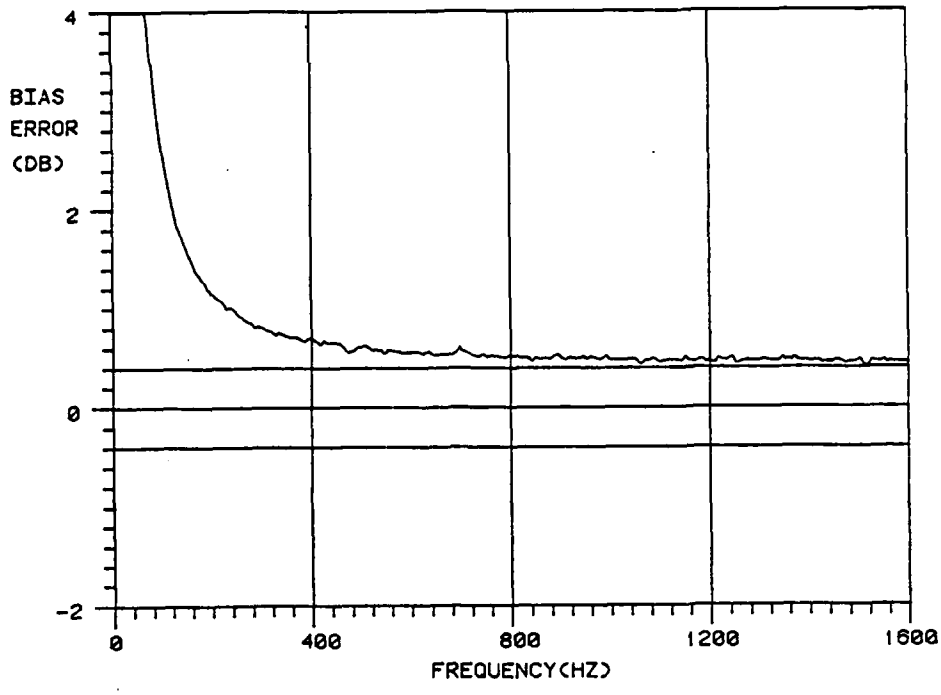

Figure 5.11(a): The Bias Error Resulting from the Phase Difference Between the Two 1/2" Microphone Cartridges as Measured by the Plane-Wave Duct System

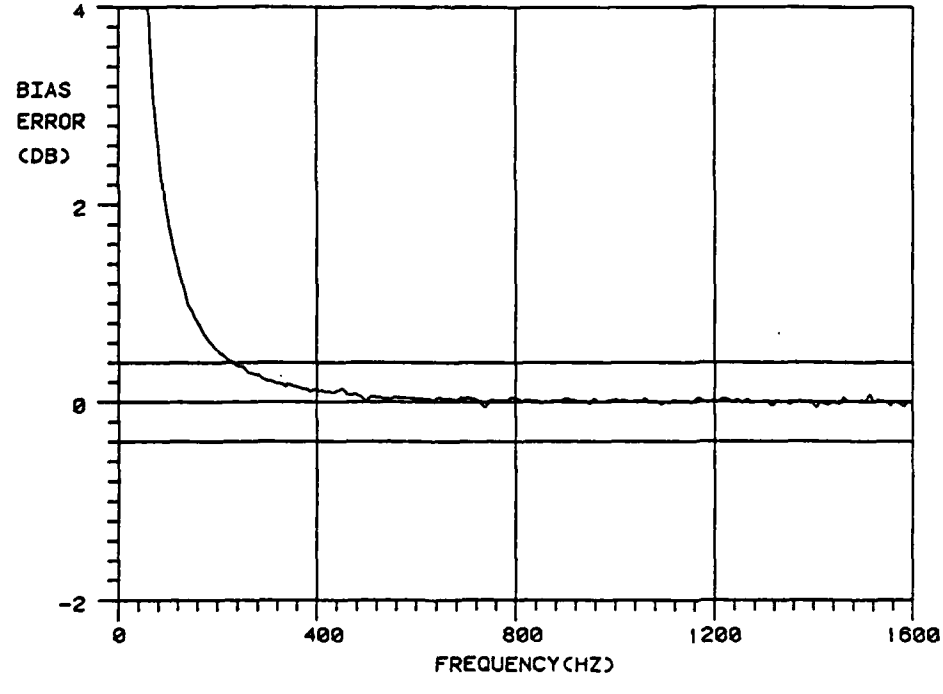

Figure 5.11(b): The Bias Error Resulting from the Phase Difference Between the Two 1/4" Microphone Cartridges as Measured by the Plane-Wave Duct System

5.5 Effect of Mismatch Errors Upon the Directional Characteristics

The relative phase shift between the two microphone channels produces consequential distortions in the directivity response of the two-microphone intensity meter which appears as a difference of the absolute sensitivity for the two opposing directions of the incident wave. For low frequencies, a very small phase difference between the two measuring systems will give noticeable distortions in the dipole response. Also, even though the directivity of the intensity probe is highly sensitive to small phase errors at low frequencies, the device is not as susceptable to magnitude differences between the two measuring systems.

The following directionality plots presented in this section are all theoretical calculations assuming plane-wave incidence of sound upon the two-microphone intensity device. It is assumed that experimental results of these analytical directivity plots would approximately duplicate the theoretical predictions. The polar plots represent the directivity response of the two-microphone array governed by the expression $I_\theta = I_n \cos\theta$ where θ is the measured angle between the axis of the sound source and the axis of the intensity probe, I_n the maximum intensity obtained at the angle $\theta = 0^o$, and I_θ the intensity component measured at some angle of wave incidence θ. All directivity response plots are normalized on a logarithmic (dB) scale rather than a linear scale.

Using the same phase differences between the microphone cartridges exemplified in Section 5.4 (from Figures 5.6 and 5.7), directivity plots

of those results are performed. Figure 5.12 shows the directivity responses of the 1/2" and the 1/4" microphone pairs for the specific frequency of 100 Hz using their respective experimental phase errors of 1.0^{o} and 0.8^{o}. Figure 5.13 gives similar results for the frequency of 200 Hz using the 1/2" and 1/4" microphone phase differences of 0.8^{o} and 0.4^{o} respectively. Comparing the directivity plot of Figure 5.12(a) with the directional response of the two-microphone device containing no phase error (Figure 3.3), the distortion of the expected dipole response is very noticeable. For the 1/4" microphone pair with a smaller phase error of 0.8^{o}, Figure 5.12(b), an improvement in the directivity response can immediately be observed. Similarily, with the phase errors at 200 Hz for the 1/2" and 1/4" microphone pairs, Figures 5.13(a) and 5.13(b) display an improvement in the directional characteristics of the intensity meter, but still the expected dipole response is slightly deformed even for a very small phase error (0.4^{o} phase error for Figure 5.13(b)).

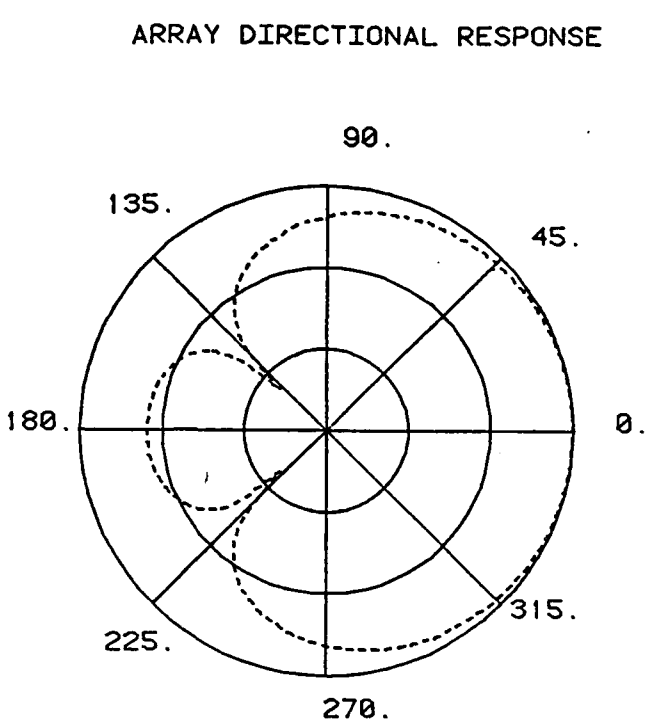

Figure 5.12(a): The Directivity Response of the Two-Microphone Intensity Meter Using 1/2" Microphones Having a Phase Difference of 1.0^{o} at 100 Hz

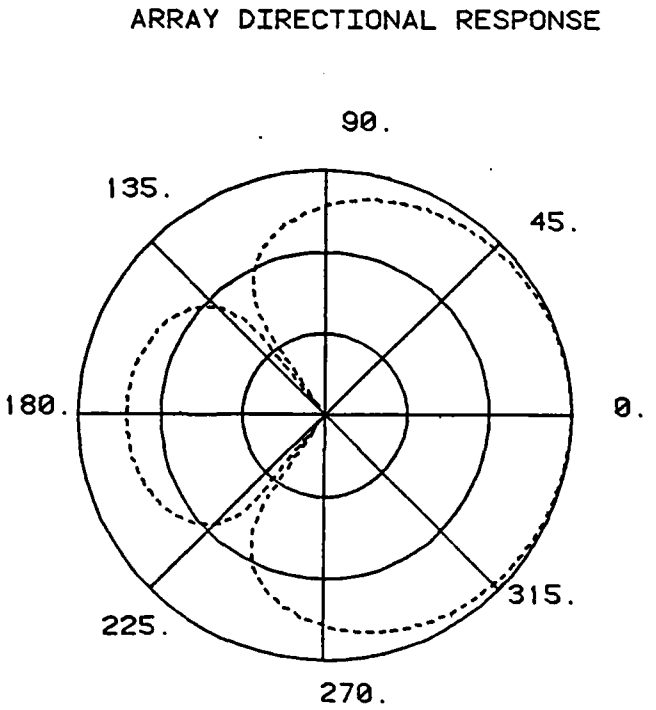

Figure 5.12(b): The Directivity Response of the Two-Microphone Intensity Meter Using 1/4" Microphones Having a Phase Difference of 0.8^{o} at 100 Hz

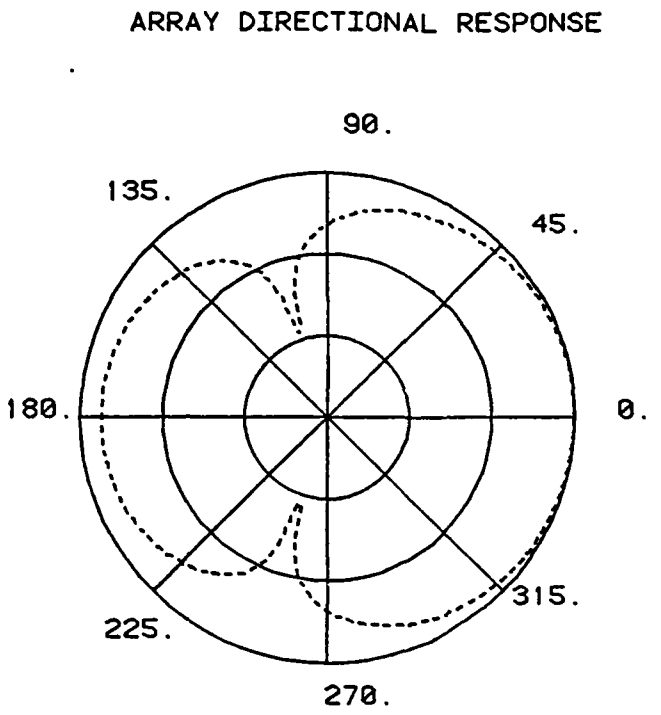

Figure 5.13(a): The Directivity Response of the Two-Microphone Intensity Meter Using 1/2" Microphones Having a Phase Difference of 0.8^{o} at 200 Hz

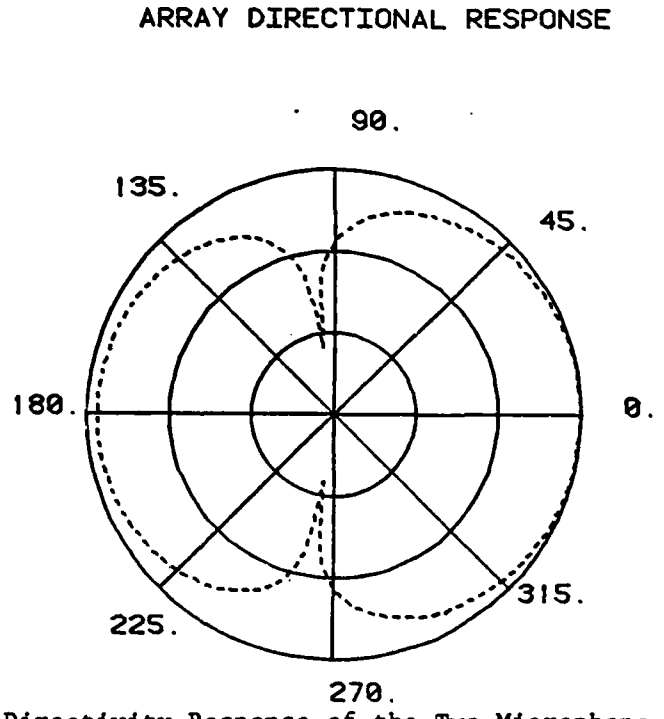

Figure 5.13(b): The Directivity Response of the Two-Microphone Intensity Meter Using 1/4" Microphones Having a Phase Difference of 0.4^{o} at 200 Hz

CHAPTER 6

INTENSITY PROBE OBSTACLE EFFECTS

6.1 Acoustical Scattering by the Intensity Probe

It must not be forgotten that the two-microphone probe for measuring the cross-spectral sound intensity has a finite physical size and therefore is an obstacle which can deflect a sound wave from its original course. When a sound wave strikes a body in its path, in addition to the undisturbed sound wave, there is a scattered wave,[1] spreading out from the obstacle in all directions, distorting the incident sound wave. This scattering of the sound field by the intensity probe (consisting of both the microphones and the two-microphone holder) can cause changes in the amplitude and phase between the two finite-size microphones especially if the obstacle is similar in dimension to the wavelength of the incident sound wave. If the obstacle (the intensity probe or microphones) is very small compared with the wavelength, all of the scattered wave is propagated out in all directions, and there exists no sharp-edged shadows thereby minimizing scattering effects. When the obstacle is about the same size as the wavelength of the incident wave, a variety of interference phenomena can occur.

---

[1] the scattered wave is defined as the difference between the actual wave and the undisturbed wave, which would be present if the obstacle were not present (39).

Imperfections of the measuring components result as a consequence of the finite size of the closely-spaced microphones and their holder. This effect becomes more important at higher frequencies where larger phase and magnitude deviations occur. At the same time, phase deviations are less important at higher frequencies with respect to the accuracy. This fact can be understood better if the bias error from the obstacle effect is modeled by the mathematical expression for the normalized bias error developed originally for the errors due to the measuring instrumentation in Chapter 5 (Equation 5.22);

$$\varepsilon_b(f) = |H_a(f)||H_b(f)|(\cos\Delta\phi_{ab} + \cot\phi_{12}\sin\Delta\phi_{ab}) - 1 \ , \qquad (6.1)$$

where it can not be assumed that $\Delta\phi_{ab}$ is so small that $\cos\Delta\phi_{ab} \simeq 1$ and $\sin\Delta\phi_{ab} \simeq \Delta\phi_{ab}$ as in Equation 5.23. Therefore, if the errors due to the measuring instrumentation are not included, $|H_a(f)|$ and $|H_b(f)|$ are the magnitude perturbations and $\Delta\phi_{ab}(f)$ the phase perturbation between the "true" acoustic pressures P_1 and P_2 at the microphone measuring positions induced by the acoustic shadowing of the intensity probe.

6.2 Scattering by the Intensity Probe Used in This Study

At the present time, two basic microphone configurations are used for intensity measurements. The most practical two-microphone configuration used to date is the placement of the two cylindrically-shaped microphones in parallel with their respective membranes in one plane (this is the microphone arrangement employed in this work and shown in Figure 3.2). The other possible arrangement is to place both microphones on one axis so that their membranes are in two parallel

planes at a chosen distance. The cathode followers are then located in opposite directions from the microphone capsules (1,49).

Considering the microphone configuation used for the intensity measurements in this paper, it would be useful to examine the microphone-proximity interference (the disparate scattering effect that each individual microphone will have on the other with respect to the microphones' separation distance) analytically. Cook et al (20,21) modeled the scattering by microphones by considering the theory of scattering between two spheres. Of course, the microphones should be modeled as finite-length rigid cylinders, but a rigorous mathematical anlysis for scattering by two semi-infinite cylinders is not available. If first-order approximations for the scattered wave of very long wavelengths on a rigid sphere or rigid cylinder are considered (38), it can be concluded that small obstacles appear even smaller to an incident sound wave. Consequently, sound is scattered almost uniformly in all the backward directions. As the frequency is increased toward obstacle size similar to wavelength of the incident wave, the angle distribution becomes more and more complicated, diffraction peaks appear and move forward from the cylinder(s). In this transition region, general simplifications of the scattered sound will not be applicable.

In addition to the microphone-proximity effect, the microphones are positioned on a finite-size holder. Therefore, the intensity probe can not be practically modeled solely as two finite-length cylinders but is a cloud of scatterers, each producing a scattered wave, and these wavelets reinforce in some directions and interfere in other directions. Because of the complicated nature of the acoustic scattering from the

intensity probe, only experimental results of these effects (the intensity probe scattering and microphone proximity interference) are investigated without theoretical confirmation.

6.3 Experimental Investigation

The device used to investigate the intensity probe acoustic scattering is described in detail in Chapter 3 and shown in Figure 3.2. The 1/2" B&K microphone cartridges were directly mounted onto the cathode followers while the 1/4" B&K microphone cartridges used adapters (model UA-0035) for mounting onto the cathode followers. Experiments were conducted in the previously described laboratory room with a flat-diaphragm loudspeaker (53) operating in the piston range (the frequency response is shown in Figure 6.1). The microphone pair (either the 1/2" or the 1/4" microphones) were placed on-axis to and in the direct field of the sound source, not near any significant sound reflectors (experimental set-up shown in Figure 6.2).

When investigating the intensity probe acoustic scattering, the procedure used eliminated the effects of the loudspeaker and microphone frequency response. First, the transfer function between a single reference microphone output (microphone 1) and the loudspeaker input was measured by the SD360 spectral analyzer (Figure 6.2(a)). Then a second "dummy" microphone (microphone 2) was carefully located directly behind the reference microphone at desired distances typical of the intensity measurements, and a second transfer-function measurement of the reference microphone was performed (Figure 6.2(b)). Using the computer, the ratio of the two transfer functions was calulated and plotted.

AD-A117 767 PENNSYLVANIA STATE UNIV UNIVERSITY PARK APPLIED RESE--ETC F/G 9/1
INVESTIGATION INTO BIAS ERRORS OF THE TWO-MICROPHONE CROSS-SPEC--ETC(U)
JUN 82 P D KITECK N00024-79-C-6043
UNCLASSIFIED ARL/PSU/TM-82-135 NL

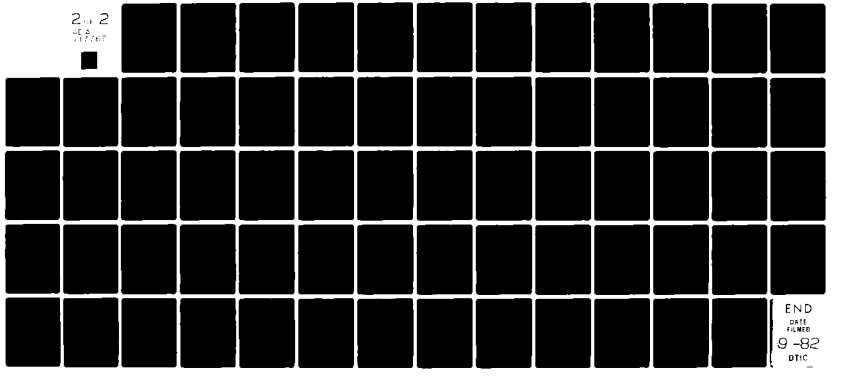

END
DATE FILMED
9-82
DTIC

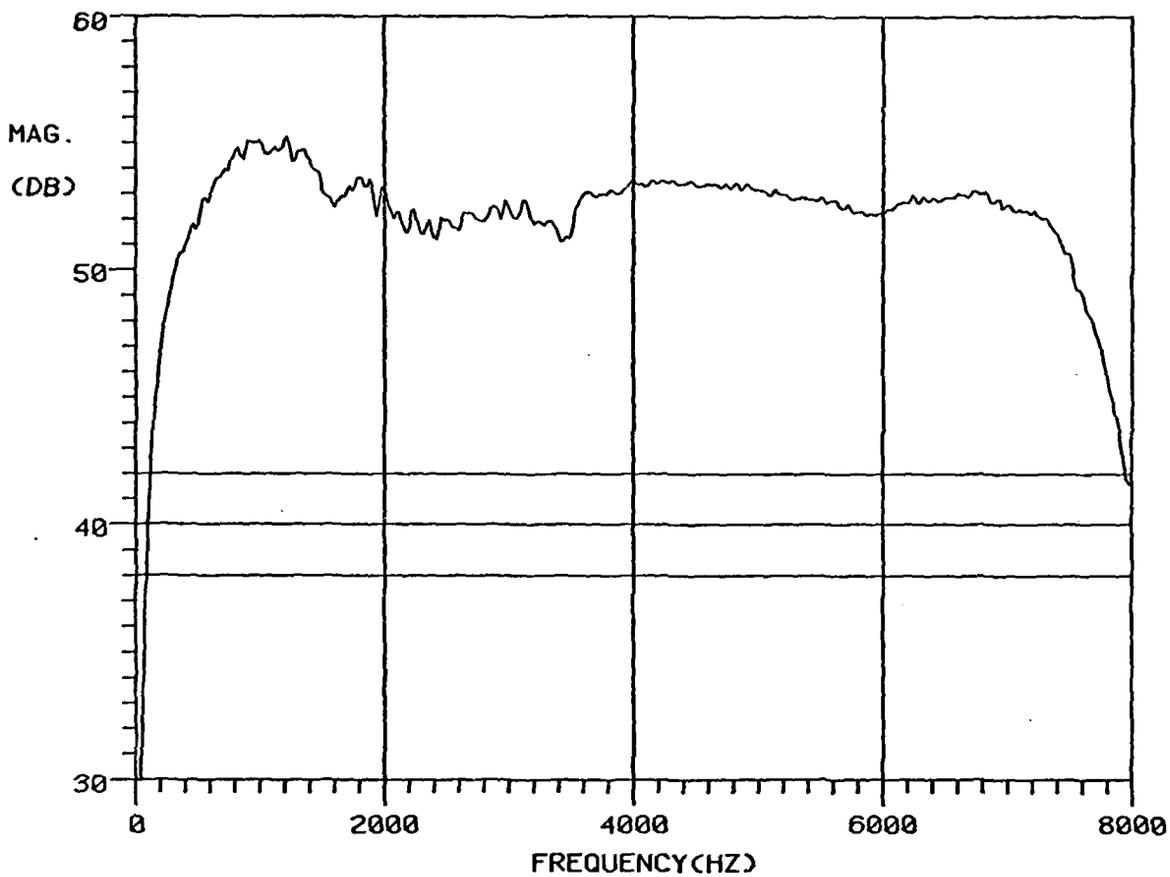

Figure 6.1: The Sound Pressure Magnitude of the Flat-Diaphragm Loudspeaker Used for the Experimental Investigation of the Intensity Probe Obstacle Effect

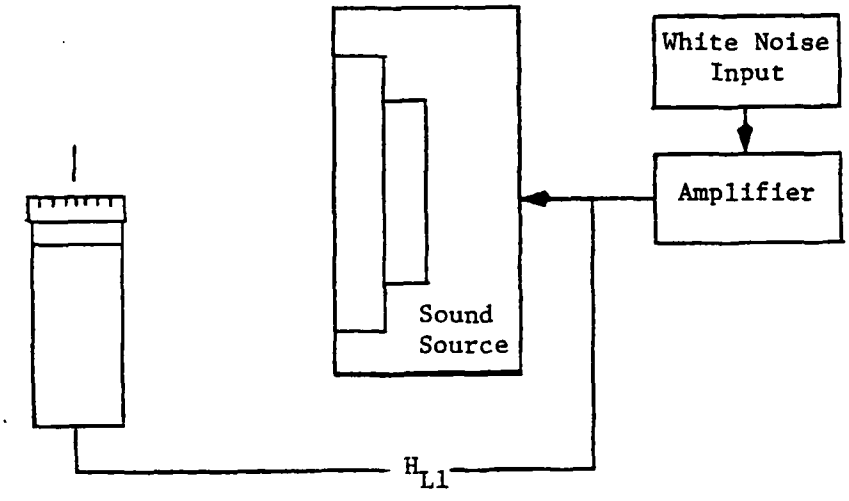

Figure 6.2(a): The Experimental Set-Up to Measure the Transfer Function Between the Loudspeaker Input and the Reference Microphone

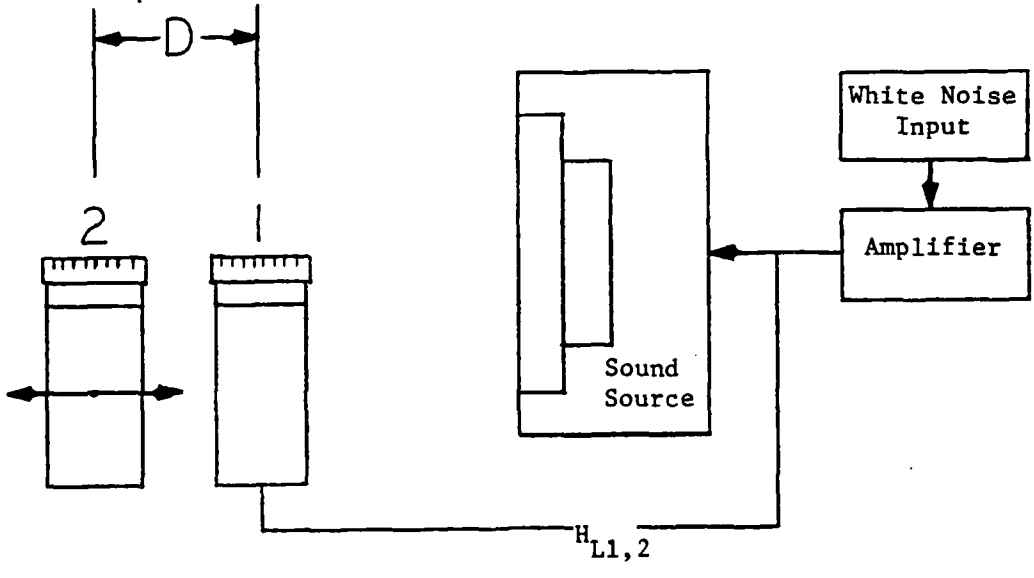

Figure 6.2(b): The Experimental Set-Up to Measure the Transfer Function Between the Loudspeaker Input and the Reference Microphone with the Addition of a "Dummy" Microphone

Therefore, the plots show both magnitude and phase differences of the complex sound pressure at the membrane of the first microphone due to the presence of the other microphone.

Figures 6.3 and 6.4 show the combined effects of the second dummy microphone and the microphone holder of both the 1/2" and 1/4" microphones while varying the separation distance between the microphones' center axes from 13 to 35 mm.[2] The phase and magnitude changes were unexpectantly large for the frequency region of 3000 Hz. In this critical frequency range of 2000-3200 Hz, the 1/2" microphone differences in magnitude were a maximum of ± 0.5 dB for 13 mm separation and -1.5 dB for 25 mm separation with corresponding maximum phase differences of $+5^{\circ}$ and $+7^{\circ}$ respectively (Figure 6.3). For the same procedure, using 1/4" microphones, the results were much better by an approximate factor of two in the same frequency range (Figure 6.4). After extending the microphone cartridges with 210 mm long goosenecks (B&K model UA-0196), these changes were reduced (see Figures 6.5 and 6.6). These measurements confirmed that the microphone holder was causing significant distortions of the measured acoustic field.

With the removal of the scattering from the microphone holder, the microphone-proximity interference can now be investigated. As expected, the effect of the second dummy microphone was increasing with frequency and was less pronounced for the 1/4" microphones than with the 1/2" microphones. It can be noticed from Figures 6.5 and 6.6 that the

---

[2] 13 mm is the minimum separation that is physically possible for 1/2" microphones, and 12.5 mm is the minimum physical separation for 1/4" microphones when using 1/2" cathode followers.

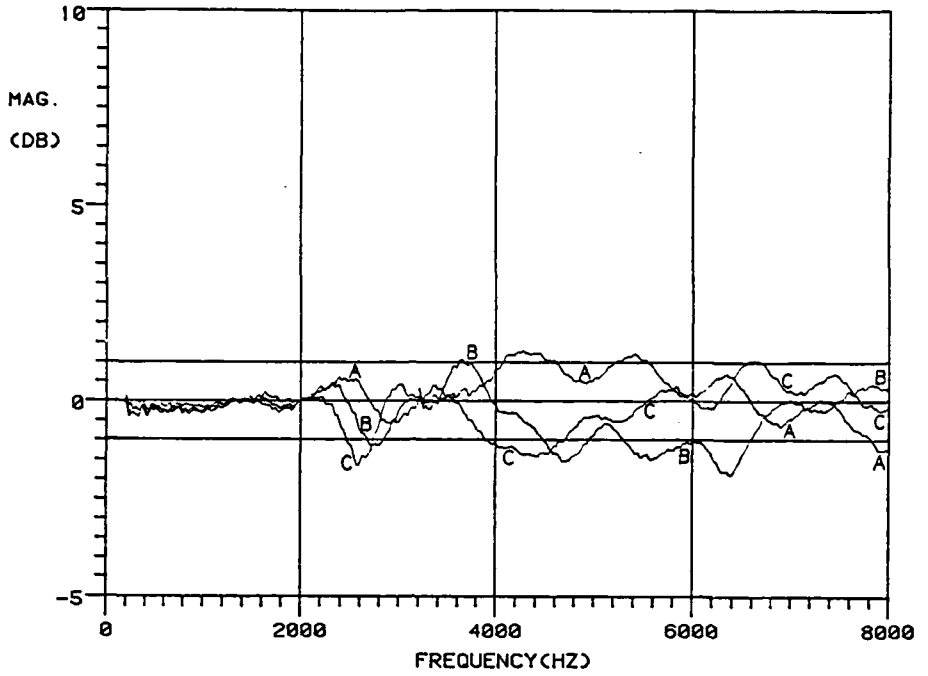

Figure 6.3(a): The Effect of Microphone 2 on the Magnitude Response of Microphone 1 for Various Distances D (1/2" Microphones) Curve A: D=13mm; Curve B: D=25mm; Curve C: D=35mm

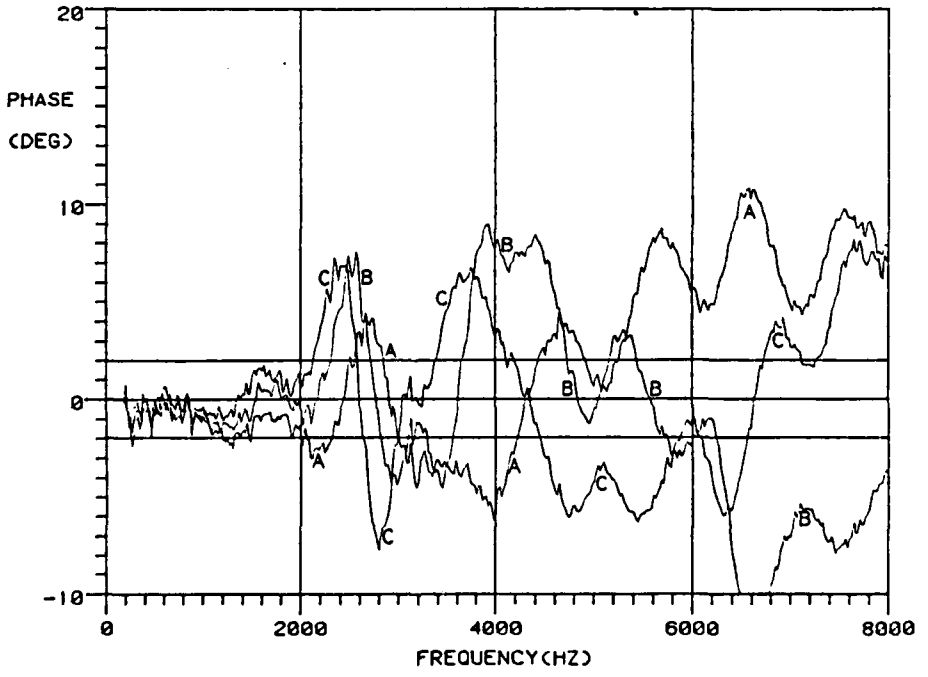

Figure 6.3(b): The Effect of Microphone 2 on the Phase Response of Microphone 1 for Various Distances D (1/2" Microphones) Curve A: D=13mm; Curve B: D=25mm; Curve C: D=35mm

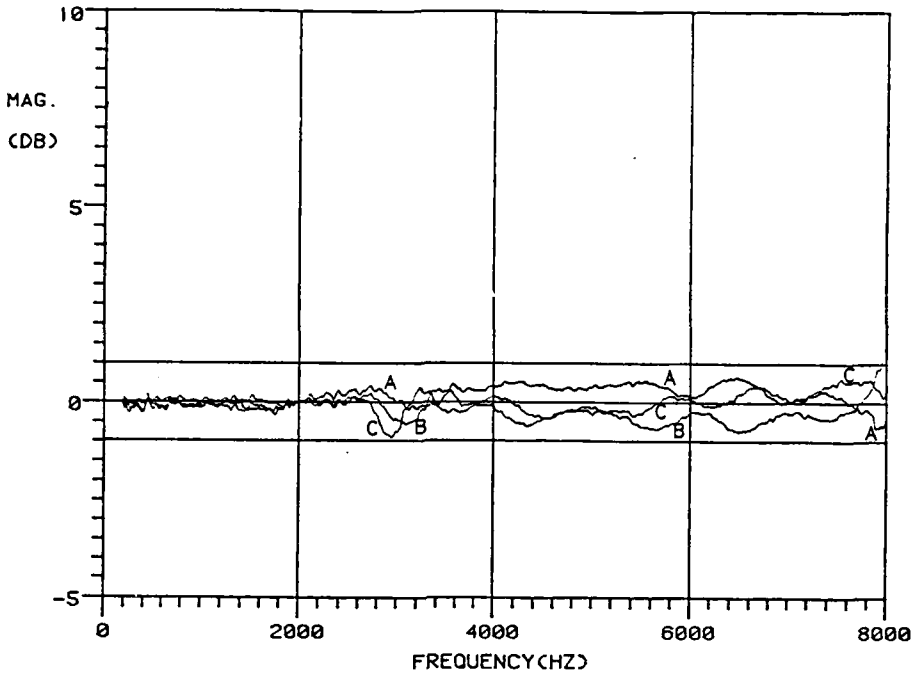

Figure 6.4(a): The Effect of Microphone 2 on the Magnitude Response of Microphone 1 for Various Distances D (1/4" Microphones) Curve A: D=13mm; Curve B: D=25mm; Curve C: D=35mm

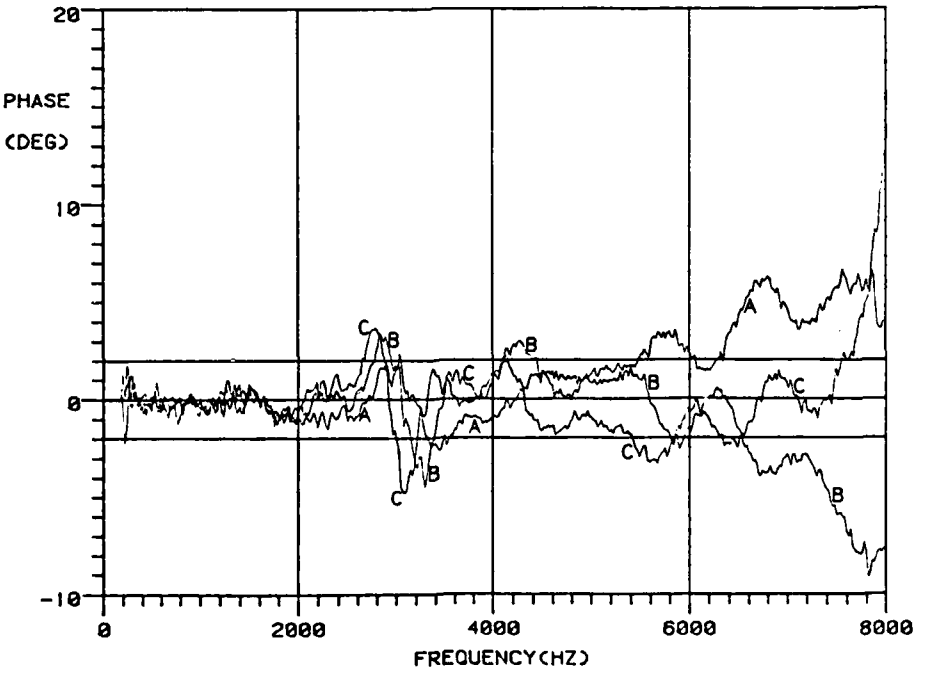

Figure 6.4(b): The Effect of Microphone 2 on the Phase Response of Microphone 1 for Various Distances D (1/4" Microphones) Curve A: D=13mm; Curve B: D=25mm; Curve C: D=35mm

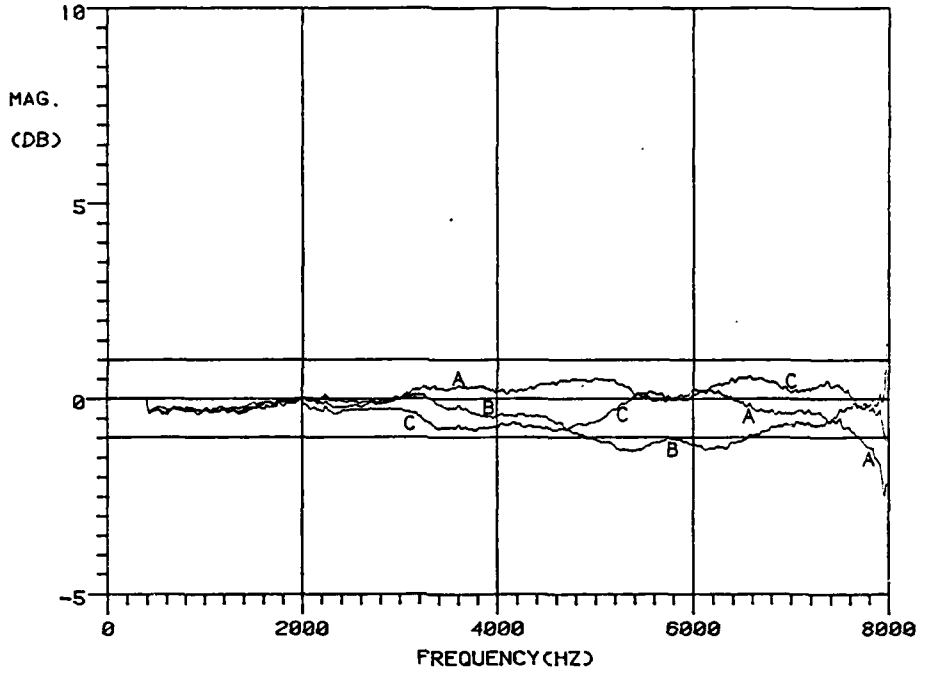

Figure 6.5(a): The Effect of Microphone 2 on the Magnitude Response of Microphone 1 for Various Distances D with the Microphones Extended by Goosenecks (1/2" Microphones)
Curve A: D=13mm; Curve B: D=25mm; Curve C: D=35mm

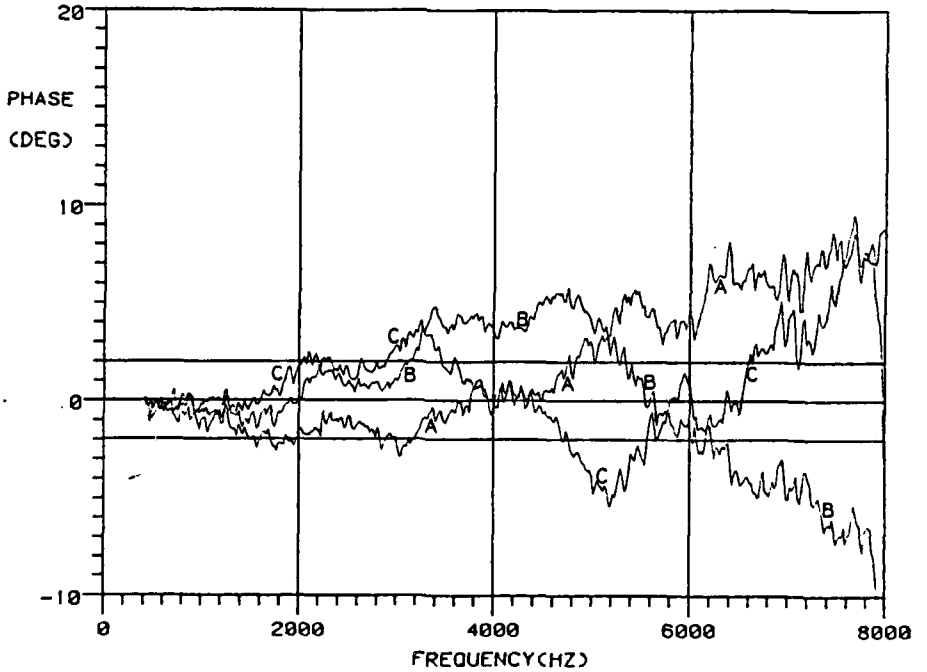

Figure 6.5(b): The Effect of Microphone 2 on the Phase Response of Microphone 1 for Various Distances D with the Microphones Extended by Goosenecks (1/2" Microphones)
Curve A: D=13mm; Curve B: D=25mm; Curve C: D=35mm

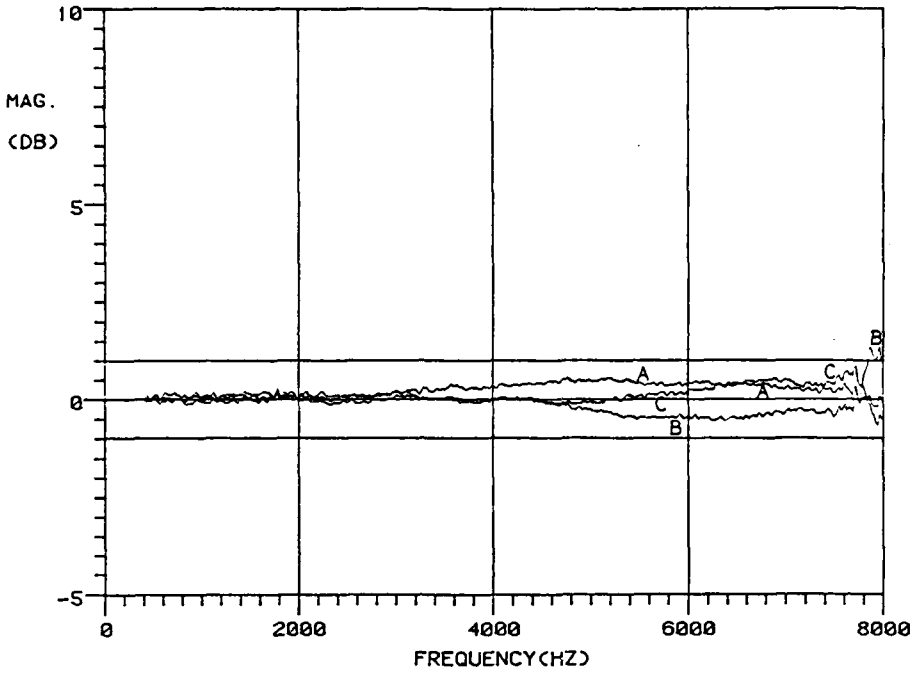

Figure 6.6(a): The Effect of Microphone 2 on the Magnitude Response of Microphone 1 for Various Distances D with the Microphones Extended by Goosenecks (1/4" Microphones)
Curve A: D=13mm; Curve B: D=25mm; Curve C: D=35mm

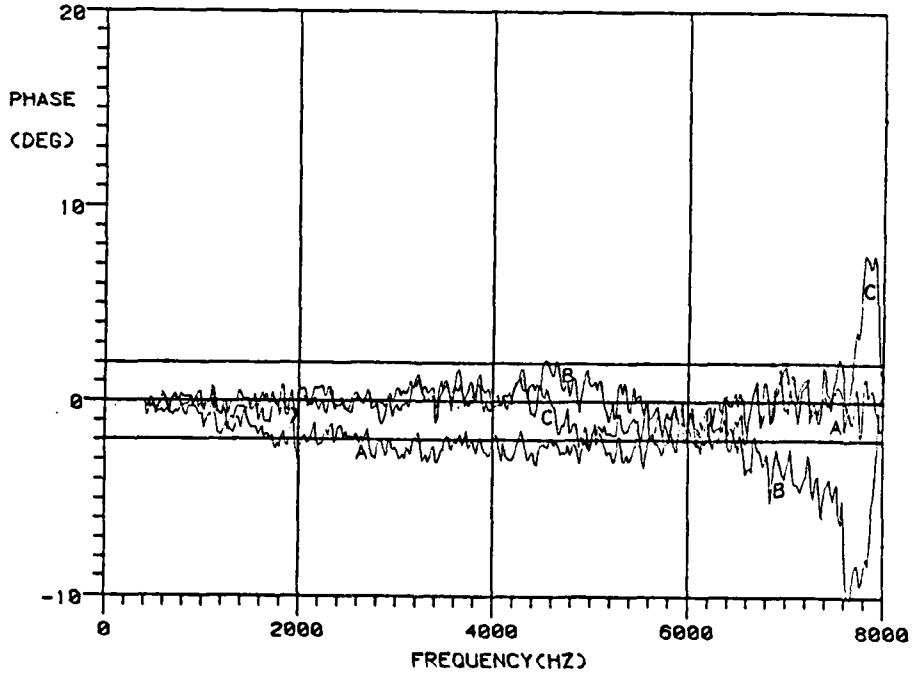

Figure 6.6(b): The Effect of Microphone 2 on the Phase Response of Microphone 1 for Various Distances D with the Microphones Extended by Goosenecks (1/4" Microphones)
Curve A: D=13mm; Curve B: D=25mm; Curve C: D=35mm

magnitude of the sound pressure below 4000 Hz was affected very little, but the phase changes were still moderately large. The scattering effects were less with both the smaller size microphones and the smaller microphone separation distances.

The results in Figures 6.3 to 6.6 show only the phase and magnitude effects when the dummy microphone was positioned directly behind the reference microphone and on the opposite side of the sound source. Now, Figures 6.7 and 6.8 show the results when the role of the microphones were reversed (the dummy microphone was located between the sound source and the measuring microphone and extended on goosenecks). As in the previous situations, the effects were much smaller with 1/4" microphones, but essentially no different than the results of Figures 6.5 and 6.6.

The above results present the effect of one microphone only. It can be expected that when both microphones are placed in the acoustic field, a mutual effect will result creating partial cancellation of the amplitude changes and the phase shifts. To investigate this effect, the transfer function between two microphones was measured, and the results are presented in Figures 6.9 and 6.10. Because the phase and amplitude responses of both microphones were slightly different, appropriate corrections were made by the computer. Also, the distances of the microphones from the sound source were not equal, and therefore, the phase plots of the transfer function were represented by lines having different angles with the frequency axis according to the microphone distance. To make the evaluation of these graphs more convenient, the phase delays from the different microphone-separation distances, Δr,

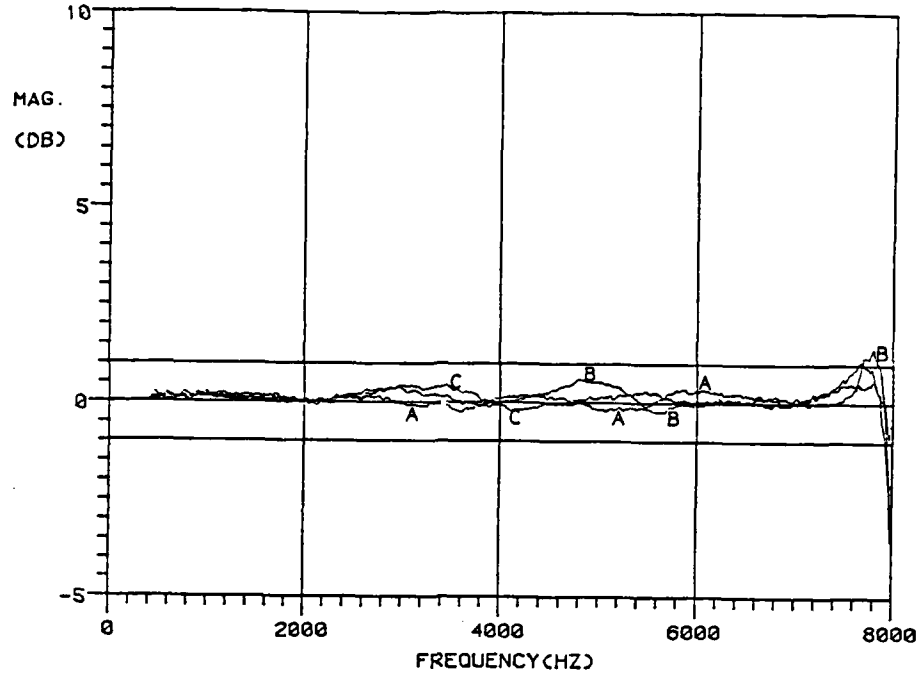

Figure 6.7(a): The Effect of Microphone 1 on the Magnitude Response of Microphone 2 for Various Distances D with the Microphones Extended by Goosenecks (1/2" Microphones)
Curve A: D=13mm; Curve B: D=25mm; Curve C: D=35mm

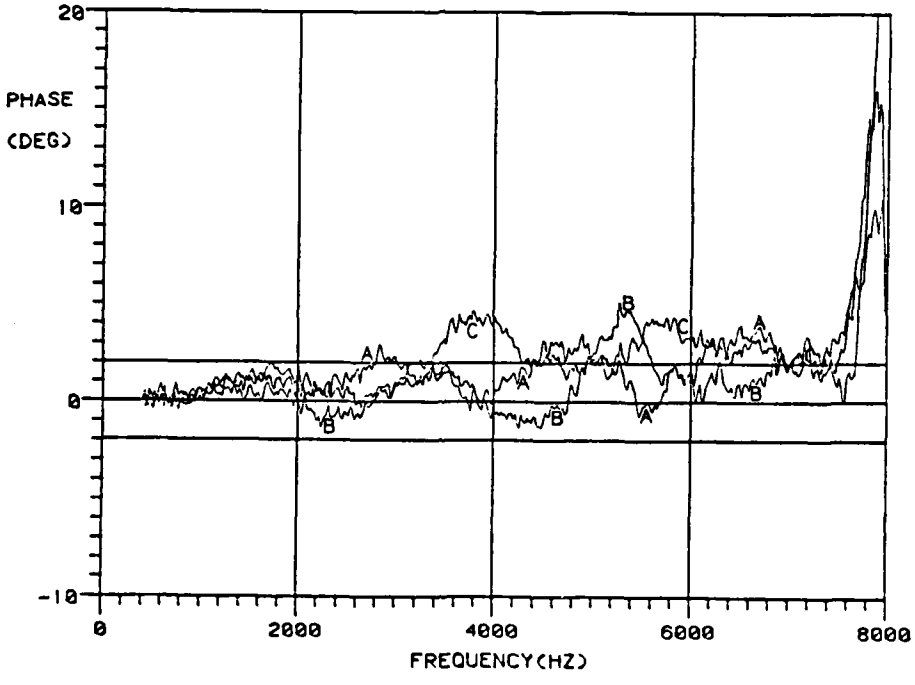

Figure 6.7(b): The Effect of Microphone 1 on the Phase Response of Microphone 2 for Various Distances D with the Microphones Extended by Goosenecks (1/2" Microphones)
Curve A: D=13mm; Curve B: D=25mm; Curve C: D=35mm

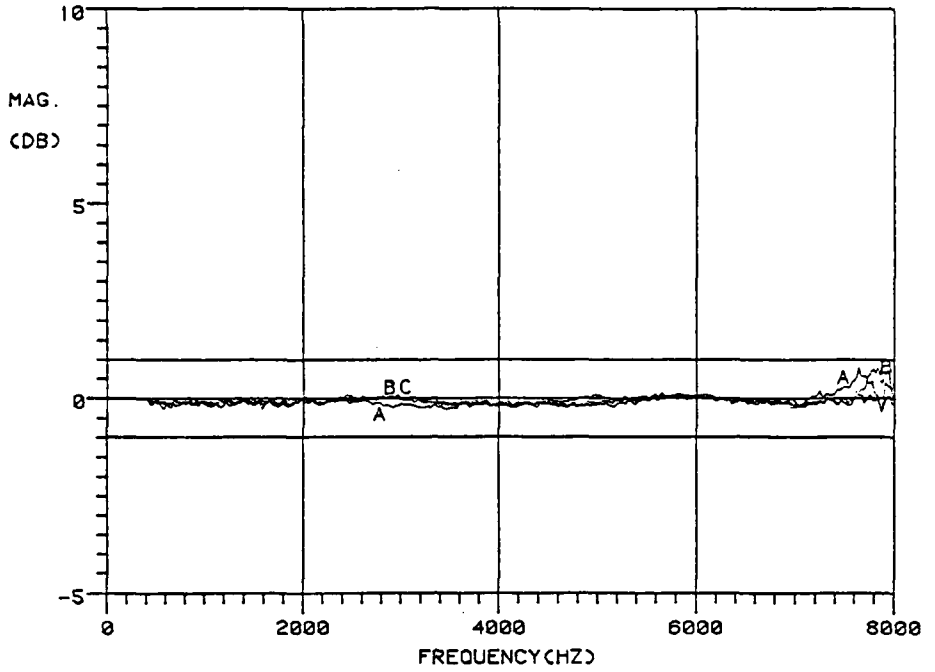

Figure 6.8(a): The Effect of Microphone 1 on the Magnitude Response of Microphone 2 for Various Distances D with the Microphones Extended by Goosenecks (1/4" Microphones)
Curve A: D=13mm; Curve B: D=25mm; Curve C: D=35mm

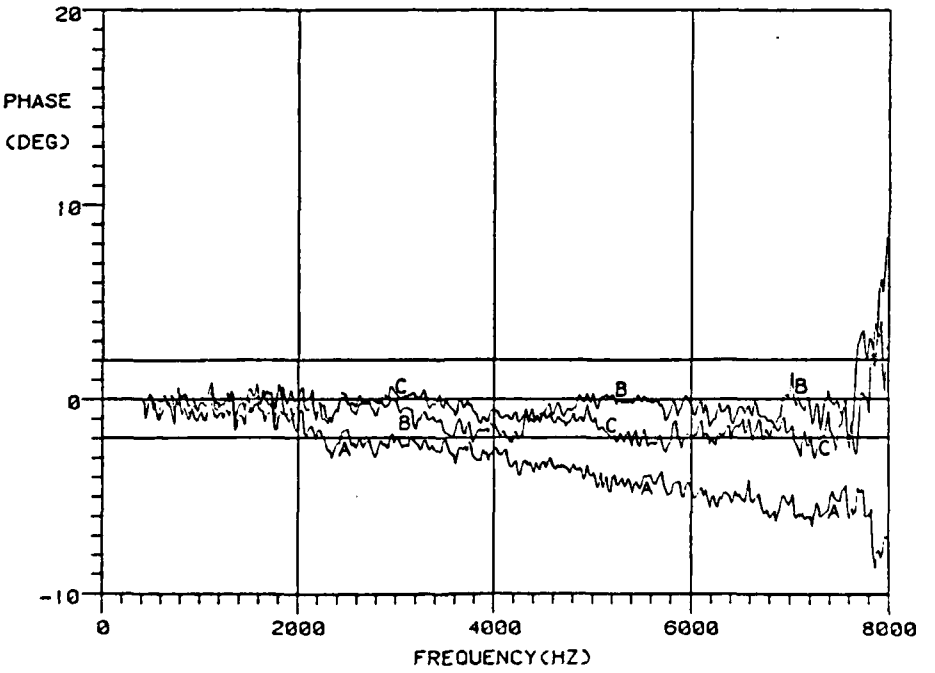

Figure 6.8(b): The Effect of Microphone 1 on the Phase Response of Microphone 2 for Various Distances D with the Microphones Extended by Goosenecks (1/4" Microphones)
Curve A: D=13mm; Curve B: D=25mm; Curve C: D=35mm

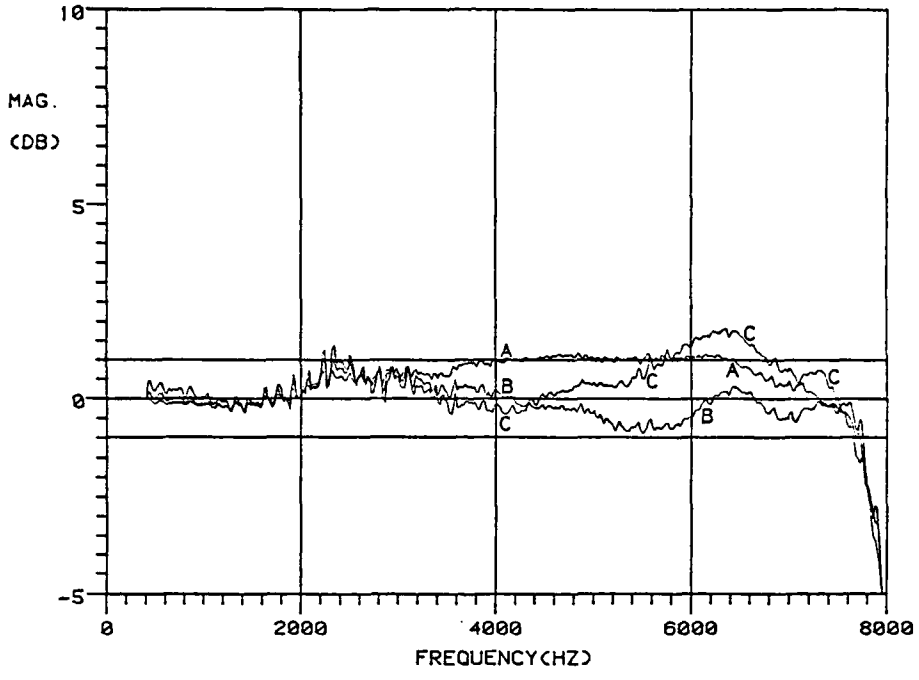

Figure 6.9(a): The Transfer Function Between the Two Microphones for Various Distances D and Extended by Goosenecks (1/2" Microphones) Curve A: D=13mm; Curve B: D=25mm; Curve C: D=35mm

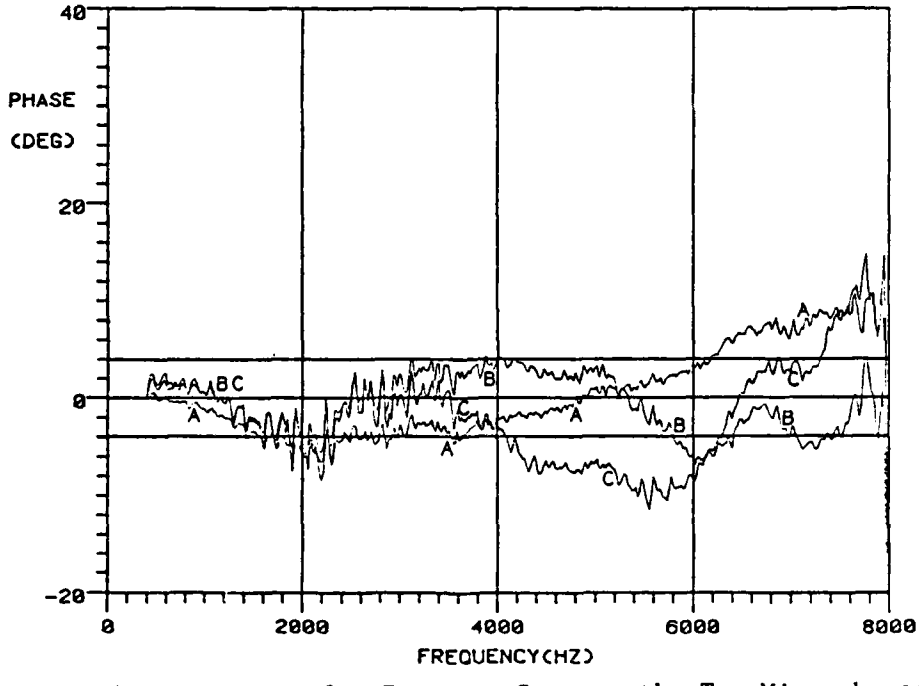

Figure 6.9(b): The Transfer Function Between the Two Microphones for Various Distances D and Extended by Goosenecks (1/2" Microphones) Curve A: D=13mm; Curve B: D=25mm; Curve C: D=35mm

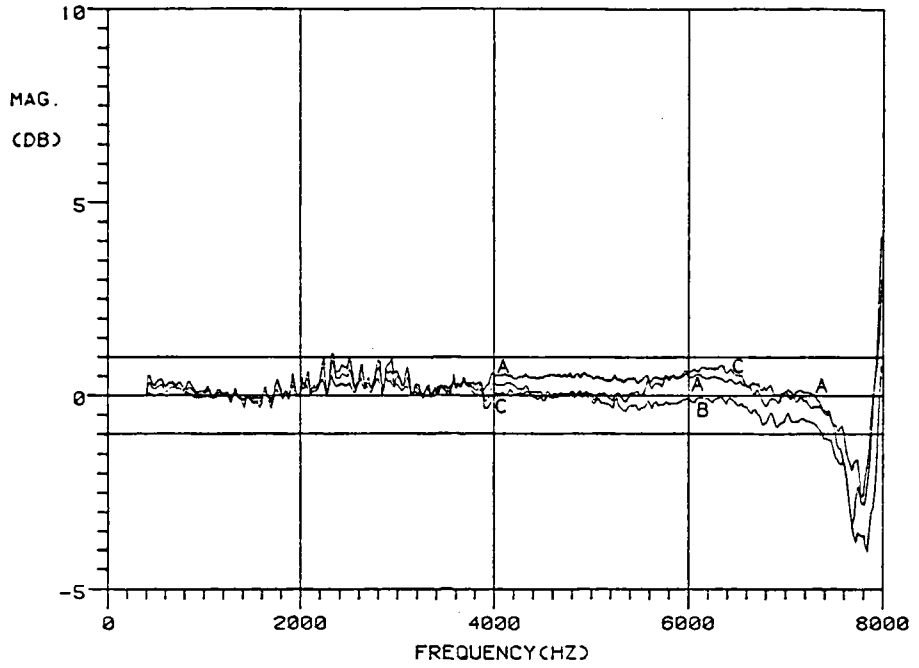

Figure 6.10(a): The Transfer Function Between the Two Microphones for Various Distances D and Extended by Goosenecks (1/4" Microphones)
Curve A: D=13mm; Curve B: D=25mm; Curve C: D=35mm

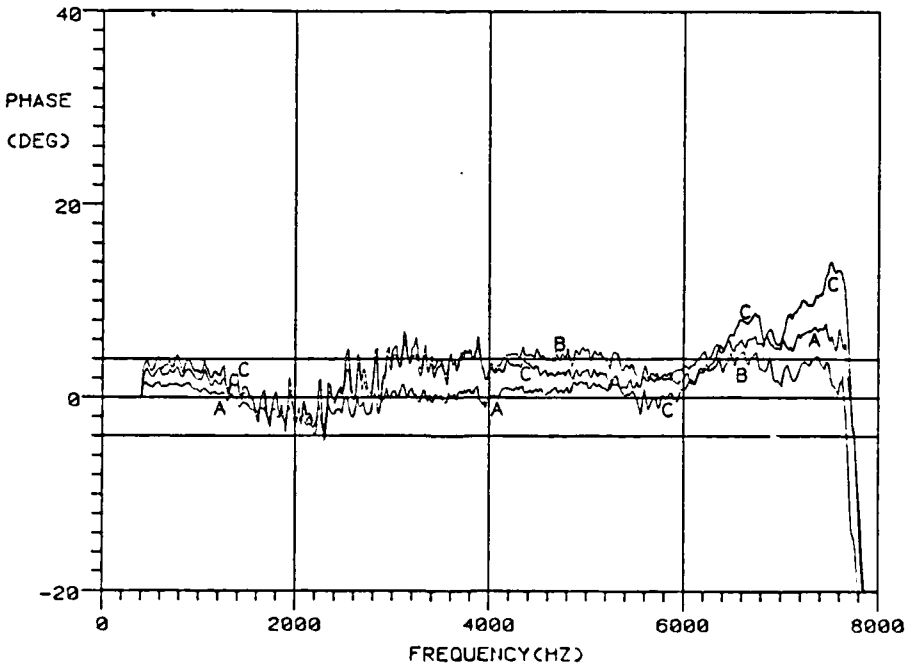

Figure 6.10(b): The Transfer Function Between the Two Microphones for Various Distances D and Extended by Goosenecks (1/4" Microphones)
Curve A: D=13mm; Curve B: D=25mm; Curve C: D=35mm

were corrected by the computer so that, ideally, both the amplitude and phase responses should have been represented by straight horizontal lines.

However, as Figures 6.9 and 6.10 reveal, the transfer functions were only slightly dependent on the frequency, and the effect was again smaller with the 1/4" microphones. As expected, the disturbance of the sound field by the 1/4" microphones was smaller with amplitude deviations of less than ± 1 dB. However, the phase deviations were several degrees at the higher frequencies.

CHAPTER 7

ERRORS FROM SECONDARY SOURCES AND THE MEASURING ENVIRONMENT

7.1 Introduction

All previous results pertaining to bias errors of the cross-spectral intensity method have been produced assuming only the measurement of a single sound source. Of course, in a normal measuring environment (in-situ), there could be more than a single sound source present when measuring a specific source that would contaminate the intensity measurement of this specific noise source. This secondary contaminating sound source may not only be an individual radiating source but could also be any reflections of the measuring sound field from nearby physical surfaces. The two-microphone intensity device may also be adversely influenced by a significant reverberant sound field. If there are errors in the intensity results caused by the reverberant environment, the intensity measurements would have to be performed closer to the primary sound source to insure that the direct field predominates. Therefore, the surrounding environment may substantially influence the qualification of a primary sound source in-situ, and empirical knowledge of these limitations of the cross-spectral intensity device is extremely important before excepting the results as accurate.

It should be noted that any influence by a secondary source upon the intensity measurement of the primary source will vary with the direction of sound-wave propagation from the secondary source because of the directional characteristics of the two-microphone acoustic intensity

device. Therefore, theoretically, a secondary sound source (a point source) located on-axis and perpendicular to the two-microphone intensity probe will not contaminate the intensity measurement of the primary source.

7.2 Uncorrelated Secondary Sources

In its simpliest form, errors introduced in the estimation of acoustic intensity by a second, uncorrelated[1] acoustic source may be evaluated by considering the bivariate stochastic process of Figure 7.1. The general theory of bias errors arising from a secondary source was derived very recently by Seybert (58), but no experimental data were given to support the basic conclusions.

7.2.1 The Normalized Bias Error

Using the schematic representation of an idealized acoustic intensity measurement (Figure 7.1), source 0 is considered the primary source being measured while source 0' is the second (contamination) source. The transfer functions H_{10}, $H_{10'}$, H_{20}, and $H_{20'}$ characterize the linear systems between each source and the measurement points 1 and 2. The influence of the primary source and the secondary source upon the measuring points 1 and 2 is represented by the respective Fourier-transformed pressures $P_1(f)$, $P_2(f)$ and $P_1'(f)$, $P_2'(f)$. If there exists phase and gain-mismatch errors from the measuring instrumentation, then the intensity results will also include the complex frequency responses

---

[1] the correlation quantity of zero specifies that two random variables x and y are said to be uncorrelated (4).

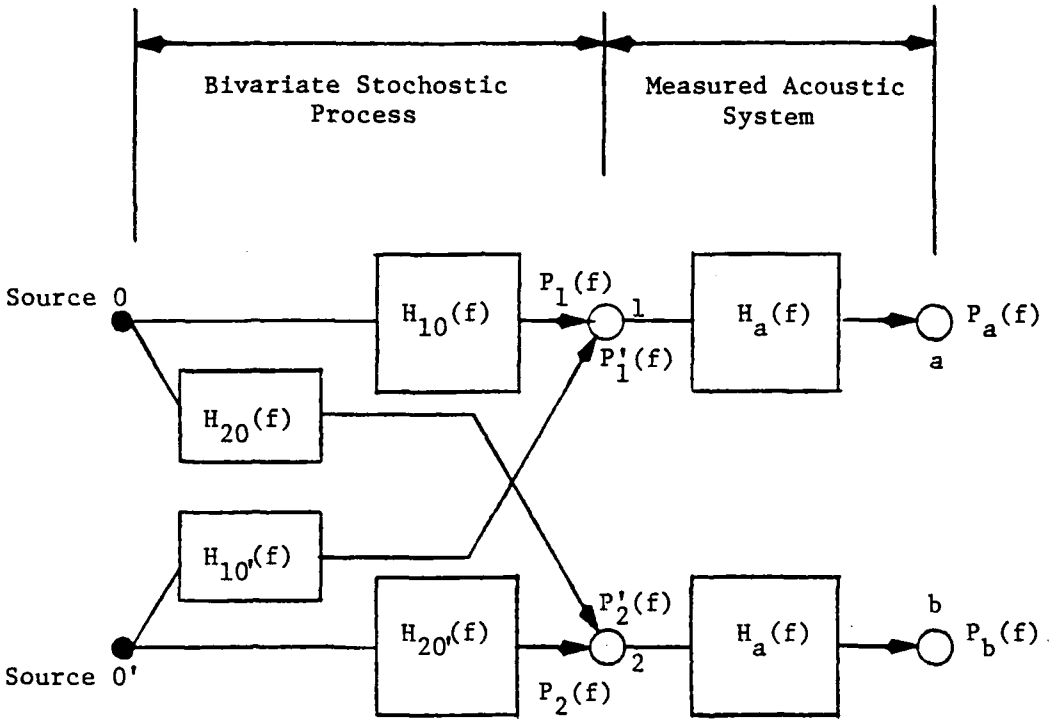

Figure 7.1: Schematic Representation of the Idealized Acoustic Intensity Measurement in the Presense of a Secondary Sound Source

of each individual microphone channel, $H_a(f)$ and $H_b(f)$, defined by Equations 5.11 and 5.12.

The total pressures at each measurement point via the instrumentation are

$$P_a(f) = [P_1(f) + P_1'(f)]H_a(f) \tag{7.1}$$

and

$$P_b(f) = [P_2(f) + P_2'(f)]H_b(f) \ . \tag{7.2}$$

Because the acoustic intensity method is proportional to the cross-spectrum between two measuring points, it is necessary to obtain the estimated cross-spectrum from the Fourier transforms of $P_a(f)$ and $P_b(f)$ by way of the cross-spectral definition (5),

$$\hat{G}_{ab}(f) = (\frac{2}{T})\langle P_a^*(f)P_b(f)\rangle \ , \tag{7.3}$$

where $P_a^*(f)$ is the complex conjugate of the transform $P_a(f)$ and T is the length of the raw data record. The expected value symbols of Equation 7.3 indicate that the quantity $\hat{G}_{ab}(f)$ is a smoothed cross-spectral estimate obtained by averaging n_d individual raw estimates of the cross-spectrum; i.e.

$$\langle P_a^*(f)P_b(f)\rangle = (\frac{1}{n_d})\sum_{i=1}^{n_d} P_{ai}^*(f)P_{bi}(f) \ . \tag{7.4}$$

Placing the total pressure values due to both the primary and secondary sources (Equations 7.1 and 7.2) into the estimated cross-spectral equation (7.3), the resulting cross-spectrum for the pressure values at points a and b due to the primary and secondary sources becomes

$$\hat{G}_{ab}(f) = [G_{12}(f) + G'_{12}(f)]|H_a(f)||H_b(f)|e^{-j\Delta\phi_{ab}} , \qquad (7.5)$$

where $G'_{12}(f)$ is the cross-spectrum due only to the secondary source. Notice that the cross-spectral products between P'_1 and P_2, P_1 and P'_2 do not appear because of the assumption that sources 1 and 2 are uncorrelated.

The normalized bias error (ε_b) was defined in Chapter 5 (Equation 5.19), and is repeated here as:

$$\varepsilon_b(f) = [E\{\hat{I}(f)\} - I(f)]/_{I(f)} . \qquad (7.6)$$

I(f), in this case, is the true acoustic intensity due only to a single primary source,[2]

$$I(f) \sim Im[G_{12}(f)] , \qquad (7.7)$$

and $E\{\hat{I}(f)\}$ is the estimated acoustic intensity influenced by both the primary and the secondary source and written as

$$E[\hat{I}(f)] \sim Im[\hat{G}_{ab}(f)]$$

$$\sim Im[G_{12}(f) + G'_{12}(f)]|H_a(f)||H_b(f)|e^{-j\Delta\phi_{ab}(f)} . \qquad (7.8)$$

Therefore, placing Equations 7.7 and 7.8 into the expression representing the normalized bias error (7.6), the bias due to a secondary source via instrumentation can be written as

$$\varepsilon_b(f) = |H_a||H_b|[|G_{12}|\sin(\phi_{12}+\Delta\phi_{ab})+|G'_{12}|\sin(\phi'_{12}+\Delta\phi_{ab})]/_{|G_{12}|\sin\phi_{12}} . \qquad (7.9)$$

---

[2] the proportionality symbol ~ is used because the factor $4\pi f\rho\Delta r$ is unnecessary for the final result and therefore ommitted.

For small $\Delta\phi_{ab}$, where $\cos\Delta\phi_{ab}\approx 1$ and $\sin\Delta\phi_{ab}\approx\Delta\phi_{ab}$, this expression (7.9) reduces to

$$\varepsilon_b(f) \approx |H_a||H_b|[(1 + \Delta\phi_{ab}\cot\phi_{12}) + (\underline{I}') + (\underline{I}'\Delta\phi_{ab}\cot\phi_{12}')] - 1 \ . \quad (7.10)$$

If there is no phase or gain mismatch between the measuring instrumentation, the normalized bias error (Equation 7.10) will simplify to

$$\varepsilon_b(f) = I'(f)/_{I(f)} \ , \quad (7.11)$$

the ratio of the secondary source intensity to the primary source intensity.

7.2.2 Experimental Setup and Procedure

The experimental setup for testing the effect of a secondary sound source upon the acoustic intensity measurement of a primary source is shown in Figure 7.2. The primary source was the previously-described enclosed flat-diaphragm loudspeaker, used for most of the cross-spectral intensity measurements. The secondary sound source consisted of a 4-1/2 in. cone-type loudspeaker (Philips model AD-5060/W8) placed at one end of a closed-back tube (a 4-1/2 in. diameter PVC pipe with a length of 3 ft.). This tube source, as it will be referred to, was a non-baffled sound source which hopefully models a point source in its operating range. Each sound source was electrically driven by its own separate random white-noise generator and amplifier to assure that two independent sources were used.

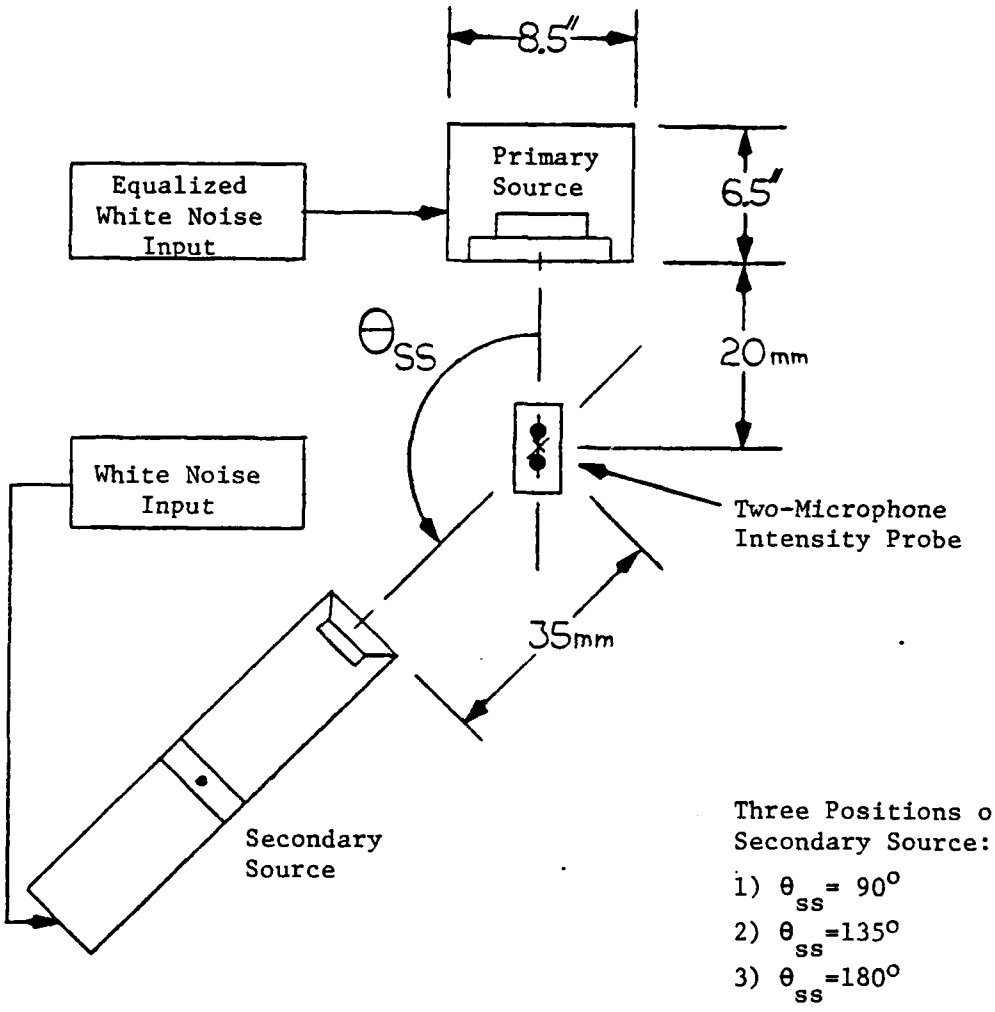

Figure 7.2: Experimental Set-Up Used to Investigate the Bias Errors of the Acoustic Intensity Technique from a Secondary Source

The intensity probe was generally located on-axis and normal to the primary source at a distance of 20 cm. The secondary source (the tube source) was placed 35 cm from the intensity probe at three separate angle positions; approximate secondary source angles of θ_{ss} = 90°, 135°, and 180° (see Figure 7.2). In addition, three different input levels to the tube source were used to provide a range of the secondary source strength upon the primary source intensity measurement. These secondary source input levels were established such that the intensity ratio (L_{ps}-L_{ss}) of the primary source intensity level (L_{ps}) to the secondary source intensity level (L_{SS}) was approximately 10 dB, 5 dB, or 0 dB. The specific angle θ_{ss} of secondary source incidence was set at 135° for the frequency range of 1500-4000 Hz.

All measurements were accomplished in the previously-described laboratory room and in the direct field of both sources where no significant sound-reflecting surfaces were present. However, the sound source itself (either the primary or secondary source) was a sound-reflecting surface. Therefore, to eliminate as much sound reflection from each source as possible, fiberglass surrounded the non-radiating area of the primary source to prevent source reflections (the tube source worked exceptionally well as a non-reflecting surface without adding acoustical treatment).

The general measuring procedure for these experiments was as follows: the primary source intensity was determined with the secondary source turned off; then the secondary source was added to the sound field and the intensity due to the combined sources was measured; also, while both sources were operating, the coherence function between the

two microphones was measured[3]; and lastly, the intensity of only the secondary source was measured. With these results stored on the computer, the experimental bias error from uncorrelated secondary sound sources could be compared to the theoretical bias error calculated from Equation 7.11 (note that all of the cross-spectral intensity data were corrected for any phase and gain-mismatch error between the microphone measuring systems).

7.2.3 Results

For all the intensity measurements related to bias errors from a secondary source (sometimes abbreviated ss), the sound pressure frequency response of the primary source (sometimes abbreviated ps) was approximately uniform over the frequency range 80-4000 Hz, and the sound pressure frequency response of the secondary source was essentially no different than that of the primary source for the frequency range 1500-4000 Hz.

Before describing the experimental results, it should be noted that all plots labeled "INT. MAG. (DB)" contain lettered curves which display the following measurements: curve A, the measurement of only the primary source intensity; curve B, the intensity measurement when both the primary and secondary sources are operating; and curve C, the intensity level of only the secondary source. For the related plots labeled "BIAS ERROR (DB)", curve A represents the experimental bias error calculated

---

[3] typically, the coherence function between the two microphones of the intensity probe is approximatly unity (perfect coherence) for a single sound source measurement in the direct field.

by subtracting the intensity level of the combined primary and secondary sources from the individual primary source intensity level, and curve B represents the theoretical bias error calculated using Equation 7.11 (where $I'(f)$ and $I(f)$ are the intensity levels due only to the individual secondary source and primary source respectively). Note also that all experimental calculations of the bias error contain some anomalies created by the random error associated with the finite averaging of n_d individual raw estimates of the cross-spectrum. This random error was reduced considerably (to an approximate value of less than ± 0.5 dB) by taking the largest possible averaging of each cross-spectral measurement available on the SD360 spectral analyzer (2^{12}, equilvalent to 4096 samples). Figures 7.3(a) and 7.3(b) show the random error of the intensity measurement for $n_d = 256$ and $n_d = 4096$ respectively. These random error plots were accomplished by comparing two separate intensity samples of the same sound source.

Figure 7.4(a) exhibits the influence of a secondary sound source upon the primary source intensity when $L_{ps}-L_{ss} = 10$ dB and radiating at an angle $\theta_{ss} = 135^{o}$. Figure 7.4(b) displays the bias error (both the experimental and theoretical bias error) for the results of Figure 7.4(a). For this particular test (Figure 7.4), there was a small but noticeable amount of error caused by the additional sound source upon the primary source intensity (0.5 dB maximum), and the coherence departs from the unity value above the frequency range where the secondary source has the greatest influence (above 1500 Hz). It also can be realized that the experimental bias error compares favorably with the calculated value of bias error. Because the bias error for this

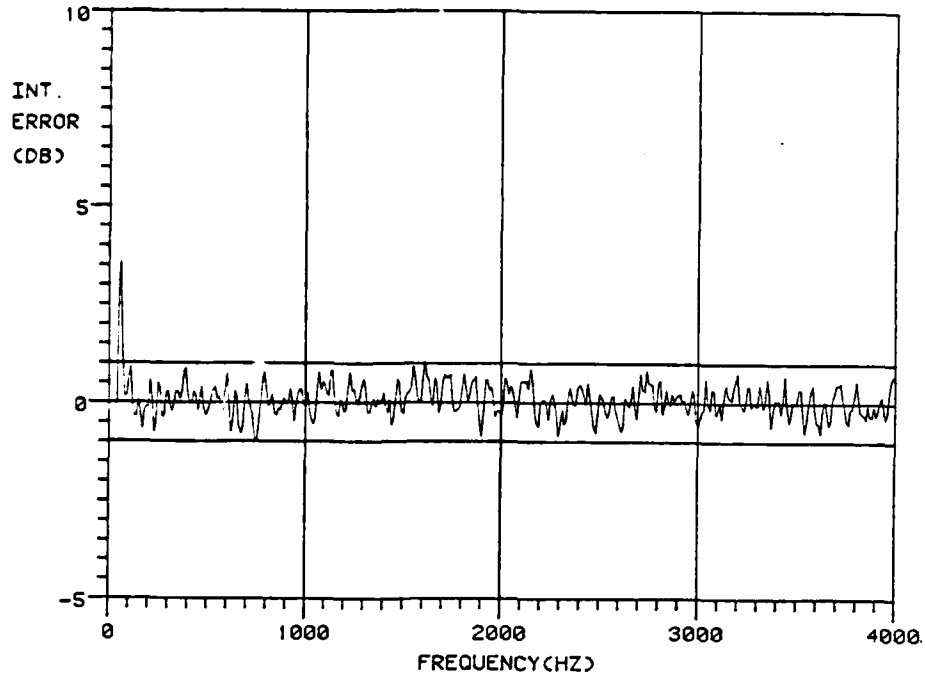

Figure 7.3(a): The Random Error of the Intensity Measurements Associated to a Finite Averaging of n_d = 256

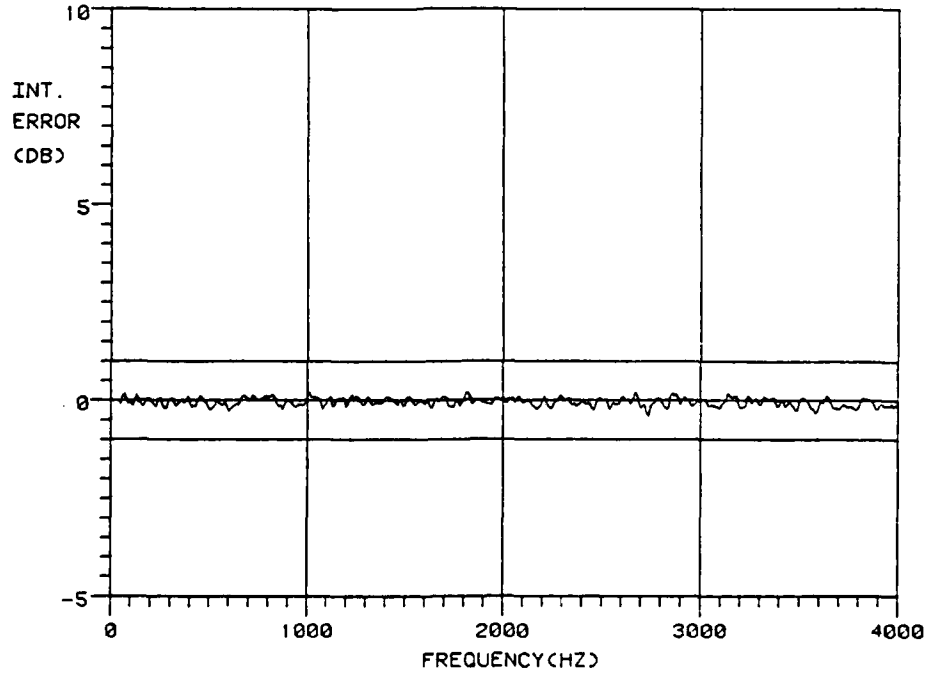

Figure 7.3(b): The Random Error of the Intensity Measurements Associated to a Finite Averaging of n_d = 4096

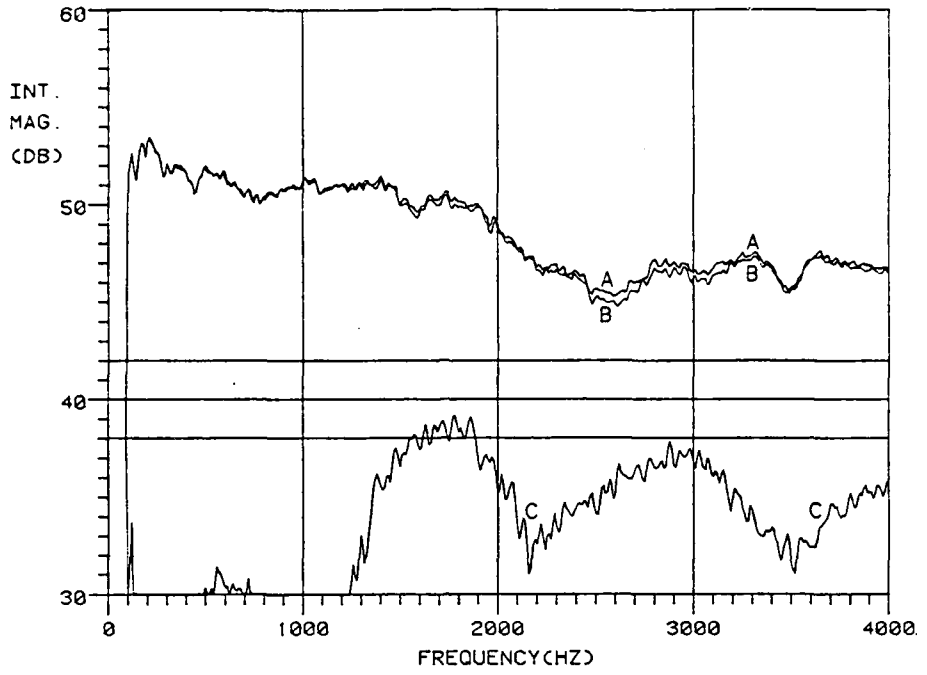

Figure 7.4(a): Cross-Spectral Intensity Measurements for L_{ps}-L_{ss}= 10 dB and θ_{ss}= 135°
Curve A: The Intensity of Only the Primary Source
Curve B: The Intensity with Both PS and SS Operating
Curve C: The Intensity of Only the Secondary Source

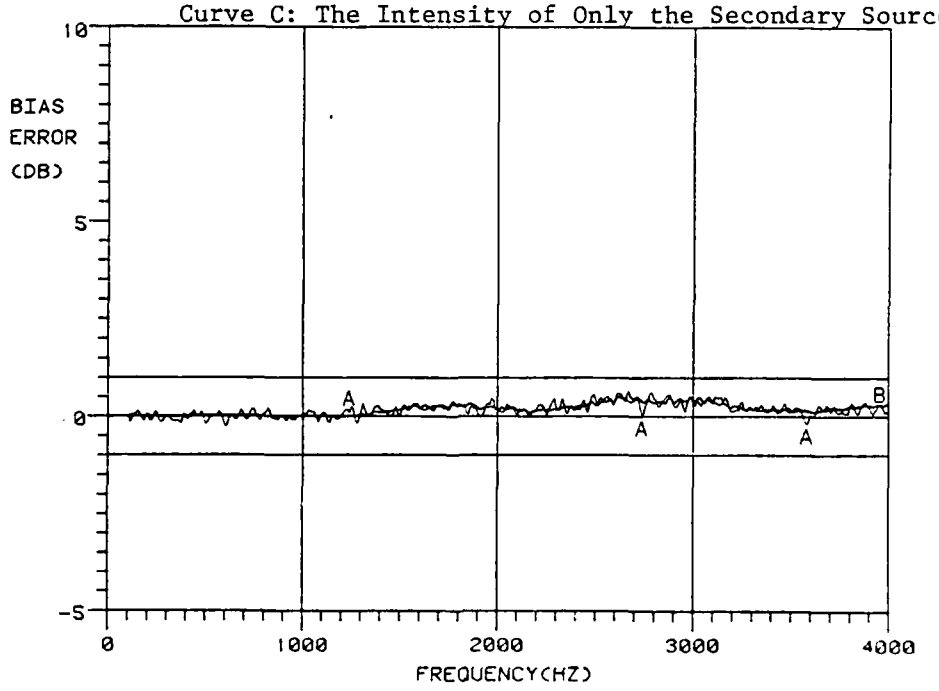

Figure 7.4(b): Bias Error Due to the Secondary Source for L_{ps}-L_{ss}= 10 dB and θ_{ss}= 135°
Curve A: The Experimental Bias Error
Curve B: The Theoretical Bias Error

particular intensity ratio, $L_{ps}-L_{ss}$ = 10 dB, was insignificant, larger secondary source intensity levels were then tried, and no other measurements were attempted for $L_{ps}-L_{ss}$ = 10 dB.

The next set of experiments (Figures 7.5-7.7) display the influence of a secondary source upon the primary source intensity for for $L_{ps}-L_{ss}$ = 5 dB and radiating at angles θ_{ss} = 90°, 135°, and 180°. For Figure 7.5, where θ_{ss} = 135°, the bias error becomes more significant than that of the measurement for $L_{ps}-L_{ss}$ = 10 dB and follows the trend of greater error for a smaller intensity ratio of primary source level to secondary source level. This finding is exactly the result predicted by the theoretical bias error equation (7.11). Then, using the same input for $L_{ps}-L_{ss}$ = 5 dB at θ_{ss} = 135°, the secondary source configuration was placed at the angle θ_{ss} = 90° (Figure 7.6). It can be immediately noticed that the secondary source intensity was reduced substantially even though the input level was the same as with the test configuration of Figure 7.5 (where θ_{ss} = 135°), and no doubt that this result was due to the directional characteristics of the two-microphone intensity device.

The resulting bias errors from the primary-secondary source configuration of Figure 7.6(b) are interesting because they show bias errors which have both positive and negative values. This indicates that the intensity flow of the secondary source adds to the primary source intensity in some frequency regions and subtracts from the primary source intensity in other frequency regions. A similar analogy would be the addition and subtraction of vector quantities whereby the vector intensity of the secondary source flowing in the same direction

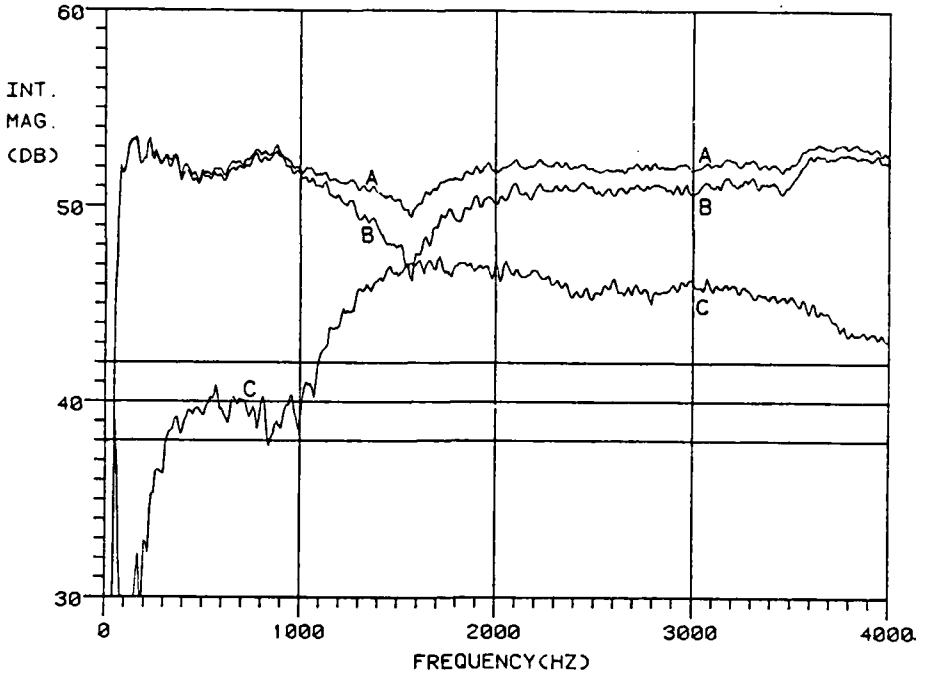

Figure 7.5(a): Cross-Spectral Intensity Measurements for L_{ps}-L_{ss}= 5 dB and θ_{ss}= 135°
Curve A: The Intensity of Only the Primary Source
Curve B: The Intensity with Both PS and SS Operating
Curve C: The Intensity of Only the Secondary Source

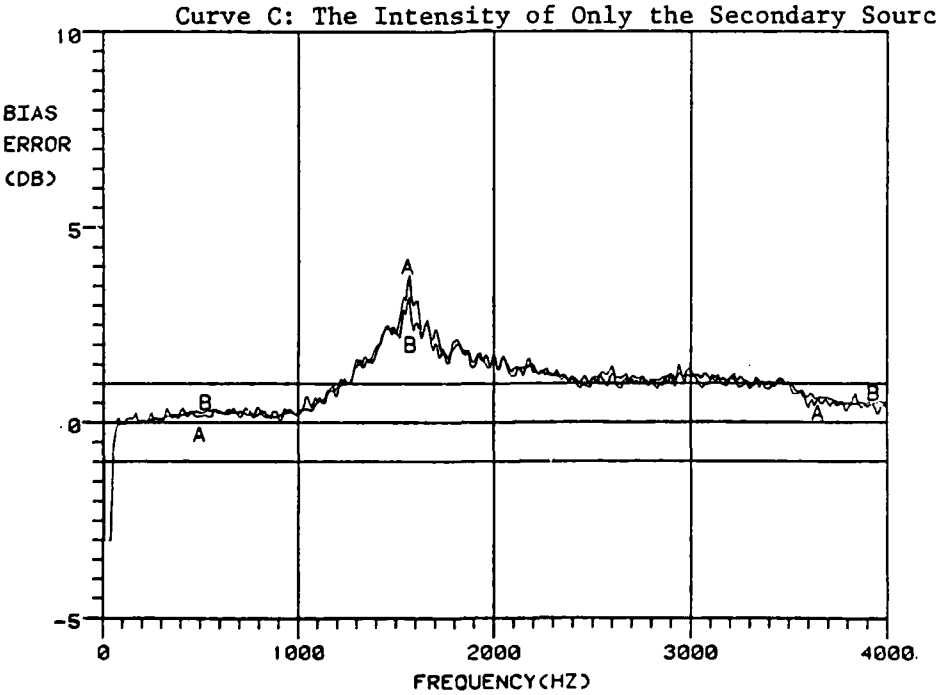

Figure 7.5(b): Bias Error Due to the Secondary Source for L_{ps}-L_{ss}= 5 dB and θ_{ss}= 135°
Curve A: The Experimental Bias Error
Curve B: The Theoretical Bias Error

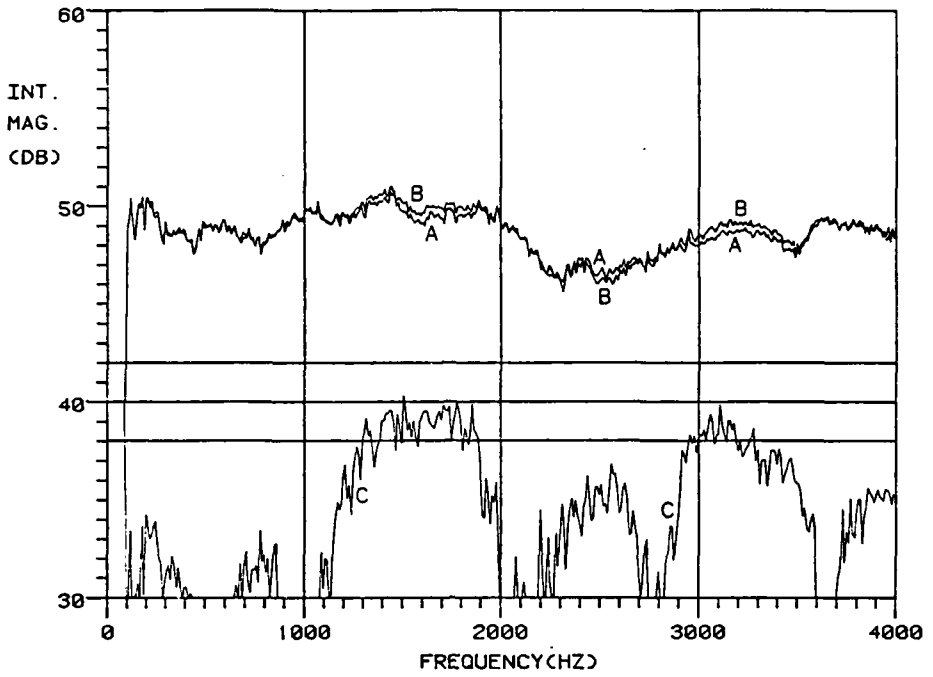

Figure 7.6(a): Cross-Spectral Intensity Measurement for L_{ps}-L_{ss}= 5 dB and θ_{ss}= 90°
Curve A: The Intensity of Only the Primary Source
Curve B: The Intensity with Both PS and SS Operating
Curve C: The Intensity of Only the Secondary Source

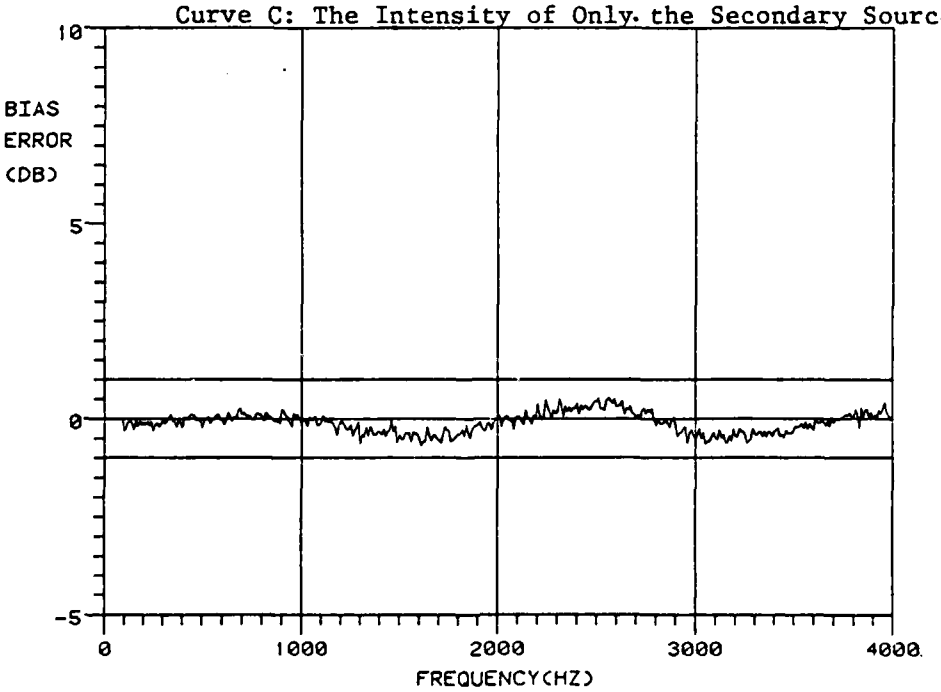

Figure 7.6(b): Bias Error (Experimental Only) Due to the Secondary Source for L_{ps}-L_{ss}= 5 dB and θ_{ss}= 90°

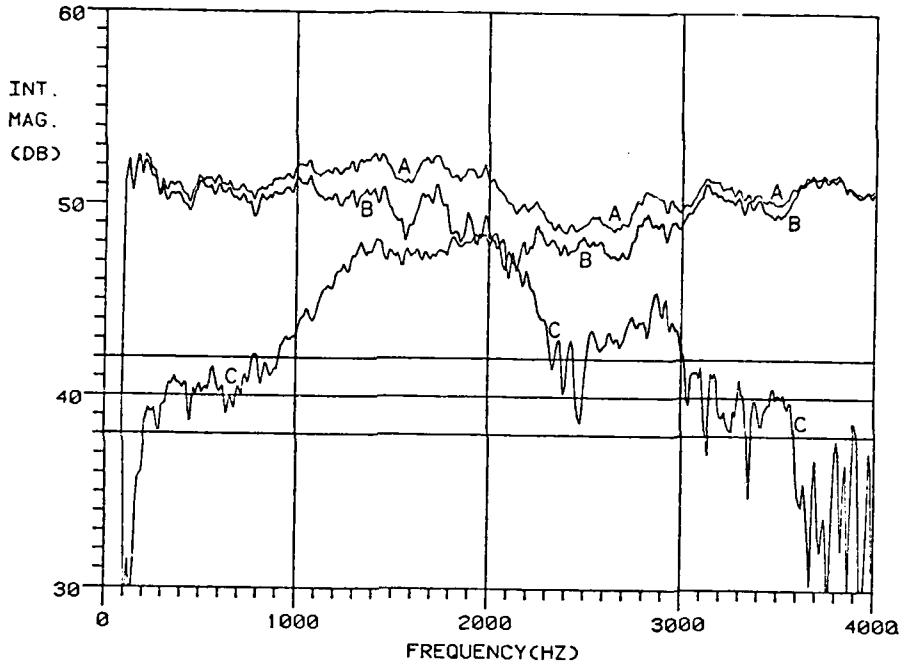

Figure 7.7(a): Cross-Spectral Intensity Measurements for L_{ps}-L_{ss}= 5 dB and θ_{ss}= 180°
Curve A: The Intensity of Only the Primary Source
Curve B: The Intensity with Both PS and SS Operating
Curve C: The Intensity of Only the Secondary Source

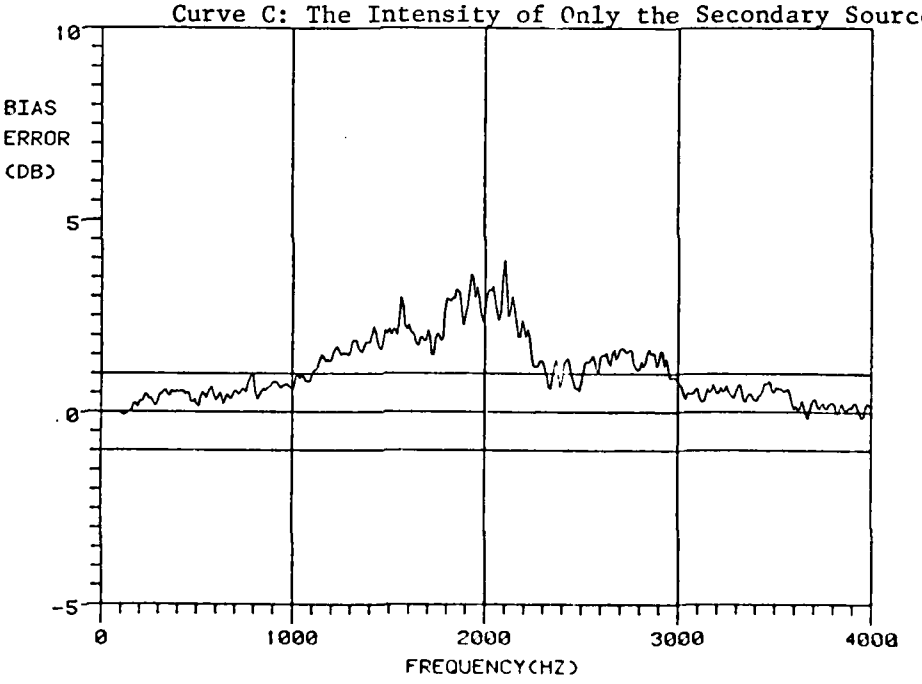

Figure 7.7(b): Bias Error (Experimental Only) Due to the Secondary Source for L_{ps}-L_{ss}= 5 dB and θ_{ss}= 180°

as the primary source intensity would give acoustic intensity values which are greater than the primary source operating alone and vice versa.

When the secondary source was located at the approximate angle $\theta_{ss} = 180^{o}$ (still using $L_{ps}-L_{ss} = 5$ dB), the influence of the secondary source upon the primary source intensity should be greater than the previous results of the primary-secondary source configurations used for Figures 7.5 and 7.6. And indeed, this fact was demonstated for the primary-secondary source arrangement using $\theta_{ss} = 180^{o}$ and $L_{ps}-L_{ss} = 5$ dB in Figure 7.7. The intensity flow of the secondary source was then opposite the intensity flow of the primary source, and the results (Figure 7.7(b)) showed an increase in the bias error. It should be noted that practically, for all the primary-secondary source configurations, there exists the possibility of significant sound reflections from the individual sound sources which could influence the data, but it was determined that any effect from these reflections was minimal after certain precautions were taken.

The last set of intensity data pertaining to bias errors from an uncorrelated secondary source (Figure 7.8) used $L_{ps}-L_{ss} = 0$ dB while locating the secondary source at an angle $\theta_{ss} = 135^{o}$. With this arrangement, the intensity level of the secondary source was essentially equal to the primary source intensity for the frequency region 2000-3500 Hz. Therefore, within this frequency range of 2000-3500 Hz, Figure 7.8(a) shows that the intensity method no longer was capable of accurately measuring the acoustic intensity flow from the primary source. The vector intensity of the secondary source can be considered

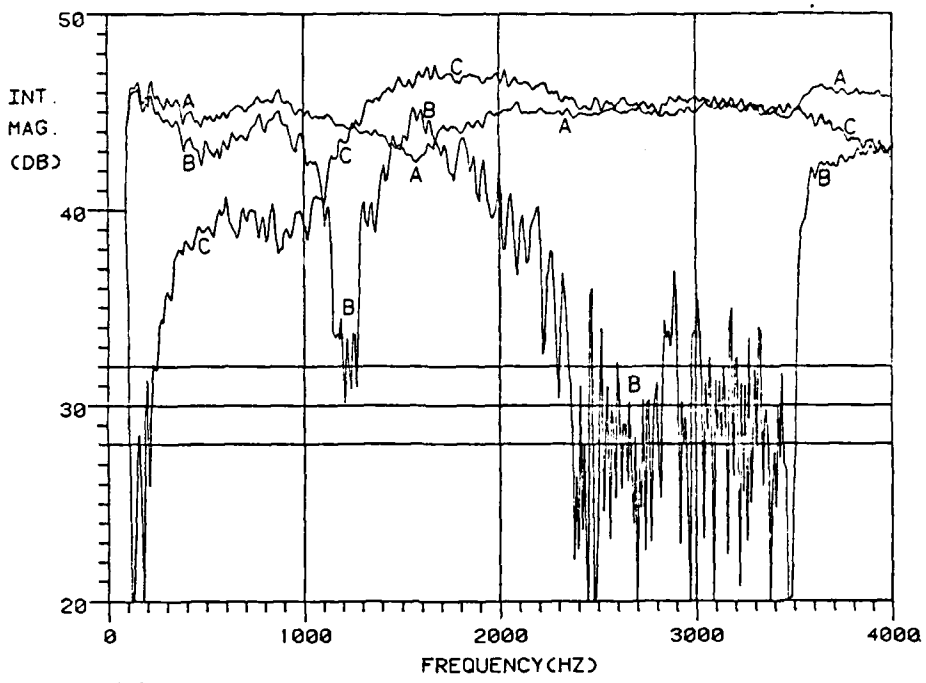

Figure 7.8(a): Cross-Spectral Intensity Measurements for L_{ps}-L_{ss}= 0 dB and θ_{ss}= 135°
Curve A: The Intensity of Only the Primary Source
Curve B: The Intensity with Both PS and SS Operating
Curve C: The Intensity of Only the Secondary Source

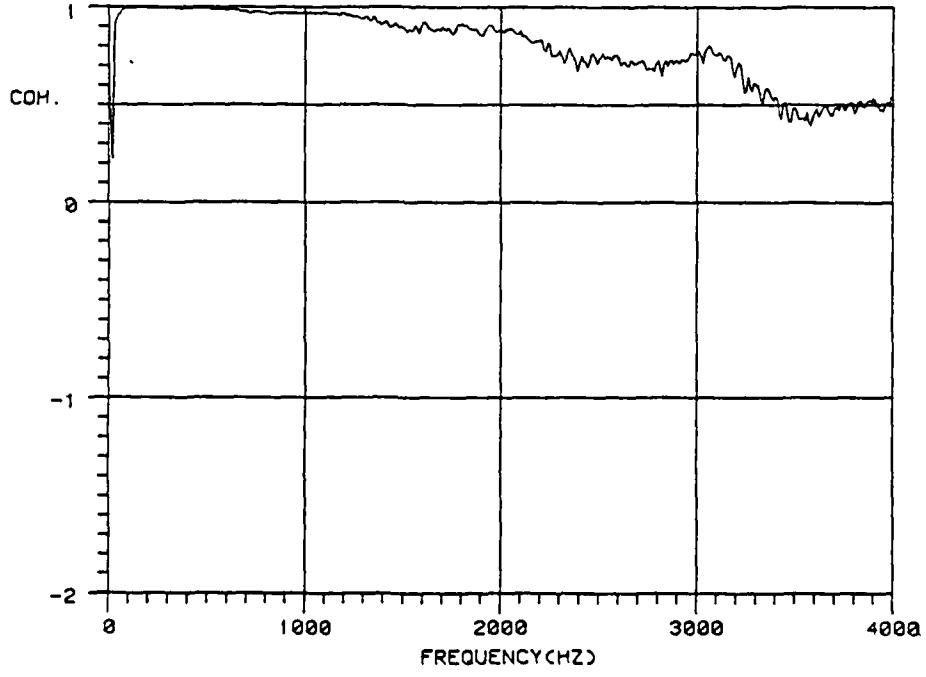

Figure 7.8(b): The Coherence Function Between the Two Microphones Used for the Cross-Spectral Intensity Measurement with Both Primary and Secondary Sources Operating (L_{ps}-L_{ss}= 0 dB)

to be equal but opposite to the primary source intensity for this specific frequency region thereby creating total cancelation of the acoustic intensities.

7.2.4 Implications of the Results when Measuring Sound Power

Up until now, only the influence of the acoustic intensity of an uncorrelated secondary source upon the primary source intensity at one spacial location was considered, but if the intensity method is used to determine the total sound power radiated from a sound source by integrating the intensity values normal to the surface area enveloping the measured primary noise source (Equation 2.1), the sound power contribution of the uncorrelated secondary source(s) exterior to the primary source measuring surface will be zero by satisfying the relation[4]

$$\iint_S I_n(\text{secondary source}) \cdot dS = 0 \ . \qquad (7.12)$$

Therefore, there would be theoretically no bias error in the measurement of the acoustic power of a specific noise source from other contaminating sources located outside the primary measuring enclosed envelop, and the precision of this measurement is then related to the number of measurement points taken and to the variance (random errors) defined by the regularity and the distribution of the normal acoustic intensities in the measuring envelop (depending on the directivity response and the stationary operation of the primary source, the effect of the exterior noise, and the choice of the position and shape of the

---

[4] assuming there is no absorption (attenuation) of sound within the volume enclosed by the measuring surface.

measuring surface).

7.3 Intensity Measurements in the Reverberant Sound Field

As stated previously in Section 3.5, the accuracy of the two-microphone cross-spectral intensity method may be influenced by the presence of a strong reverberant sound field. Whereby, the three-dimensional reverberant sound field can be described by using the acoustic parameters of pressure, three mutually perpendicular components of the particle velocity, and the corresponding three components of the intensity vector; the two-microphone intensity meter only provides the acoustic intensity component in the direction along the line joining the microphone pair. Therefore, if the total intensity vector is required at a point in the reverberant field, three separate intensity measurements have to be taken.

Cross-spectral intensity measurements can be performed successfully outside the direct field of a noise source in-situ. In an isotropic reverberant sound field which consists of modes representing standing waves, the acoustic intensity through a field point is zero. In an acoustic confinement in which the sound may be well scattered but not completely diffused, the cross-spectral intensity measurement will not be zero if there is a preferred direction of power flow within the enclosure (6).

The reflective sound field can be thought of as a background noise caused by the relevant image sound sources. Therefore, the same law of energy conservation described in Section 7.2.4 should apply when integrating the intensity measurement over a sound source surface to

evaluate sound power. Excluding any sound absorption inside the space enclosing the measuring surface, the combined intensities of the exterior (contaminating) reflected noise will yield a theoretical value of zero, and the sound power measurement accomplished by integrating the acoustic intensity over the measuring surface area suppresses the reflected sound while the radiated sound waves by the primary sound source under examination remain unbiased.

7.3.1 Experimental Investigation

To understand the capabilities of the cross-spectral intensity meter in a reverberant sound field, on-axis intensity measurements of the previously-described flat-diaphragm sound source were taken at distances extending from 20 cm (in the direct field) to 4.0 m (in the assumed reverberant field). The sound source was located in the same laboratory room used for most all the intensity results and at a physical position not near any significant sound reflectors.

Figures 7.9-7.11 display acoustic intensity data calculated from assumed free-field pressure values ($p^2/\rho c$) and the two-microphone cross-spectral procedure (using a Δr=13 mm). Figures 7.9(a) and 7.9(b) show that the intensity calculated from the free-field pressures (Curve A in all figures) and the intensity measured by the the cross-spectral method (Curve B in all figures) compared very favorably. Locating the intensity probe at 80 cm (Figure 7.10(a)) and at 160 cm (Figure 7.10(b)) from the source, more radical fluctuations of the intensity levels were obtained, and evidently, the sound receiver was beginning to be affected by the reverberant sound field. Even so, the cross-spectral intensity

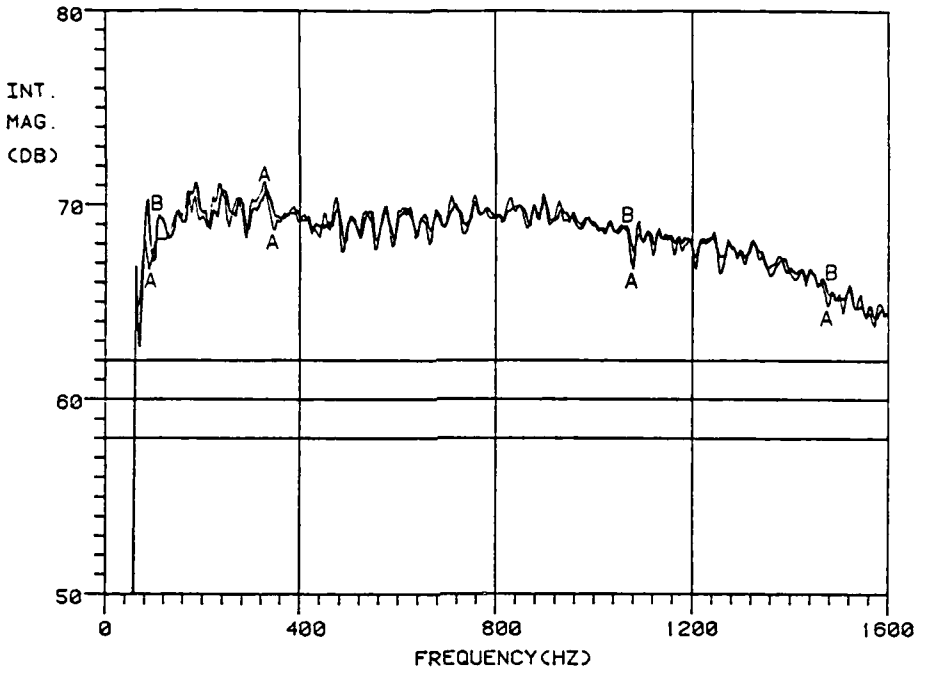

Figure 7.9(a): The Acoustic Intensity of a Loudspeaker Sound Source at a Distance of 20 cm
Curve A: Intensity Calculated Using Free-Field Pressure
Curve B: Intensity Measured by the Cross-Spectral Method

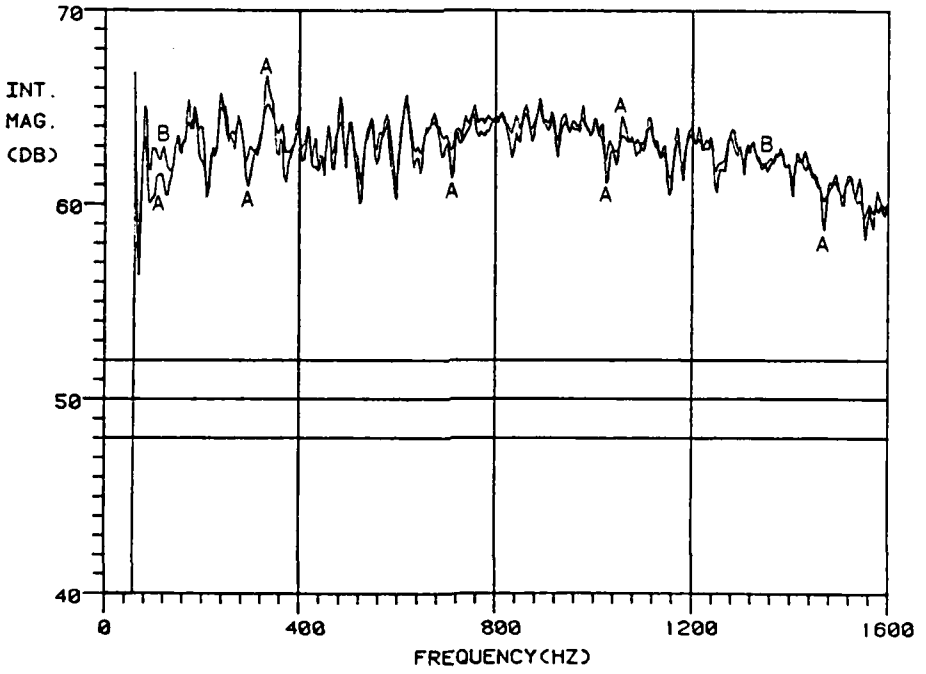

Figure 7.9(b): The Acoustic Intensity of a Loudspeaker Sound Source at a Distance of 40 cm
Curve A: Intensity Calculated Using Free-Field Pressure
Curve B: Intensity Measured by the Cross-Spectral Method

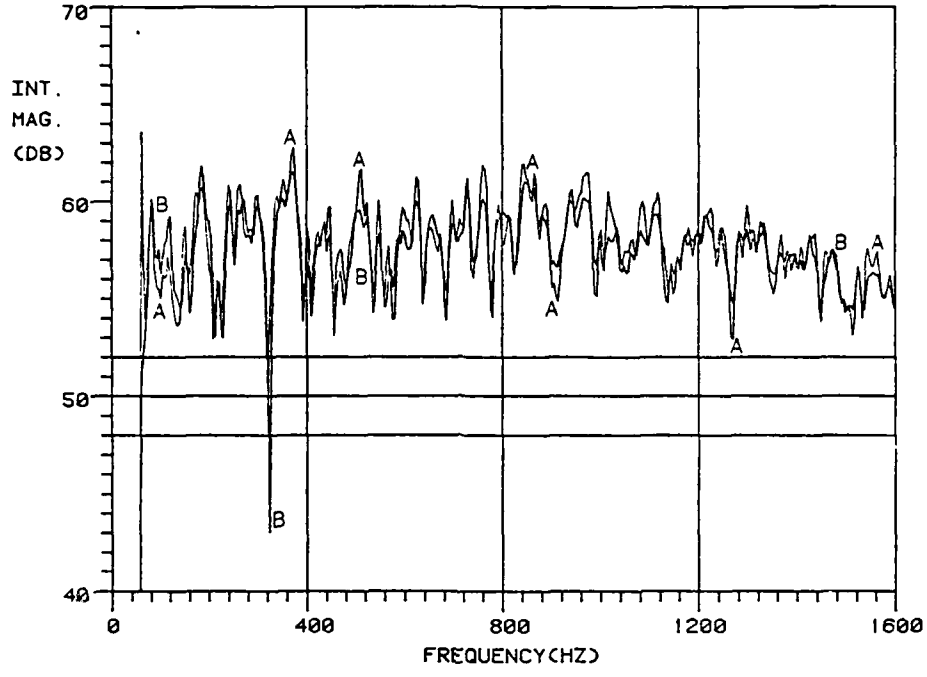

Figure 7.10(a): The Acoustic Intensity of a Loudspeaker Sound Source at a Distance of 80 cm
Curve A: Intensity Calculated Using Free-Field Pressure
Curve B: Intensity Measured by the Cross-Spectral Method

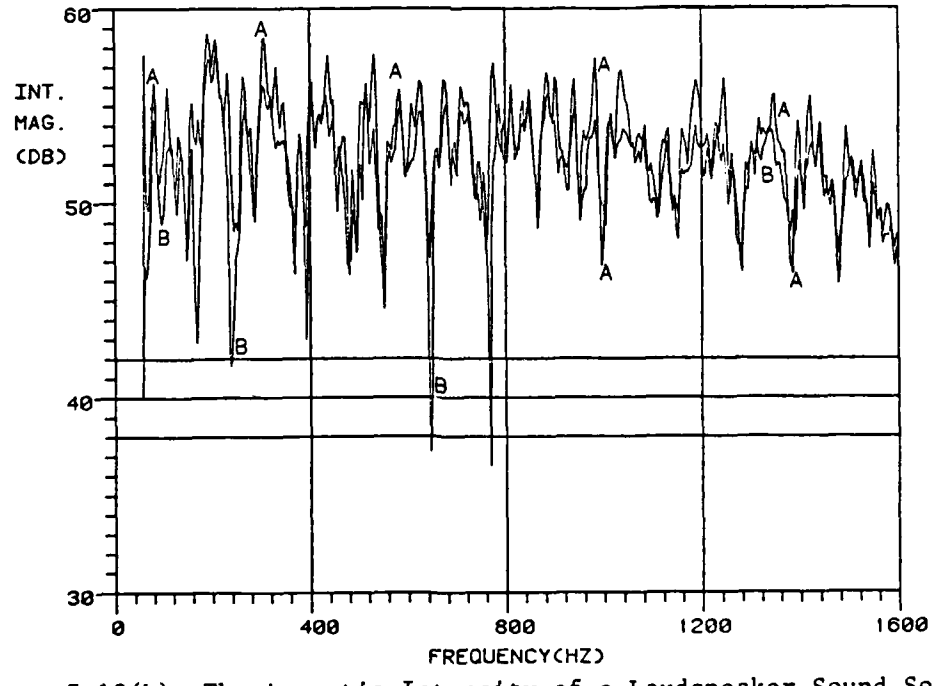

Figure 7.10(b): The Acoustic Intensity of a Loudspeaker Sound Source at a Distance of 160 cm
Curve A: Intensity Calculated Using Free-Field Pressure
Curve B: Intensity Measured by the Cross-Spectral Method

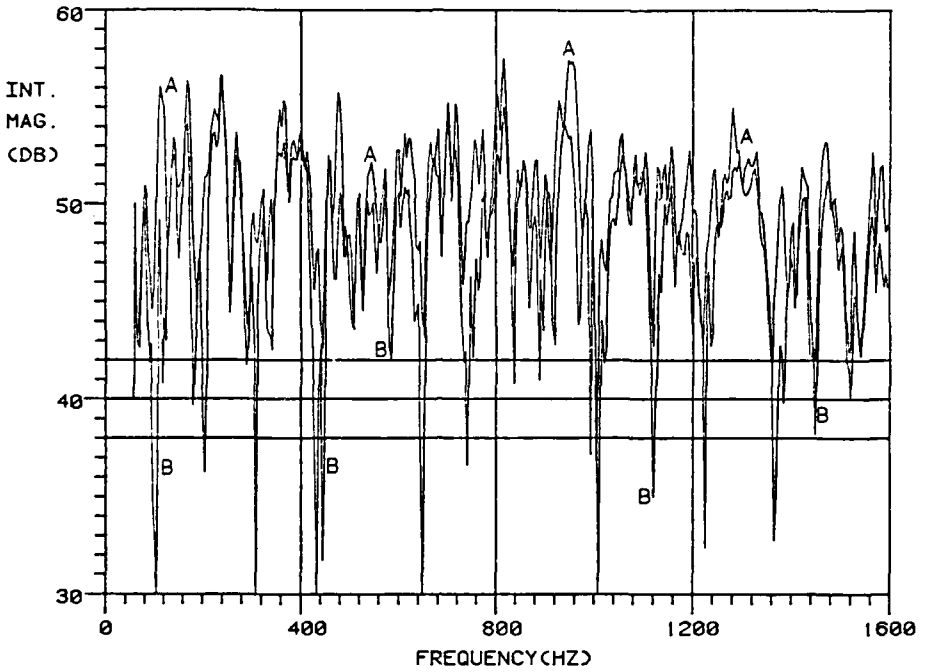

Figure 7.11(a): The Acoustic Intensity of a Loudspeaker Sound Source at a Distance of 250 cm
Curve A: Intensity Calculated Using Free-Field Pressure
Curve B: Intensity Measured by the Cross-Spectral Method

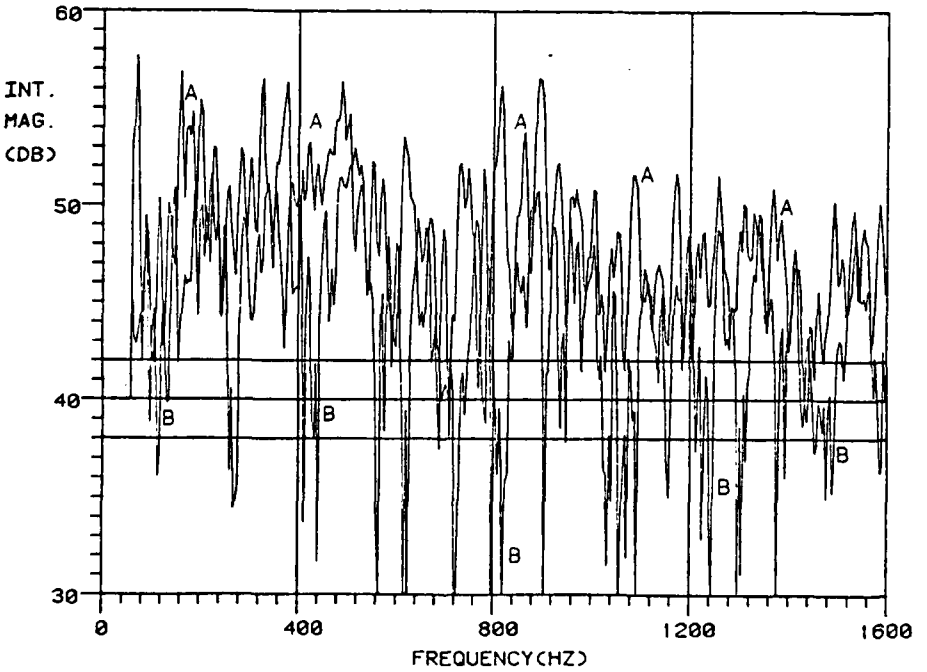

Figure 7.11(b): The Acoustic Intensity of a Loudspeaker Sound Source at a Distance of 4.0 m
Curve A: Intensity Calculated Using Free-Field Pressure
Curve B: Intensity Measured by the Cross-Spectral Method

measurements of Figure 7.10 were approximately equal to the intensity measurements from assumed free-field sound presure levels.

Intensity measurements were then taken at the distances of 250 cm (Figure 7.11(a)) and 4.0 m (Figure 7.11(b)). These intensity measurements of Figure 7.11 indicate that there was a more significant influence of the reverberant field upon the measurements. Also, the intensity levels calculated from the pressure values were consistantly higher than that of the cross-spectral intensity.

Even though the intensity plots of Figures 7.9-7.11 show tendencies, it was very difficult to make any conclusions about the data because of the fluctuating nature of the measurements in the more reverberant field. Therefore, a smoothing process was utilized with all the intensity data of Figures 7.12-7.14 depending upon the amount of variation in the measurements. This smoothing processs was a continuous linear average of each individual intensity data with other neighboring intensity data over the frequency range of interest. For example, if the intensity value at 400 Hz was smoothed with a smoothing factor (S.F.) of 10, then the 10 intensity values directly before and after the data point of interest would be averaged with that intensity value at 400 Hz.

The smoothed intensity levels calculated from free-field pressure values and the smoothed cross-spectral intensity levels at the distances of 20 cm (Figure 7.12(a)), 40 cm (Figure 7.12(b)), and 80 cm (Figure 7.13(a)) were equilvalent for all practical purposes. Increasing the intensity probe distance from the source, the intensity levels from the two different measurement procedures began to separate at the distance

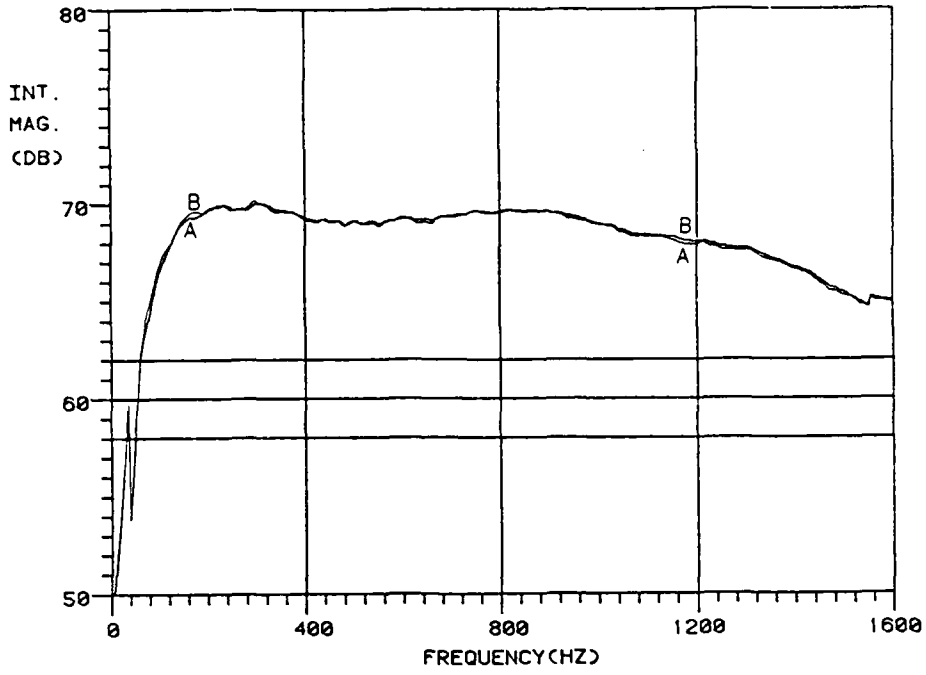

Figure 7.12(a): The "Smoothed" Acoustic Intensity of a Loudspeaker Sound Source at a Distance of 20 cm (Smoothing Factor = 10)
Curve A: Intensity Calculated Using Free-Field Pressure
Curve B: Intensity Measured by the Cross-Spectral Method

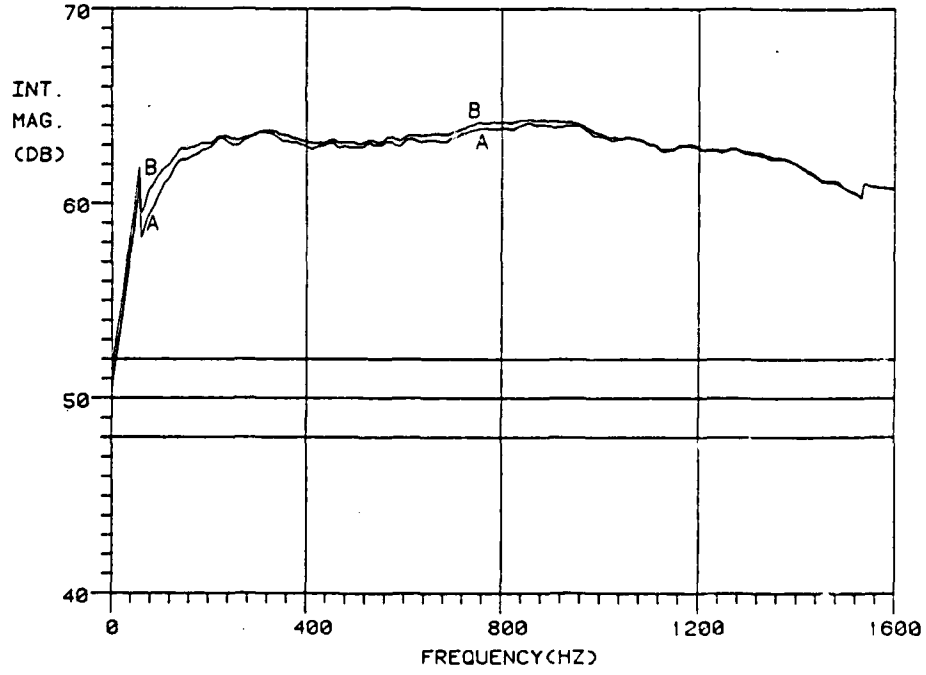

Figure 7.12(b): The "Smoothed" Acoustic Intensity of a Loudspeaker Sound Source at a Distance of 40 cm (S.F. = 15)
Curve A: Intensity Calculated Using Free-Field Pressure
Curve B: Intensity Measured by the Cross-Spectral Method

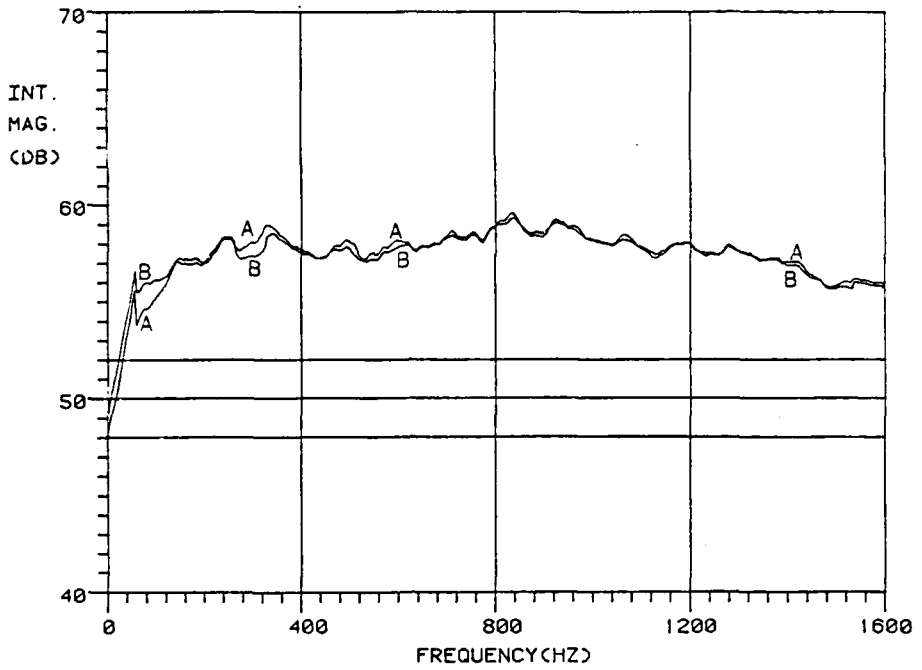

Figure 7.13(a): The "Smoothed" Acoustic Intensity of a Loudspeaker Sound Source at a Distance of 80 cm (S.F. = 20)
Curve A: Intensity Calculated Using Free-Field Pressure
Curve B: Intensity Measured by the Cross-Spectral Method

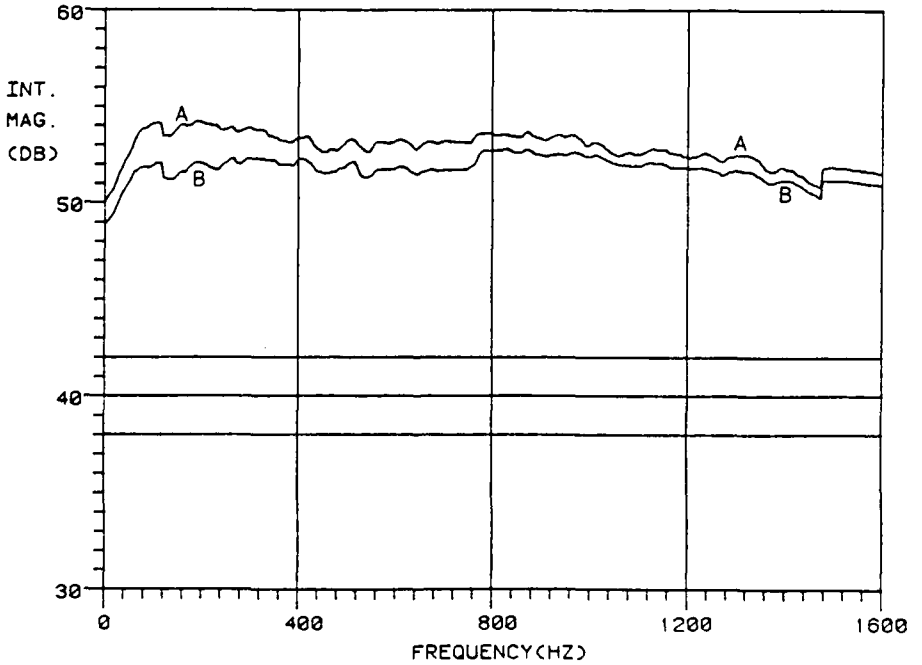

Figure 7.13(b): The "Smoothed" Acoustic Intensity of a Loudspeaker Sound Source at a Distance of 160 cm (S.F. = 30)
Curve A: Intensity Calculated Using Free-Field Pressure
Curve B: Intensity Measured by the Cross-Spectral Method

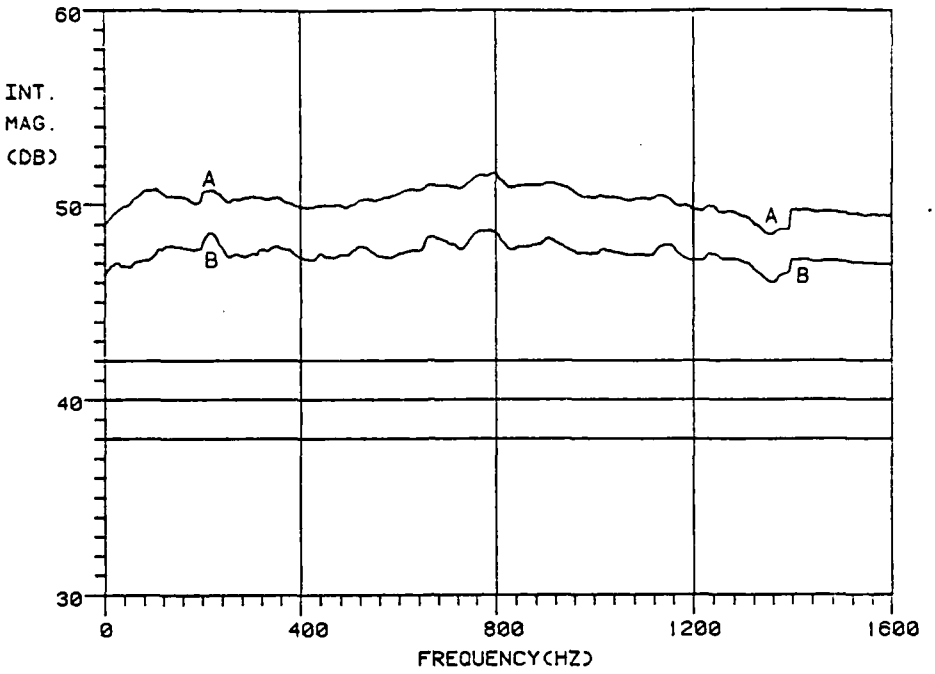

Figure 7.14(a): The "Smoothed" Acoustic Intensity of a Loudspeaker Sound Source at a Distance of 250 cm (S.F. = 50)
Curve A: Intensity Calculated Using Free-Field Pressure
Curve B: Intensity Measured by the Cross-Spectral Method

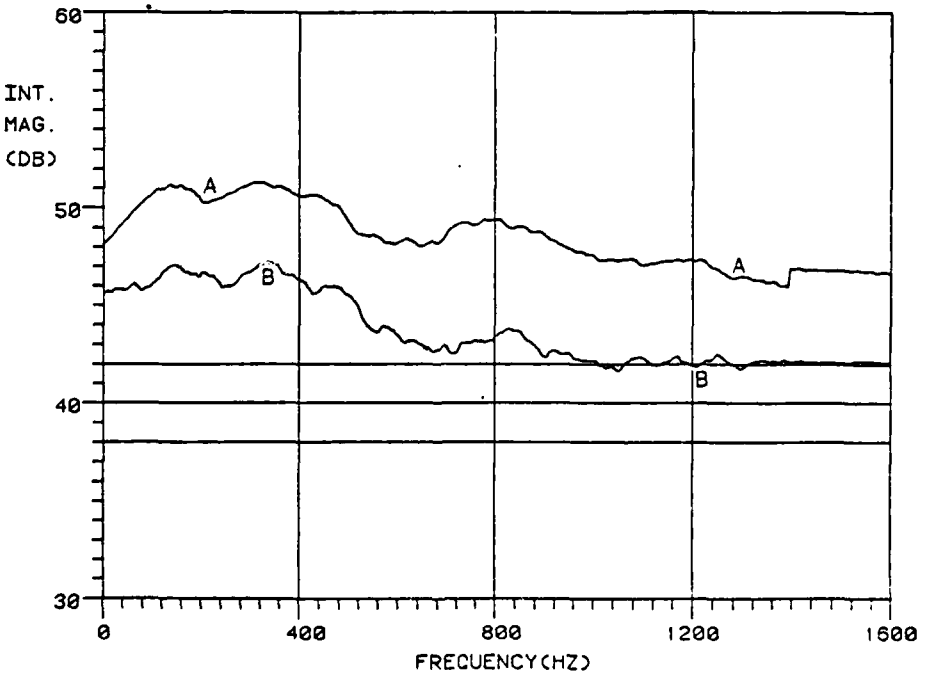

Figure 7.14(b): The "Smoothed" Acoustic Intensity of a Loudspeaker Sound Source at a Distance of 4.0 m (S.F. = 50)
Curve A: Intensity Calculated Using Free-Field Pressure
Curve B: Intensity Measured by the Cross-Spectral Method

of 160 cm from the source (Figure 7.13(b)). It could then be noticed that the intensity levels from pressure values at 250 cm (Figure 7.14(a)) and 4.0 m (Figure 7.14(b)) remain very similar while the cross-spectral intensity levels at the same distances from the sound source continued to decrease.

To understand the implications of the results of Figures 7.12-7.14, the intensity levels calculated from free-field pressures (Curve A) and the cross-spectral method (Curve B) were plotted (Figures 7.15-7.16) as a function of distance from the sound source for four specific frequencies (200 Hz, 400 Hz, 800 Hz, and 1200 Hz). The intensity values can then be compared to the theoretical free-field decay (6 dB/doubling distance) of intensity calculated from $p^2/\rho c$ (Curve C). In all the results of Figures 7.15-7.16, the cross-spectral intensity levels corresponded reasonable well to the theoretical free-field intensity while the intensity measurements from sound pressure values tend to level off to a constant value as would be expected of sound pressure measurements in a reverberant sound field.

Though the measurement conditions far from the source (4 m) were evidently not entirely reverberant because the pressure-squared data did not completely level to a constant value (except for the data of Figure 7.15(b)), it can be logically deduced from the presented results of Figures 7.15-7.16 that the two-microphone cross-spectral method of measuring acoustic intensity performs well under semi-reverberant (reverberant) situations. It would be useful and necessary to perform more experimental measurements in a highly reverberant environment to totally quantify the accuracy of the intensity meter in highly reverberant circumstances.

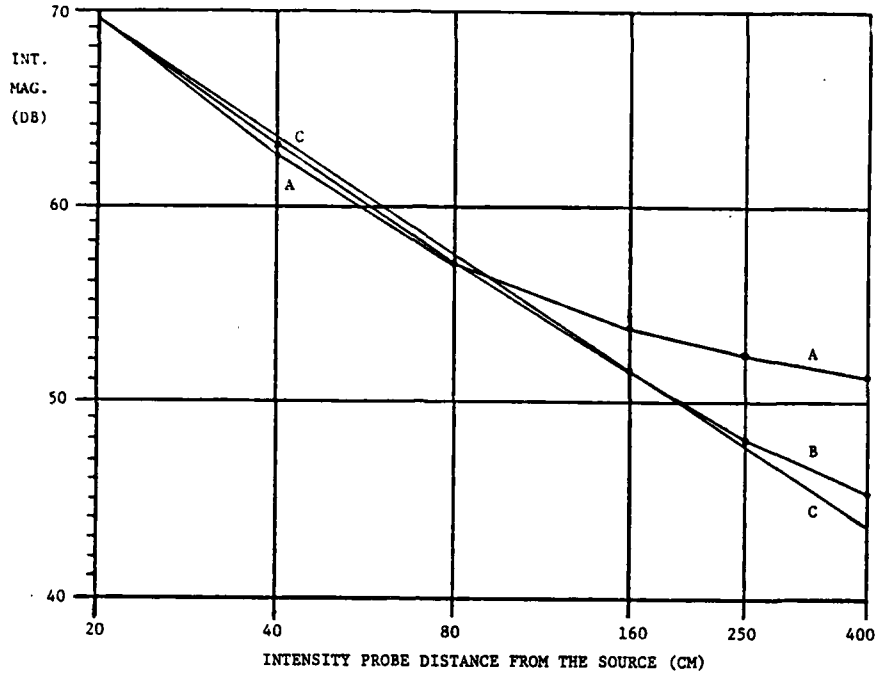

Figure 7.15(a): Measured Intensity Levels as a Function of Distance from a Loudspeaker Sound Source in a Reverberant Room (200 Hz)
Curve A: Intensity Calculated Using Free-Field Pressure
Curve B: Intensity Measured by the Cross-Spectral Method
Curve C: Theoretical Decay of Free-Field Intensity

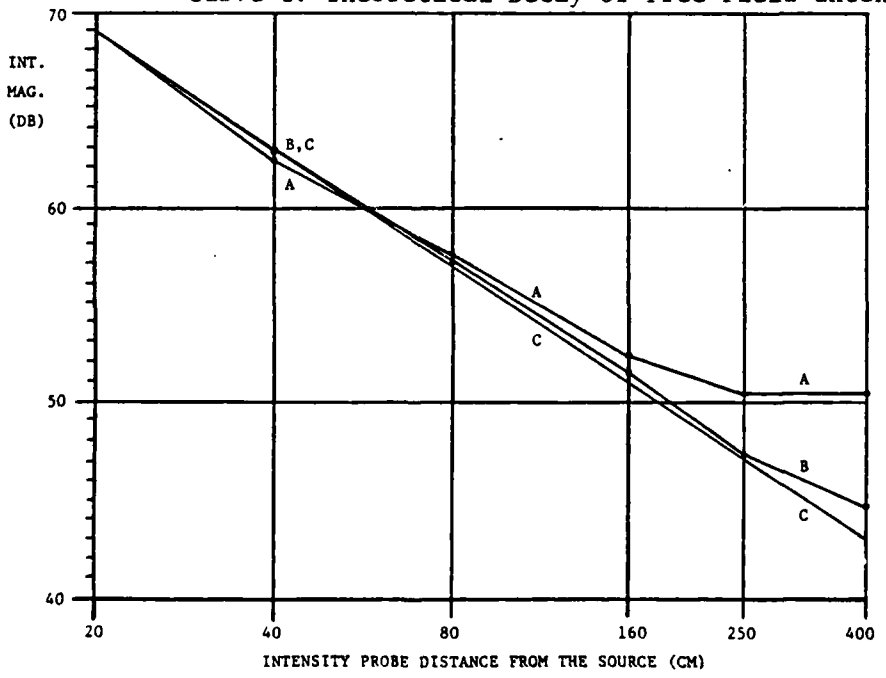

Figure 7.15(b): Measured Intensity Levels as a Function of Distance from a Loudspeaker Sound Source in a Reverberant Room (400 Hz)
Curve A: Intensity Calculated Using Free-Field Pressure
Curve B: Intensity Measured by the Cross-Spectral Method
Curve C: Theoretical Decay of Free-Field Intensity

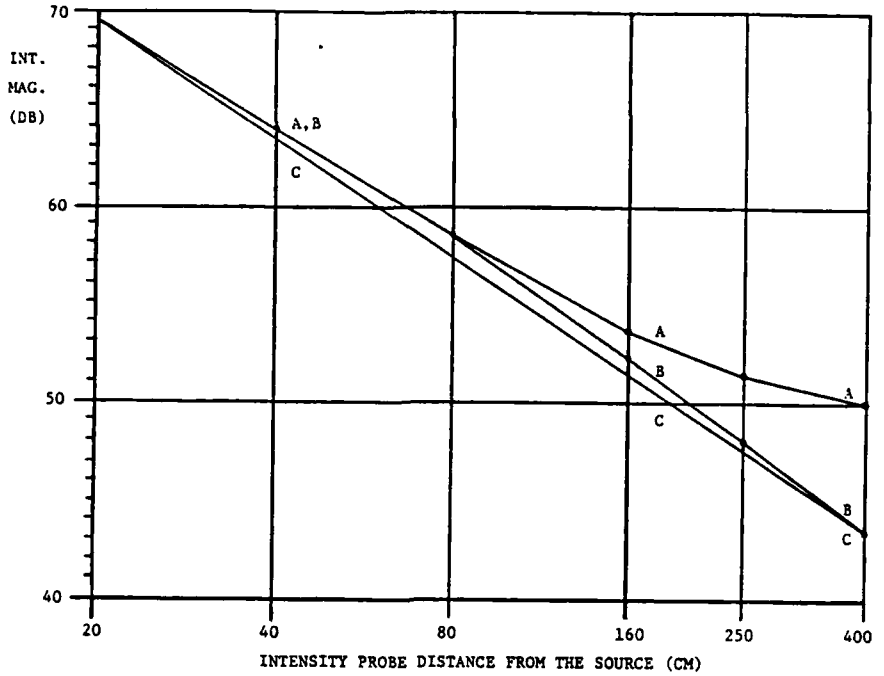

Figure 7.16(a): Measured Intensity Levels as a Function of Distance from a Loudspeaker Sound Source in a Reverberant Room (800 Hz)
Curve A: Intensity Calculated Using Free-Field Pressure
Curve B: Intensity Measured by the Cross-Spectral Method
Curve C: Theoretical Decay of Free-Field Intensity

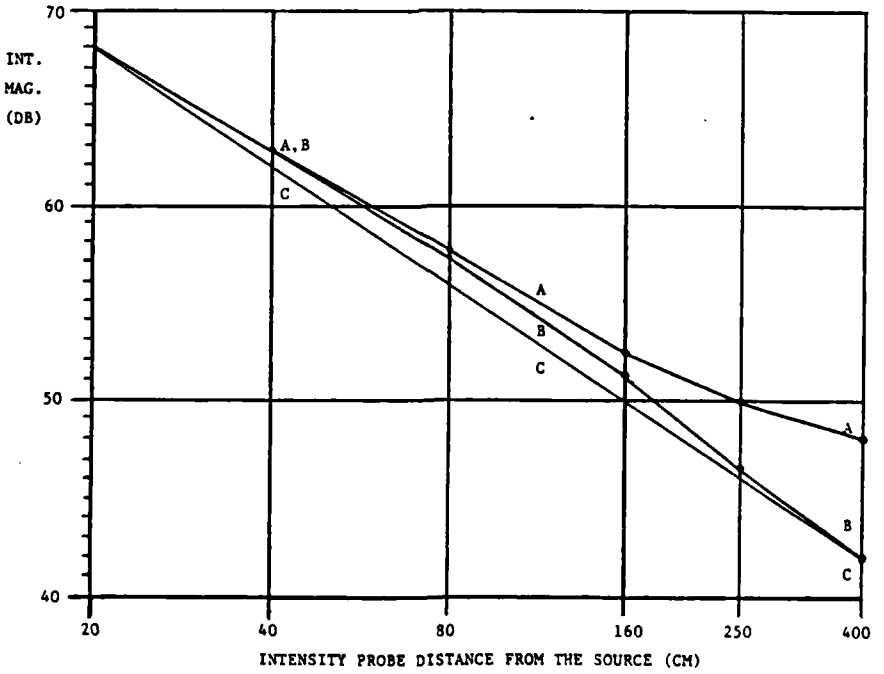

Figure 7.16(b): Measured Intensity Levels as a Function of Distance from a Loudspeaker Sound Source in a Reverberant Room (1200 Hz)
Curve A: Intensity Calculated Using Free-Field Pressure
Curve B: Intensity Measured by the Cross-Spectral Method
Curve C: Theoretical Decay of Free-Field Intensity

These intensity results using the cross-spectral intensity device were limited to the frequency range of 1600 Hz. With a two-microphone spacing of 13 mm, accurate measurements approaching the frequency range of 4000 Hz should be possible with the intensity meter, but as the measurement frequency increases, the variance (random error) of the intensity process increases when located in the more reverberant sound field (this subject is discussed in more detail in the following text, Section 7.3.2).

7.3.2 Variance and Coherence in the Reverberant Field

The estimation of the acoustic intensity in actual multiple reflective sound fields may be influenced by the variance of the measurement which depends on the measured coherence function between the two closely-spaced microphone signals (theoretically presented in Section 3.7 and in reference 58). The measured values of coherence can be much lower than the expected value of one due to the resolution bandwidth (B) of the spectral analysis relative to the density of the acoustic modes (m) in an enclosure (49). At the one extreme where the resolution bandwidth includes numerous modes, the measured coherence will tend to decrease with increasing frequency. For the limiting condition of an undamped acoustic enclosure and a measurement with a bandwidth such that mB>>1, the true coherence function will approach the form (49)

$$\gamma_{12}^2(f) = \{\sin(k\Delta r)/_{k\Delta r}\}^2 , \qquad (7.13)$$

which is identical to the coherence function for a diffused sound field. At the other extreme where the resolution band includes a few modes, the coherence function will tend to oscillate with changing frequency due to the standing wave patterns in the enclosure.

Figure 7.17 displays the coherence function measured between the two closely-spaced receivers used for the experimental investigation pertaining to cross-spectral intensity results in a reverberation sound field (Section 7.3.1). Figure 7.17(a) exhibits the measured coherence function between the two receivers when located at a distance of 250 cm from the sound source for a frequency range of 1600 Hz. Notice that the coherence function was approximately equal to 1.0 for the lower frequencies and began to deviate from the value 1.0 as the measurement frequency increased. This predicted event was more prominent for the frequency range of 4000 Hz (Figure 7.17(b)). Also, the decrease of coherence in both Figure 7.17(a) and Figure 7.17(b) at the very low frequencies (below 80 Hz) was due to background noise and 60 Hz ground-loop problems in the measuring systems.

7.4 The Reactive Sound Field

The accuracy of sound power measurements normal to a radiating surface with an intensity meter may be affected by a large reactive component of the measuring sound field. This reactive (non-radiating) part of the complex intensity will intuititively become more significant and unpredictable with a greater complexity of source radation. If there is the presence of a reactive sound field, then it is necessary to recognize the constraints, if any, added to the measurement of the real acoustic intensity.

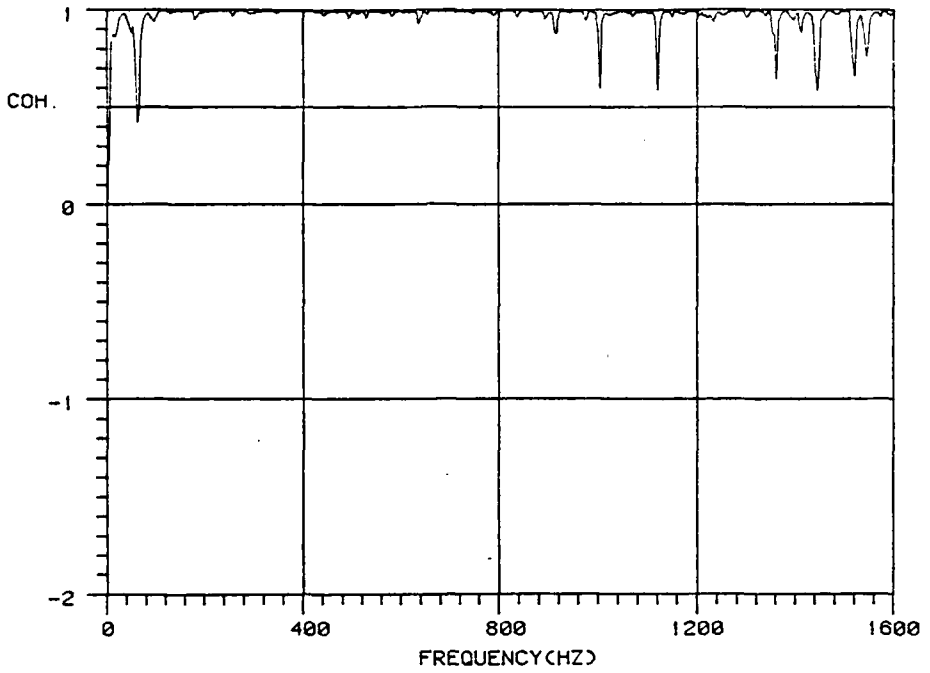

Figure 7.17(a): The Measured Coherence Between the Two Microphones Used for Cross-Spectral Intensity Measurements at a Distance of 250 cm from the Sound Source (1600 Hz Range)

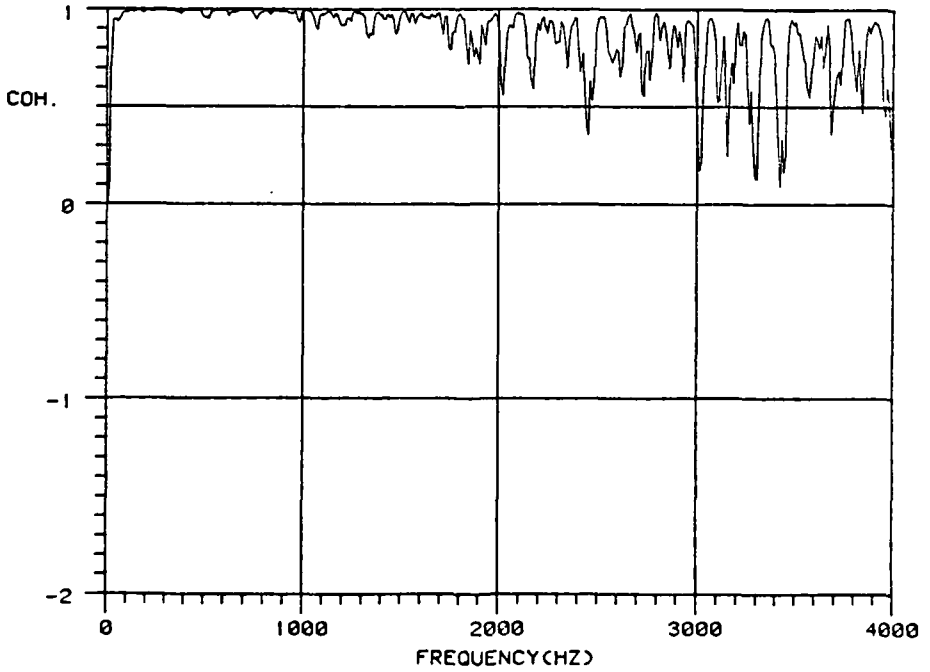

Figure 7.17(b): The Measured Coherence Between the Two Microphones Used for Cross-Spectral Intensity Measurements at a Distance of 250 cm from the Sound Source (4000 Hz Range)

In the nearfield of a noise source, the resulting acoustic intensity evaluated by the two-microphone method involves not only the imaginary part of the cross-spectral density (formulated in Chapter 3) but also a similar derivation of the reactive sound field. The measurement of the reactive acoustic intensity using the two-microphone method was recently described in a publication by Stanton and Beyer (58), and the theory, pertaining to complex intensity measurements using the cross-spectral method, was similarly developed in the work of Pascal (46).

The reactive intensity expression was derived in Section 3.2 (Equation 3.21) and restated here as

$$\hat{I}_{IM}(f) = [G_2(f) - G_1(f)]_{/8\pi f\rho\Delta r}, \qquad (7.14)$$

which utilizes the difference between the power spectral density functions (autospectra) of the two measuring microphone pressures. This difference in the autospectra magnitude between the two measuring points can be significant and may not be ignored when measuring the acoustic intensity in the nearfield of a sound source. Also, a stronger reactive sound field will usually exist in the lower frequencies of the measurements.

7.4.1 The Normalized Bias Error

The phase and gain-mismatch errors discussed in Chapter 5 and the intensity probe obstacle effects examined in Chapter 6 will consequently induce errors in the measurement of the reactive intensity. Also, the finite-difference approximation will behave differently in the presence

of a strong reactive sound field (reviewed in Chapter 4 and analyzed in the related literature (23,46,61)).

If it is assumed that $\Delta r << \lambda_{min}$, then any bias error of the reactive intensity will be caused by instrumentation errors and scattering effects of the intensity probe. Utilizing Equation 5.19, the normalized bias error for the cross-spectral reactive intensity can be written as

$$\varepsilon_{b_{IM}}(f) = [E\{\hat{I}_{IM}(f)\} - I_{IM}(f)]/I_{IM}(f) \tag{7.15}$$

where

$$I_{IM}(f) = \{G_2(f) - G_1(f)\}/4\pi f\rho\Delta r \tag{7.16}$$

$$\hat{I}_{IM}(f) = \{\hat{G}_2(f) - \hat{G}_1(f)\}/4\pi f\rho\Delta r \ . \tag{7.17}$$

Using the expressions for the true reactive intensity (7.9) and the estimated reactive intensity (7.10), the normalized bias error for the reactive intensity develops into the form

$$\varepsilon_{b_{IM}}(f) = \{(\hat{G}_2(f) - G_2(f)) - (\hat{G}_1(f) - G_1(f))\}/\{G_2(f) - G_1(f)\} \tag{7.18}$$

with

$$\hat{G}_1(f) = |H_a(f)|G_1(f) \tag{7.19}$$

$$\hat{G}_2(f) = |H_b(f)|G_2(f) \ . \tag{7.20}$$

Notice that if $|H_a(f)| = |H_b(f)| = 1$, then the normalized bias error $\varepsilon_{b_{IM}}(f)$ will be equal to zero, and there will be no bias of the measurment of the cross-spectral reactive intensity provided that the finite-difference approximation is not appreciable.

7.4.2 Intensity Measurements Compared with Pressure Values in the Nearfield

Assuming that the phase and magnitude differences between the two microphone measuring systems has been corrected by calibration and the scattering effects by the intensity probe are very minimal, the two-microphone intensity technique should provide an accurate measurement of the real (active) intensity as compared to the intensity calculated from free-field pressure values when the sensor(s) are located in the nearfield of a noise source.

To qualify the above deduction, the following experiment was performed, and the results are shown in Figure 7.18. First, the acoustic intensity at a point very close to a 10" diameter loudspeaker sound source (at a distance of 5 cm) was measured using both the free-field pressure method (Figure 7.18(a), Curve A) and the two-microphone cross-spectral technique (Figure 7.18(a), Curve B). Then, the acoustic intensity using both methods was measured at a 30 cm distance from the loudspeaker. This was considered to be in the far-field but still in the direct sound field (Figure 7.18(b)).

The results displayed in Figure 7.18(a) (the "nearfield" condition) show that the acoustic intensity calculated from assumed free-field pressure levels gave higher values than that of the cross-spectral intensity method, but after making similar measurements at a greater distance from the sound source (Figure 7.18(b)), the two intensity methods compared very favorably. Though not totally conclusive, these experimental results suggest that the intensity values calculated from the free-field pressure tend to be overestimated when very near the

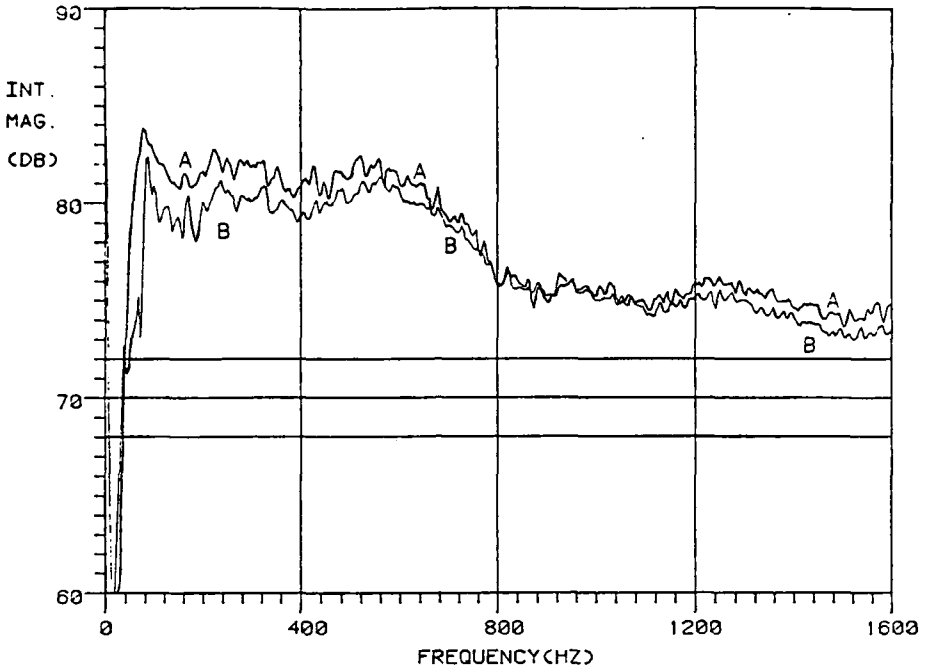

Figure 7.18(a): The Acoustic Intensity Measured in the Nearfield of a Loudspeaker Sound Source (at a Distance of 5 cm)
Curve A: Intensity Calculated Using Free-Field Pressure
Curve B: Intensity Measured Using the Cross-Spectral Method

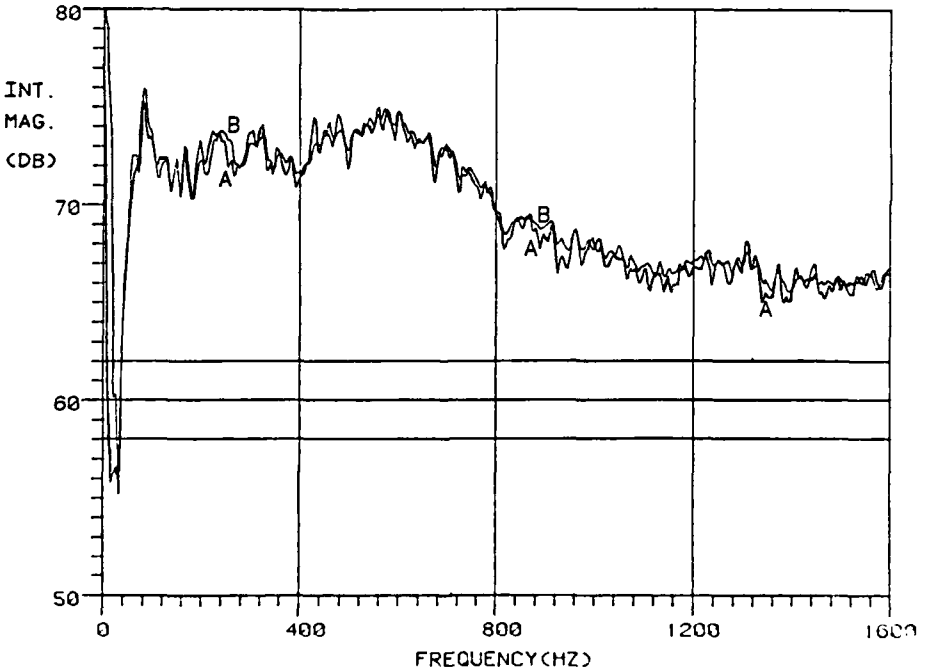

Figure 7.18(b): The Acoustic Intensity Measured in the Far-Field of a Loudspeaker Sound Source (at a Distance of 30 cm)
Curve A: Intensity Calculated Using Free-Field Pressure
Curve B: Intensity Measured by the Cross-Spectral Method

sound source while the two-microphone cross-spectral method gives acceptable intensity values even in the nearfield of a noise source.

CHAPTER 8

CONCLUSIONS

8.1 Summary and Conclusions

The two-microphone cross-spectral method of measuring acoustic intensity has proven to be a viable method of determining the sound power of a noise source when located in-situ, and the technique therefore provides a useful and practical alternative to traditional methods of measuring the sound power of a noise source.

The two-microphone acoustic intensity device is considered to be a sound receiver of the first-order having a dipole-type directional characteristic. Because the intensity meter measures the acoustic power flow, it has a definite advantage over the traditional pressure receiver when quantifying a noise source in-situ. Due to its scalar nature, the omni-directional microphone would be influenced significantly by the reactive sound field, diffraction due to its own physical geometry, other secondary (contaminating) sources, and the reverberant environment. The two-microphone intensity meter provides a more accurate sound power determination in-situ and because of its directionality, allows additionally for an easier source identification.

The cross-spectral intensity technique has limitations which must be fully understood before accepting the results as absolute and rigorous. There are four categories of bias errors related to the intensity technique: (1) errors associated with the finite-difference approximation; (2) errors due to the measuring instrumentation; (3)

errors from the intensity probe obstacle effects; and (4) errors influenced by secondary sources and the measuring environment. This work investigated experimentally these bias errors of the cross-spectral method of measuring acoustic intensity, and the conclusions, along with a brief summary, are now presented.

(1) The finite-difference error defines the high-frequency limitation of the cross-spectral intensity technique and is associated with the mathematical approximation of the acoustic intensity by finite-sum and difference quantities from two separate pressure measurements. This finite-difference error is a function of the separation distance between the two microphones and the measurement distance from the source (a proximity error), and these effects will be more substantial for the more complex-radiating sound sources. In general, the finite-difference error cannot be avoided,. and the only method of extending the upper frequency range of the two-microphone intensity device is to decrease the finite separation between the two sensors. Also, because the intensity is proportional to the measured phase shift (in the direction of wave propagation) between the two sound receivers, the relative phase difference between the two microphone measuring systems will affect the precision of the intensity measurement in the lower frequencies (corresponding to a small phase shift) of operation.

If intensity measurements in the immediate vicinity of the sound source are excluded, the expression for the bias error using plane-wave or point monopole conditions gives an adequate indication of the measurement accuracy. Using the above requisite and an error below 1.0 dB as the design criteria for the intensity measurements, the two-

microphone intensity device gives acceptable results up to the 1/3 octave frequency band of 4000 Hz for a 13 mm separation distance between the microphones and 8000 Hz for a 6.5 mm separation distance.[1]

(2) The two microphone measuring systems (consisting of microphones and the associated electronics) used to measure the cross-spectrum will contain phase and magnitude differences which can induce errors in the intensity measurements, and these instrumentation errors (particularly the phase differences) define the low-frequency limitation of the cross-spectral intensity technique. This relative phase shift between the two microphone channels can also significantly distort the expected directional response of the intensity meter for low frequencies.

Typically, the phase and magnitude differences of the electronics associated with the two measuring systems (the cathode followers, power supplies, pre-amplifiers, and the FFT analyzer) are very minimal. The most severe phase difference are usually contributed by the microphone cartridges, and these phase differences occur in the low-frequency region where phase errors between the two measuring systems are much more critical.

These phase and magnitude differences between the two measuring systems can be corrected by calibration. The calibration procedure of this work and frequently used in the field is the calibration-transfer-function method. The two common transfer-function methods to calibrate for phase and magnitude-mismatch errors, the plane-wave duct method and

---

[1] when using the two-microphone arrangement of this work, this separation distance of 6.5 mm can be realized by employing 1/4" microphones with corresponding 1/4" cathode followers.

the dual-electrostatic acutator method, gave different results in the critical low-frequency region. It was determined that the phase-difference values measured by the dual-actuator test were incorrect for the lower test frequencies because the electrostatic actuator does not apply an acoustic signal to the equalization vent of the measuring microphones. Therefore, the plane-wave duct method provides the more accurate low-frequency acoustic intensity results. It should be noted that the plane-wave duct method has a high-frequency limitation related to the radial modes of the duct, but practically, if the plane-wave duct method is used only below the radial mode cut-off frequency, this calibration procedure offers sufficient high-frequency correction of the phase and magnitude differences between the two microphone measuring systems. In general, phase-matched microphones are the best sensors to use for this type of cross-spectral operation, but even these microphones can have or develop low-frequency phase differences which must be corrected.

(3) The scattering of the sound field by the finite-size intensity probe (consisting of both the microphones and their microphone holder) can produce changes in the amplitude and phase between the two measuring microphones. These obstacle effects are very difficult to model theoretically, and only an experimental evaluation of the errors from this scattering was investigated.

The intensity probe used for this work consisted of two B&K 1/2" or 1/4" microphones placed in parallel with their respective membranes in one plane. This two-microphone arrangement is a very common and physically practical configuration for measuring the acoustic intensity with two microphones.

The presented experimental evidence shows that this two-microphone configuration causes errors in the measurement results due to the scattering effects. These scattering effects are less with the smaller-size microphones and the smallest separation distances between the two measuring microphones. It was also found that the two-microphone holder produces noticeable distortions of the measured field, and therefore, it is suggested that the physical size of the two-microphone holder be as small as possible. In conclusion, when certain precautions are taken (i.e., using 1/4" microphones with a small separation distance on a physically small holder), the scattering of sound by the intensity probe produces only a minimal amount of error in the cross-spectral intensity measurements.

(4) Since the greatest advantage of the two-microphone intensity device is the ability to determine the sound power of a noise source in-situ, it is necessary to understand the errors created by the measuring environment. This measuring acoustical environment may include secondary noise sources radiated by other machines which are not the subject of the sound power determination. Also, reflections from the room boundaries (the reverberant field) and/or by sound-reflecting surfaces in the vicinity of the measuring area can influence the measuring environment.

It is shown that the cross-spectral intensity measurement of a specific sound source at a given spacial point can be biased by an uncorrelated contaminating source according to the ratio of the secondary source intensity to the primary source intensity. The experimental results using a secondary source verifies the theoretical

bias error prediction in which the contaminating sound source intensity is considered to be a vector quantity which adds to or subtracts from the primary source intensity measurement depending on the secondary source intensity flow and position. Therefore, if the secondary source vector intensity is equal but opposite the primary source intensity, then there would be total cancellation of the acoustic intensities at the measurement point.

The conclusions from the measured results using a secondary sound source exhibit only the intensity measurement at one spacial location, but when estimating the sound power of the primary source, the acoustic power flow would be measured about a surface area enclosing only the primary source thereby eliminating any bias (contribution) by the exterior secondary source(s). Therefore, the limitations in precision of the sound power determination in-situ would then relate to the number of measurement points contained in the measuring envelop and the random, not bias, error associated directly with the coherence magnitude between the two closely-spaced microphones influenced by the measuring environment.

Determining the sound power of a noise source in-situ may also require that measurements be taken in semi-reverberant (reverberant) conditions. In this situation, there is concern that the intensity meaurements will be influenced by the presence of the reverberant sound field. If the multiple reflected sound waves are considered to be analogous to individual secondary sound sources, then the combined intensities of the reflected sound waves exterior to the measuring surface will be equal to a theoretical value of zero, and no bias of the sound power measurement from the reverberant should occur.

Acoustic intensity measurements conducted using the two-microphone cross-spectral method in a reverberant test environment provided results that closely correspond to the theoretical decay of intensity in a free-field situation. Therefore, it can be concluded that the cross-spectral intensity device provides reliable measurements in both the free-field and reverberant conditions. Also, the coherence between the two closely-spaced microphone signals decreased with increasing frequency which would indicate an increase in the variance of the intensity measurement due to resolution limitations of the analysis related to the density of acoustic modes in the enclosure. Therefore, even though the presence of perturbing noise (secondary sound sources and the reverberant sound field) does not bias the sound power estimate via the intensity meter, the contaminating noise may increase the random error of the measurement.

Locating the two-microphone intensity device in the nearfield of a sound source, the resulting acoustic intensity involves not only the imaginary part of the cross-spectral density but also the difference between the autopectrums of the two microphone outputs. The nearfield intensity measurement is biased by the same errors (instrumentation errors, obstacle effects of the intensity probe, and the finite-difference error) which could adversely affect the measurement of the active (real) acoustic intensity, but if the phase and gain mismatch is corrected by calibration and the acoustic scattering by the intensity probe is minimized, the finite-difference approximation is the major contributor to any bias error of the cross-spectral intensity estimation when placing the intensity meter in the nearfield of a noise source.

In general, when comparing the two-microphone cross-spectral intensity method to the measuring procedure using assumed free-field (plane wave) sound pressure measurements for sound power determination in-situ, the intensity device has the advantage of suppressing the bias error produced by a nearfield measurement of the noise source and reducing the effect of the measuring environment consisting of uncorrelated secondary sound sources, sound-reflecting surfaces, and the reverberant sound field. All of these acoustical conditions would give rise to an overestimation of the sound power in-situ via sound pressure measurements.

8.2 Final Comments and Recommendations for Future Study

The two-microphone cross-spectral intensity meter is a very proficient measuring device when determining and qualifying the sound power of a noise source located in its natural operating acoustic environment. With the rapid increase in the application of the cross-spectral intensity instrument for noise measurement and identification, the user must be fully aware of its limitations in practical situations. For example, the careful measurement of the phase differences between the two microphone cartridges is essential for accuracy in the low-frequency region of the analysis. Though there are methods to calibrate the phase and gain differences between the two measuring systems, the calibration techniques do have particular disadvantges, and it would be useful to possess a more convenient and relieable calibration system that would encompass the complete frequency range of application.

The cross-spectral intensity procedure exhibits exceptional accuracy even under the influence of background (exterior) noise and semi-reverberant (reverberant) conditions, but when the secondary perturbing sound field is excessive, the random error of the intensity measurement can be substantially increased. Therefore, it would be extremely useful and strongly recommended that there be additional experimental examination into the variance of the measuring procedure when the coherence between the two closely-spaced receivers deviates from the required value of one. Also, there is neither adequate theoretical modeling or empirical information pertaining to the finite number of intensity receiver positions, over the measuring surface, necessary for acceptable sound power results of a noise source in-situ, especially under less than ideal measuring conditions.

The two-microphone cross-spectral method of measuring acoustic intensity will soon become a standard tool for sound power measurements and noise source identification. The two-microphone cross-spectral process has also been successfully applied to other quantitative measurements of acoustics such as transmission loss and sound absorption where intensity is needed to characterized the acoustic properties. Also, the data acquisition time required to perform these acoustic measurements is reduced substantially.

BIBLIOGRAPHY

1. Alfredson, R.J., "The Direct Measurement of Acoustic Energy in Transient Sound Fields", J. Sound Vib., 70(2), pp. 181-186 (1980).

2. Baker, S., "Acoustic Intensity Meter", J. Acoust. Soc. Am., 27(2), pp. 269-273 (1955).

3. Bauer, B.B., "Measurement of Acoustic Intensity and Reflection Coefficient with Cardiod Microphones", J. Acoust. Soc. Am., 44(2), pp. 636-637 (1968).

4. Bendat, J.S. and Piersol, A.G., Engineering Applications of Correlation and Spectral Analysis, Wiley-Interscience, New York, 1980.

5. Bendat, J.S. and Piersol, A.G., Random Data: Analysis and Measurement Procedures, Wiley-Interscience, New York, 1971.

6. Blake, W.K. and Waterhouse, R.V., "The Use of Cross-Spectral Density Measurements in Partially Reverberant Sound Fields", J. Sound Vib., 54(4), pp. 589-599 (1977).

7. Bodlund, K., "A New Quantity for Comparative Measurements Concerning the Diffusion of Stationary Sound Fields", J. Sound Vib., 44(2), pp. 191-207 (1976).

8. Bolt, R.H. and Petrauskas, A.A., "An Acoustic Impedance Meter for Rapid Field Measurements", J. Acoust. Soc. Am., 15, p. 79(A) (1943).

9. Burger, J.F., van der Merwe, G.J.J., van Zyl, B.G., and Joffe, L., "Measurement of Sound Intensity Applied to the Determination of Radiated Sound Power", J. Acoust. Soc. Am., 53(4), pp. 1167-1168 (1975).

10. Chung, J.Y., Pope, J., and Feldmaier, D.A., "Application of Acoustic Intensity Measurement to Engine Noise Evaluation", Proc. of the Diesel Engine Noise Conference, Detroit, Michigan, pp. 353-364, Feb.26-March 2, 1979.

11. Chung, J.Y., "Cross-Spectral Method of Measuring Acoustical Intensity", GM Research Publication GMR-2617, December, 1977.

12. Chung, J.Y., "Cross-Spectral Method of Measuring Acoustic Intensity Without Error Caused by Instrument Phase Mismatch", J. Acoust. Soc. Am., 64(6), pp. 1613-1370 (1977).

13. Chung, J.Y., "A New Method of Measuring Sound Power", GM Research Publication GMR-2156, May, 1976.

14. Chung, J.Y., "Practical Measurement of Acoustic Intensity--The Two-Microphone Cross-Spectral Method", GM Research Publication GMR-2645, Feb., 1978.

15. Chung, J.Y. and Blaser, D.A., "Recent Developments in the Measurement of Acoustic Intensity Using the Cross-Spectral Method", SAE Paper No. 810396, Feb., 1981.

16. Chung, J.Y. and Blaser, D.A., "Transfer Function Method of Measuring In-Duct Acoustic Properties. I. Theory", J. Acoust. Soc. Am., 68(3), pp. 907-913 (1980).

17. Chung, J.Y. and Blaser, D.A., "Transfer Function Method of Measuring In-Duct Acoustic Properties. II. Experiment", J. Acoust. Soc. Am., 68(3), pp. 914-921 (1980).

18. Chung, J.Y. and Blaser, D.A., "A Transfer Function Technique for Determining the Acoustic Characteristics of Duct Systems with Flow", Proc. of Internoise Conference-78, pp. 901-908, May, 1978.

19. Clapp, C.W. and Firestone, F.A., "Acoustic Wattmeter", J. Acoust. Soc. Am., 13, pp. 124-136 (1941).

20. Cook, R.K., Waterhouse, R.V., Berendt, R.D., Edelman, S., and Thompson, M.C.,Jr., "Measurements of the Correlation Coefficients in Reverberant Sound Fields", J. Acoust. Soc. Am., 27(6), pp. 1072-1077 (1955).

21. Cook, R.K. and Proctor, T.M., "A Standing-Wave Tube as an Absolutely Known Source of Sound Power", J. Acoust. Soc. Am., 65(6), pp. 1542-1555 (1979).

22. Crocker, M.J., Forssen, B., Raju, P.K., and Mielnicka, A., "Measurement of Transmission Loss of Panels by an Acoustic Intensity Technique", Proc. of Internoise-80, pp. 741-746, Dec. 8-10, 1980.

23. Elliott, S.J.; Thompson, J.K., "Errors in Acoustic Intensity Measurments", J. Sound Vib. (Letters to the Editor with Author's Reply), 78(3), pp. 439-445 (1981).

24. Fahy, F.J., "Measurement of Acoustic Intensity Using the Cross-Spectral Density of Two Microphone Signals", J. Acoust. Soc. Am., 62(4), pp. 1057-1059 (1977).

25. Fahy, F.J., "Measurements with an Intensity Meter of the Acoustic Power of a Small Machine in a Room", J. Sound Vib., 57(3), pp. 311-322 (1978).

26. Fahy, F.J., "A Technique for Measuring Sound Intensity with a Sound Level Meter", Noise Control Eng., 9(3), pp. 155-162 (1977).

27. Frederiksen, E., "Low-Frequency Calibration of Acoustical Systems", Bruel&Kjaer Technical Review ISSN 0007-2621, No. 4 (1981).

28. Glaretas, C., "A New Method for Measuring the Acoustic Impedance of the Ground", Ph.D. Thesis in Acoustics, The Pennsylvania State University (1981).

29. Goff, K.W., "The Application of Correlation Techniques to Some Acoustic Measurements", J. Acoust. Soc. Am., 27(2), pp. 236-246 (1955).

30. Hodgson, T.H., "Investigation of the Surface Acoustical Intensity Method for Determining the Noise Sound Power of a Large Machine In-Situ", J. Acoust. Soc. Am., 61(2), pp. 487-493 (1977).

31. Hodgson, T.H. and Erianne, R.D., "Noise Source Location for Large Machines from Measurements of Surface Acoustic Intensity", Proc. of Internoise-76, pp. 13-18, April 5-7, 1976.

32. Jacobsen, F., "The Diffuse Sound Field--Statistical Considerations Concerning the Reverberant Field in the Steady State", The Acoustics Laboratory/Technical University of Denmark, Report No. 27, 1979.

33. Jacobsen, F., "Measurement of Sound Intensity", The Acoustics Laboratory/Technical University of Denmark, Report No. 28, 1980.

34. Jacobsen, F., "Sound Power Determination in Reverberation Rooms-- A Normal Mode Analysis", The Acoustics Laboratory/Technical University of Denmark, Report No. 26, 1979.

35. Krishnappa, G., "Cross-Spectral Method of Measurement Acoustic Intensity by Correcting Phase and Gain Mismatch Errors by Microphone Calibration", J. Acoust. Soc. Am., 69(1), pp. 307-310 (1981).

36. Laville, F., Salvan, G., and Pascal, J.C., "Sound Power Determination Using Intensity Measurements Under Field Conditions", Proc. of Internoise-80, pp. 1083-1086, Dec. 8-10, 1980.

37. Merhaut, J., Theory of Electroacoustics, McGraw-Hill International, New York, 1981.

38. Morfey, C.L., "Acoustic Energy in Non-Uniform Flow", J. Sound Vib., 14(2), pp. 159-170 (1971).

39. Morse, P.M. and Ingard, K.U., Theoretical Acoustics, McGraw-Hill, Inc., New York, 1968.

40. Munro, D.H. and Ingard, K.U., "On Acoustic Intensity Measurements in the Presence of Mean Flow", J. Acoust. Soc. Am., 65(6), pp. 1402-1406 (1979).

41. Noiseux, D.U., "Measurement of Power Flow in Uniform Beams and Plates", J. Acoust. Soc. Am., 47(1), pp. 238-247 (1970).

42. Okubo, K., "A Study of Cross-Spectrum Acoustic Intensity Measurements Applied to Continuous and Impact Noise Sources", M.S. Thesis in Mech. Eng., Michigan Tech. Univ. (1980).

43. Olson, H.F., "Field-Type Acoustic Wattmeter", J. Audio Eng. Soc., 22(5), pp. 321-327 (1974).

44. Olson, H.F., "System Response to the Energy Flow of Sound Waves", U.S. Patent No. 1,892,644 (1932).

45. Pascal, J.C., "Estimation of the Acoustic Power by Means of Intensity Meters", Proc. of the Conference of Recent Developments in Acoustic Intensity Measurement, Senlis(France), pp. 179-185, Sept. 30-Oct. 2, 1981.

46. Pascal, J.C., "Measurement of the Active and Reactive Intensity in Various Acoustic Fields", Proc. of the Conference of Recent Developments in Acoustic Intensity Measurements, Senlis(France), pp. 11-19, Sept. 30-Oct. 2, 1981.

47. Pavic, G., "Measurement of Sound Intensity", J. Sound Vib. 51(4), pp. 533-546 (1977).

48. Pavic, G., "Measurement of Structure Borne Wave Intensity, Part I: Formulation of the Methods", J. Sound Vib., 49(2), pp. 221-230 (1976).

49. Pettersen, O. Kr.Ø., "Sound Intensity Measurements for Describing Acoustic Power Flow", Applied Acoustics, 14, pp. 387-397 (1981).

50. Piersol, A.G., "Use of Coherence and Phase Data Between Two Receivers in Evaluation of Noise Measurements", J. Sound Vib., 56(2), pp. 215-228, (1978).

51. Rasmussen, G. and Brock, M., "Acoustic Intensity Measurement Probe", Proceedings, Conference of Recent Developments in Acoustic Intensity Measurements, Senlis(France), pp. 81-88, Sept. 30-Oct. 2, 1981.

52. Reinhart, T.E., "Noise Source Identification of Diesel Engines Using Acoustic Intensity Measurements", M.S. Thesis in Mech. Eng., Purdue University (1980).

53. Sakamoto, N., Satoh, K., Satoh, K., and Nobuhisa, A., "Loudspeaker with Honeycone Disk Diaphragm", J. Audio Eng. Soc., 29(10), pp. 711-719 (1981).

54. Schultz, T.J., "Acoustic Wattmeter", J. Acoust. Soc. Am., 28(4), pp. 693-699 (1956).

55. Schultz, T.J., Smith, P.W.,Jr., and Malme, C.I., "Intensity Measurement in Near Fields and Reverberant Spaces", Bolt, Beranek, and Newman, Inc., Report No. 1135, July 24, 1964; submitted to the Office of Naval Research, Washington, D.C.

56. Schultz, T.J., Smith, P.W.,Jr., and Malme, C.I., "Measurement of Acoustic Intensity in a Reactive Sound Field", J. Acoust. Soc. Am., 57(6), Pt. 1, pp. 1263-1268 (1975).

57. Seybert, A.F. and Ross, D.F., "Experimental Determination of Acoustic Properties Using a Two-Microphone Random-Excitation Technique", J. Acoust. Soc. Am., 61(5), pp. 1362-1370 (1977).

58. Seybert, A.F., "Statistical Errors in Acoustic Intensity Measurements", J. Sound Vib., 75(4), pp. 519-526 (1981).

59. Stahel, W. and Lambrich, H.P., "Development of an Instrument for the Measurement of Sound Intensity and Its Application in Car Acoustics", External Publication, Interkeller A.G., Zurich, Switzerland, 1975.

60. Stanton, T.K. and Beyer, R.T., "Complex Wattmeter Measurements in a Reactive Acoustic Field", J. Acoust. Soc. Am., 65(1), pp. 249-252 (1979).

61. Thompson, J.K. and Tree, D.R., "Finite Difference Approximation Errors in Acoustic Intensity Measurements", J. Sound Vib., 75(2), pp. 229-238 (1981).

62. Verheij, J.W.; Pavic, G., "Cross-Spectral Density Methods for Measuring Structure Borne Power Flow On Beams and Pipes", J. Sound Vib. (Letters to the Editor with Author's Reply), 70(1), pp. 133-139 (1980).

63. Walker, A.W., "The Effect of Bandwidth on the Accuracy of Transfer Function Measurements of Single Degree of Freedom System Response to Random Excitation", J. Sound Vib., 74(2), pp. 152-263 (1981).

64. Westervelt, P.J., "Acoustical Impedance in Terms of Energy Functions", J. Acoust. Soc. Am., 23, pp. 347-348 (1951).

65. Yamada, I., "Cross-Spectral Method for the Estimation of Ground-Reflection Characteristics and Free-Field Spectrum of Noise", J. Acoust. Soc. Jpn. (E), 1(4), pp. 249-259 (1980).

66. van Zyl, B.G. and Anderson, F., "Evaluation of the Intensity Method of Sound Power Determination", J. Acoust. Soc. Am., 57(3), pp. 682-686 (1975).

DISTRIBUTION LIST FOR TM 82-135

Commander (NSEA 0342)
Naval Sea Systems Command
Department of the Navy
Washington, DC 20362 — Copies 1 and 2

Commander (NSEA 9961)
Naval Sea Systems Command
Department of the Navy
Washington, DC 20362 — Copies 3 and 4

Defense Technical Information Center
5010 Duke Street
Cameron Station
Alexandria, VA 22314 — Copies 5 through 10